

**EMPIRICAL STUDY OF THE EFFECT OF OFFRAMP QUEUES ON
FREEWAY MAINLINE TRAFFIC FLOW**

A Dissertation
Presented to
The Academic Faculty

by

Christopher Stephen Toth

In Partial Fulfillment
of the Requirements for the Degree
Doctor of Philosophy in the
School of Civil & Environmental Engineering

Georgia Institute of Technology
December 2014

Copyright © 2014 By Christopher Toth

**EMPIRICAL STUDY OF THE EFFECT OF OFF-RAMP QUEUES
ON FREEWAY MAINLINE TRAFFIC FLOW**

Approved by:

Dr. Jorge Laval, Advisor
School of Civil & Environmental
Engineering
Georgia Institute of Technology

Dr. Randall Guensler, Advisor
School of Civil & Environmental
Engineering
Georgia Institute of Technology

Dr. Michael Hunter
School of Civil & Environmental
Engineering
Georgia Institute of Technology

Dr. Michael Rodgers
School of Civil & Environmental
Engineering
Georgia Institute of Technology

Dr. Baabak Ashuri
School of Building Construction
Georgia Institute of Technology

Date Approved: November 17, 2014

ACKNOWLEDGEMENTS

I wish to thank my committee members for their support, guidance, and insight during my dissertation research. I cannot express enough appreciation Dr. Jorge Laval, Dr. Randall Guensler, Dr. Michael Hunter, Dr. Michael Rodgers, and Dr. Baabak Ashuri have put toward reviewing my research work to make it the best it can be. A special thanks to Dr. Jorge Laval and Dr. Randall Guensler for encouraging me to pursue a Ph.D. degree. Their patience and flexibility have given me the opportunity to grow and succeed, and prepare me for life after graduation. Furthermore, they have made my experience at Georgia Tech not only educational, but enjoyable and invigorating at times.

My gratitude also goes to the friends I have made while at Georgia Tech, who have created memories and experiences that will be with me throughout my lifetime. Finally, the encouragement, emotional support, and love I have received from my parents and family cannot be understated. I am very grateful they were there for me throughout this entire process. Without them, none of this would have been possible.

TABLE OF CONTENTS

| | Page |
|---|------|
| ACKNOWLEDGEMENTS | iii |
| LIST OF TABLES | vi |
| LIST OF FIGURES | vii |
| LIST OF SYMBOLS AND ABBREVIATIONS | xi |
| SUMMARY | xii |
| CHAPTER 1: INTRODUCTION | 1 |
| Goals and Objectives | 3 |
| Contribution | 7 |
| Dissertation Outline | 8 |
| CHAPTER 2: LITERATURE REVIEW | 11 |
| Corridor Description | 11 |
| Reasons for Weaving | 13 |
| Relationship to Capacity | 16 |
| Effect of Weaving on Car-Following Behavior | 20 |
| Lane-Changing Models | 22 |
| Off-ramp Bottlenecks | 29 |
| Literature Review Summary | 30 |
| CHAPTER 3 CASE STUDY SITE SELECTION | 32 |
| Site | 34 |
| CHAPTER 4: DATA COLLECTION METHODOLOGY | 40 |
| Final Camera View Selections | 47 |
| Data Collection Protocols | 48 |
| CHAPTER 5: DATA COLLECTION AND PROCESSING | 50 |
| Footage Selection | 51 |
| Vehicle Trajectories | 52 |
| Lane Change Counts | 58 |
| Volume Counts | 61 |
| Peach Pass Tag Read Processing | 61 |
| Data Collection Summary | 63 |
| CHAPTER 6: MACROSCOPIC LANE CHANGING MODEL | 65 |

| | |
|---|-----|
| Preliminary Data Assessment | 67 |
| Final Model Selection | 90 |
| Lane Changes out of a Ramp Lane | 119 |
| Macroscopic Lane Changing Model Conclusion | 121 |
| CHAPTER 7: LATERAL PROPAGATION OF CONGESTION | 123 |
| Case Studies | 133 |
| Regression Analysis | 140 |
| CHAPTER 8: LANE DISTRIBUTION OF EXITING VEHICLES | 153 |
| Relationship Between Lane Choice and Freeway Speed | 155 |
| HOT Egress Behavior of Exiting Drivers | 174 |
| CHAPTER 9 FUTURE MODEL DEVELOPMENT | 183 |
| Research Utilizing Current Capabilities and Techniques | 183 |
| Research Utilizing Improved Capabilities and Techniques | 186 |
| CHAPTER 10 CONCLUSIONS AND FUTURE RESEARCH | 190 |
| Limitations | 192 |
| Future Research | 193 |
| Contributions | 196 |
| APPENDIX A: PROCEDURES FOR CHANGING TMC PTZ CAMERA VIEWS DURING I-85 VIDEO DATA COLLECTION EFFORTS | 198 |
| Procedures for Changing I-85 TMC PTZ Camera Views | 199 |
| Background | 199 |
| TMC Notification | 200 |
| Procedures for Moving Camera Views | 200 |
| APPENDIX B: SCREENSHOTS OF CAMERA VIEWS USED DURING RECORDING | 202 |
| APPENDIX C: OTHER MODEL CONSIDERATIONS | 203 |
| APPENDIX D: VIDEO PROCESSING SOFTWARE | 210 |
| Tracking | 211 |
| Calibration | 212 |
| REFERENCES | 214 |
| VITA | 218 |

LIST OF TABLES

| | |
|--|-----|
| Table 1: List of Cameras Used for Data Collection | 47 |
| Table 2: Data Collection Summary | 64 |
| Table 4: Statistical Summary of Lane Change Position | 73 |
| Table 5: Kolmogorov-Smirnov Test Results – Comparison of Distributions with Different Exit lane speeds | 76 |
| Table 6: Comparison of Statistics – Observed versus Bootstrap Best-Fit | 80 |
| Table 8: KS Test Results – Comparison of Observed Data Between Days | 84 |
| Table 9: Qualitative Assessment of a Model with a Given AIC (Burnham and Anderson, 2002) | 95 |
| Table 10: Interactive Polynomial Fit Statistics | 96 |
| Table 11: Calibration and Verification Data Set Dates | 99 |
| Table 12: Parameter Estimates Using Calibration and Verification Data Sets | 101 |
| Table 13: Chi-Squared Test Results for Best-Fit Curve (I-85) | 104 |
| Table 14: Parameter Estimates for Best-Fit Curve (Buford-Spring Conn.) | 112 |
| Table 15: Chi-Squared Test Results for Best-Fit Curve (Buford-Spring Conn.) | 115 |
| Table 16: Mechanisms of Congestion Propagation | 124 |
| Table 17: Disruption Regression Results | 147 |
| Table 18: Non-Disruption Regression Results | 150 |
| Table 19: Fraction of Drivers with Peach Pass by Time of Day (I-85 Southbound 10/1/12) | 157 |
| Table 20: Parameter Estimates for Best-Fit Curve (Inflection) | 208 |
| Table 21: Chi-Squared Test Results for Best-Fit Curve (Inflection) | 208 |

LIST OF FIGURES

| | |
|---|----|
| Figure 1: Recently Developed Tracking Software | 5 |
| Figure 2: Disruptive Lane Change into Queued Off-ramp Lane | 6 |
| Figure 3: HOV/HOT Study Corridor | 12 |
| Figure 4: Lane Changing Model Structure (Ahmed, 1999) | 23 |
| Figure 5: Time-Space Diagram for Forced and Cooperative of Lane Changes (Hidas, 2005) | 24 |
| Figure 6: Number of Peach Pass Drivers Exiting I-85 Southbound (October 2012) | 34 |
| Figure 7: I-85 Site Map | 36 |
| Figure 8: Site Location | 37 |
| Figure 9: Buford Spring Connector Study Corridor | 38 |
| Figure 10: Site Location | 39 |
| Figure 11: PTZ Camera and General View | 41 |
| Figure 12: Camera Coverage on the Study Corridor | 43 |
| Figure 13: Occlusion Example | 44 |
| Figure 14: Side of Freeway View for Monitoring Lane Changes | 45 |
| Figure 15: Overpass View for Monitoring Lane Changes | 46 |
| Figure 16: Vehicle Tracking Camera View | 54 |
| Figure 17: Frame-by-Frame Estimated Speed (Gygax) vs. Ground Truth Speed (Laser Gun) | 56 |
| Figure 18: Cumulative Distribution of Frame-by-Frame Speed Error | 56 |
| Figure 19: Vehicle-by-Vehicle Average Estimated Speed (Gygax) vs. Average Ground Truth Speed (Laser Gun) | 57 |
| Figure 20: Cumulative Distribution of Vehicle-by-Vehicle Speed Error | 57 |
| Figure 21: Underpass Occlusion | 59 |

| | |
|--|-----|
| Figure 22: Partial Graphical Representation of Peach Pass Tag Read Data (10/24/12) | 62 |
| Figure 23: Speed-Space Distribution of Observed Lane Changes | 68 |
| Figure 24: Density Histograms of Observed Lane Change Data | 68 |
| Figure 25: Spatial Distribution of All Observed Lane Changes | 70 |
| Figure 26: Spatial PDF by Speed | 72 |
| Figure 27: Average Lane Change Position Given Exit Lane Speed | 73 |
| Figure 28: Cumulative Distribution Function of Lane Changes from Lane 5 to Lane 6 Given Exit Lane Speed | 75 |
| Figure 29: Bootstrap Best-Fit Gamma Distribution | 78 |
| Figure 30: Histogram of Number of LC Versus target Lane Speed (5mph bins) | 85 |
| Figure 31: PDF of Number of Lane Changes Conditioned by Speed (5 mph bins) | 87 |
| Figure 32: Target Lane Speed vs. Average Number of Lane Changes | 88 |
| Figure 33: Bootstrap Best-Fit Poisson Distribution | 89 |
| Figure 34: Three-Dimensional and Two-Dimensional Contour Plots for Best Fit Model | 97 |
| Figure 35: Average Lane Change Position Predicted by Model (I-85) | 102 |
| Figure 36: Model Standard Deviation Lane Change Position Predicted by Model (I-85) | 103 |
| Figure 37: Observed (5/7/13) vs. Final Model | 105 |
| Figure 38: Observed (5/8/13) vs. Final Model | 107 |
| Figure 39: Observed (5/9/13) vs. Final Model | 109 |
| Figure 40: Average Lane Change Position | 113 |
| Figure 41: Standard Deviation of Lane Change Position | 113 |
| Figure 42: Three-Dimensional and Contour Plots for Best Fit Model (Spring- Buford Conn.) | 115 |

| | |
|---|-----|
| Figure 44: Spatial PDF of All Lane Changes from Lane 6 to Lane 5 (5/7/13 - 5/9/13) | 119 |
| Figure 45: Cumulative Distribution Function of Lane Changes from Lane 6 to Lane 5 | 120 |
| Figure 46: Types of Congestion Propagation | 126 |
| Figure 47: Lane-by-Lane VDS Speed in the Vicinity of the Ramps to I-285 WB | 128 |
| Figure 48: Disruptive Lane Change Progression Example (May 8, 2013) | 132 |
| Figure 49: Disruption Case Study 1 | 135 |
| Figure 50: Disruption Case Study 2 | 136 |
| Figure 51: Disruption Case Study 3 | 138 |
| Figure 52: Disruption Case Study 4 | 139 |
| Figure 53: Hybrid Speed Visualization | 144 |
| Figure 54: Regression Data Visualization | 145 |
| Figure 55: Disruption Regression Fit | 147 |
| Figure 56: Disruption Regression Residuals | 147 |
| Figure 57: Non-Disruption Regression Residuals | 150 |
| Figure 58: Fraction of Drivers with Peach Pass by Time of Day (I-85 Southbound 10/1/12) | 157 |
| Figure 59: Lane Distribution - Beginning of Corridor to End of Corridor (weekdays, October, 2012) | 163 |
| Figure 60: Misaligned General Purpose Detector | 166 |
| Figure 61: Lane Distribution - Beginning of Corridor to I-285 Eastbound (weekdays, October, 2012) | 167 |
| Figure 62: Lane Distribution - Beginning of Corridor to I-285 Westbound (weekdays, October, 2012) | 169 |
| Figure 63: HOT Usage Comparison | 172 |
| Figure 64: HOT Egress Counts by Location (weekdays, October 2012) | 173 |

| | |
|--|-----|
| Figure 65: HOT Egress Behavior (10/23/12) | 176 |
| Figure 66: Average HOT Egress Location (exiting to I-285 WB/EB) | 179 |
| Figure 67: Average HOT Egress Location Vs. Previous and Next Segment GP Speed | 181 |
| Figure 68: Best-Fit Model | 191 |
| Figure 69: Spatial Distribution of Last-Minute Lane Changes by Speed | 204 |
| Figure 70: Relationship between Ramp Lane Speed and Last-Minute Lane Changing | 204 |
| Figure 71: Three-Dimensional and Contour Plots for Best Fit Model With Inflection | 208 |

LIST OF SYMBOLS AND ABBREVIATIONS

| | |
|------|--------------------------------------|
| AIC | Akaike Information Criterion |
| BIC | Bayesian Information Criterion |
| GDOT | Georgia Department of Transportation |
| GP | General Purpose |
| HD | High Definition |
| HOT | High Occupancy Toll |
| HOV | High Occupancy Vehicle |
| PTZ | Pan-Tilt-Zoom |
| RFID | Radio Frequency Identification |
| SRTA | State Road and Tollway Authority |
| VDS | Vehicle Detection System |

SUMMARY

Proper management and design of highway facilities requires knowledge of how varying freeway conditions affect driver behavior. Understanding how congestion propagates throughout a network of freeways is an essential component of freeway design and congestion mitigation. Video data collected on the I-85 corridor in Atlanta are processed to analyze driver lane changing behavior on a macroscopic level and identify behavior that results in congestion propagation. The quality and quantity of data collected using state-of-the-art object tracking techniques is unprecedented, and can be used for other traffic flow studies in the future.

Lane change location data and ramp speed data are used to derive a macroscopic lane-changing model for vehicles changing lanes from a freeway through lane to an exit lane that leads to another freeway. The dissertation examines the relationship between the number of lane changes, the speed of the ramp lane (using tracked vehicle data), and the location upstream of the ramp split through statistical analyses. Results of the analyses indicate the number of lane changes is approximated by a non-homogeneous Poisson distribution, with a parameter which is a function of ramp lane speed and distance upstream of the off-ramp. Analyses indicate the number of lane changes exhibits a parabolic relationship with respect to the ramp lane speed, and the number of lane changes exhibits gamma-distributed relationship with respect to the distance upstream of the ramp. The parameters of the gamma distribution are a function of ramp lane speed. Data were collected from a secondary site, and fit to the model to provide an initial assessment of model validity and model transferability. A discussion regarding the role of

how other access points may affect the shape of the model is opened. The macroscopic lane changing model presented in this dissertation is best characterized as the development of generalized lane-changing relationships, and provides a starting point from which more complex corridor-level models can be developed.

This study also identifies an unusual car-following behavior exhibited by certain lane-changing drivers. Typically found when the ramp lanes are moving at slow speeds, some lane-changing drivers will slow down, causing a disruption in their initial lane. Several case studies are used to showcase certain aspects of such driver behavior. Regression analysis is used to analyze the predictability of upstream speed of the initial lane to indicate the lane-changing disruption is responsible for the lateral propagation of congestion upstream of the location of the disruption.

The lane choice of exiting vehicles is also studied. As speeds in the general purpose lanes decreases, exiting vehicles are more likely to wait longer to move into the exit ramp lanes, resulting in an increased lane changing density. Vehicle egress from a high-occupancy toll lane is studied, and the results indicate that general purpose lane speeds play a role in the exit location distribution for vehicles as they leave the HOT lane and move toward the exit.

Results from this study are expected to have the greatest impact on microscopic lane-change model validation. The data-driven macroscopic lane change model presented can be compared against simulation results to assess whether simulated drivers are behaving in a realistic manner. Additionally, results reinforce the importance of maintaining a certain speed on the roadway, as well as implications for design of freeway ramps and safety issues associated with congested freeway ramps. As data collection

technologies improve and data (from high-definition cameras) becomes increasingly available, this research provides the basis for the further development of larger and more elaborate lane-changing models.

CHAPTER 1: INTRODUCTION

The extension of off-ramp queues back onto the mainline of a freeway is arguably one of the leading causes of freeway mainline capacity drops. Previous research has shown that there is a relationship between off-ramp queues extending onto the exit lane on the mainline and discharge on the mainline (Cassidy, Annai, and Haigwood 2002). However, there has not been an in-depth analysis on why this occurs. Cassidy, Annai and Haigwood (2002) proposed that the capacity drop was due to drivers in the through lanes being unwilling to travel above a certain speed, while vehicles in the exit lane are in a stop-and-go state.

Lane changing and weaving are two of the least-understood aspects in the field of traffic flow theory. There are no models that adequately describe the conditions under which drivers make lane changes, or how those lane changes affect freeway operations. This is unfortunate because lane changing appears to be a leading cause for bottlenecks on freeways. Field data show that reserving a lane for carpools on congested freeways induces a smoothing effect that is characterized by significantly higher bottleneck discharge flows (capacities) in adjacent lanes (Cassidy, et al, 2008). The effect appears to arise because disruptive vehicle lane changing diminishes in the presence of a carpool lane. The effect is reproducible across days and freeway sites and was observed, without exception, in all cases tested (Cassidy, et al, 2008). Weaving patterns resulting from the presence of the carpool lane were favorable for increasing mainline throughput. However, given the right conditions, not all weaving activity in the presence of managed

lanes along the left side of the freeway can be expected to increase general purpose lane throughput.

A friction factor may exist along the boundary between two adjacent lanes when a speed differential exists between them. If drivers in the faster-moving lane anticipate that drivers in the slower-moving lane may move into their lane (i.e., in front of them), drivers in the faster-moving lane may leave larger reaction gaps between their vehicle and the vehicle in front of them to reduce the likelihood of collision. Again, the lower traffic density for a given speed would reduce traffic flow and lower the effective capacity of the roadway (Guin, Hunter, and Guensler, 2008).

Weaving may constitute the only source of congestion in managed lane facilities, such as high-occupancy toll (HOT) lanes, which are becoming increasingly popular in the United States as cities search for ways to manage freeway congestion and provide reliable travel options. Drivers moving from the managed lane to a downstream exit may create additional constraints on mainline discharge, especially if there is a queue on the off-ramp. Only a thorough understanding of the driver behavior mechanisms at weaving sections will lead to proper modeling and ultimately the efficient management of these types of facilities.

Examining the findings of previous research will lay the groundwork for variables to consider in the development of a macroscopic lane changing model. Recent advances in traffic flow theory and the upcoming availability of high resolution empirical data make it possible to derive successful models. High-resolution data will be collected using state-of-the-art software to extract vehicle trajectories data from video streams, which has been developed by researchers at Georgia Tech.

The remainder of the introduction will introduce and describe the goals and objectives of this research, state the contribution this research provides in the transportation field, and outlines the remaining chapters of the dissertation.

Goals and Objectives

To accomplish the goals of this research project, six objectives have been identified. Each objective is discussed in detail its own section.

1. Identify road segment where off-ramp queues affect mainline throughput
2. Collect video footage, extract vehicle trajectories with in-house image-processing software, and extract lane change counts
3. Develop statistical relationships between the number of lane changes, target lane speed and distance upstream of ramp by analyzing processed video data
4. Examine potential causes of the lateral propagation of congestion and validate using regression analysis
5. Study the lane choice of exiting vehicles using Peach Pass data
6. Identify the next steps toward establishing a generalizable model that can account for complex corridor-level interactions

Identify Areas of Roadway Where Off-ramp Queues Affect Mainline Throughput

Using Peach Pass tag read data provided by the State Road and Tollway Authority (SRTA), Georgia Tech researchers assessed which weaving sections are most likely to have an impact on mainline flow. Video collected from pan-tilt-zoom (PTZ) cameras in the field and vehicle detection system (VDS) speed data already indicate that recurring bottlenecks arise in the vicinity of certain weaving sections. Observations from field video are supplemented with VDS speed data to locate sections of freeway where off-

ramp queues are impacting mainline flow. Examination of available video footage and VDS data provides sufficient evidence for establishing a case study analysis.

Collect Footage and Extract Vehicle Trajectories with Image-Processing Software

The main deterrent to assessing the impact of weaving on effective capacity in previous research has been the lack of vehicle trajectory data for weaving sections. As a consequence, existing traffic simulation models, including commercial software packages, are unable to replicate traffic dynamics in the vicinity of weaving sections. Unfortunately, current analytical tools and guidelines, e.g. the Highway Capacity Manual, rely on these models.

Another unique aspect of this research is inclusion of a larger quantity of data and more detailed data than has been available for most previous research. Due to the advances in image processing, vehicle position and speed data can be quickly and accurately extracted from camera recordings. The expectation is that larger quantities of data and better quality data will lead to more meaningful and robust models. Figure 1 shows the software actively tracking vehicles and the time-space trajectories that are generated from its output. Time-space trajectories are a graphical representation of a vehicle's position (y-axis) through time (x-axis). Each vehicle is represented by a line, as it passes through the time-space window of the video. Taking the derivative of a point along the line yields the speed of the vehicle. Thus, vehicle trajectories should always be moving forward in time and space to ensure the vehicle is always moving in the direction

of the freeway with speed greater than zero (the vehicle trajectory for a stopped vehicle is a horizontal line).



Figure 1: Recently Developed Tracking Software

Examine Effects of Off-ramp Queues on Mainline Flow

One of the main goals of this research will be to improve our understanding of the fundamental diagram of traffic flow by determining how queue formation and dissipation is correlated with lane-changing frequency and disruptions on other mainline lanes. Once data have been collected, they are analyzed to develop a model that represents the relationship between off-ramp speeds, distance from the off-ramp, and lane-changing frequency between mainline and ramp lanes. Results from the macroscopic lane changing model can be used to improve microscopic lane changing models (Laval and Leclercq, 2008).

Examine Potential Causes of Lateral Propagation of Congestion

Another goal of the research will be to study the progression of traffic states across lanes in the vicinity of the exit ramp and its queue. The presence of off-ramp queues is negatively correlated with mainline throughput (Cassidy, Annai, and

Haigwood, 2002). However, the mechanism that results in decreased flow has not been studied. In Figure 2, a driver has stopped to move into the jammed ramp lanes, resulting in the formation of a jammed traffic state in the rightmost through lane, and reducing the capacity of that lane. If we are better able to understand the causes of weaving behavior in the vicinity of off-ramp queues and estimate the impacts of weaving on the speed of other lanes, we will be better able to understand characteristics of traffic flow and better model potential traffic conditions on highways.



Figure 2: Disruptive Lane Change into Queued Off-ramp Lane

Study Vehicle Lane Choice

In October 2011, the Georgia Department of Transportation (GDOT) and Georgia State Road and Tollway Authority opened the high-occupancy toll (HOT) lanes on I-85 between I-285 and SR-316, providing a unique opportunity to study how vehicles move throughout the corridor. Availability of RFID data allows behavior of the subset of

vehicles with RFID toll tags (Peach Pass) to be studied (Guensler, et al, 2013). More specifically, the relationship between freeway speeds, lane choice, and weaving behavior of HOT drivers can be studied because RFID tag readers were placed not only in the managed lane, but at various locations in the general purpose lanes. Knowledge of this relationship can yield insight on the density of lane changes that occurs upstream of a ramp.

Contribution

Previous studies do not analyze multi-lane HOT-to-ramp weaving, and do not consider the mechanism by which off-ramp queues propagate to the mainline. In addition, the previous use of NGSIM data, the lack of large quantities of new data, and lack of more thorough validation techniques are all issues in current lane-changing model research. Since NGSIM datasets were generated in 2005, there are very few studies that rely on small amounts of empirical data to support results.

This research will use a large quantity of new data from freeways in Atlanta, Georgia to provide more insight about how off-ramp queues decrease mainline flow and a deeper understanding of how concentrated multi-lane weaving affects flow. If driver behavior can be better understood, congestion can be more accurately forecast and reducing congestion on the freeway system through better design.

This paper focuses on the factors that affect lane changing, as well as the relationships between lane changing on both the initial and target lanes. Many of the microscopic lane-changing models developed to date (discussed in the literature review) use a comparison of cumulative curves to compare the correctness of the model against

observation, and do not analyze spatial or speed properties of macroscopic lane-changing behavior for model validation.

Many of the interesting problems concerning lane changes revolve around weaving sections, where high-demand movements to freeway ramps result in large concentrations of lane changing. In this research, a freeway segment is selected where a high-demand for weaving is observed so that empirical analyses can be performed on different aspects of lane-changing activity. The lane changing activities that were analyzed include:

- Lane changes versus target lane speed
- Spatial distribution of lane changes
- Impacts of disruptive lane changes on the initial lane

Analysis reveals that lane changing activities are not as random as they may seem, especially on a macroscopic level.

Dissertation Outline

A review of relevant literature is outlined in Chapter 2. Previous research (Cassidy, Jang and Daganzo, 2001, Munoz and Daganzo, 2000) has indicated correlation between off-ramp congestion and mainline congestion. Furthermore, traffic states between lanes become more homogeneous further upstream of an offramp (Munoz and Daganzo, 2000). Thus, an investigation of the lateral propagation of congestion is warranted. Lane-changing activities are expected to play a role in the homogenization of lane-by-lane traffic states upstream of the congested off-ramp.

After the literature review, the dissertation describes the criteria for freeway site selection (Chapter 3), the data collection plan (Chapter 4), and the data processing techniques (Chapter 5) used to obtain the final analytical data used in this research.

A data-driven, macroscopic lane changing model for the corridor (Chapter 6) is based upon the analysis of lane change data from a through lane to a congested freeway ramp lane. Relationships between the location of lane changes, target lane speed and the intensity of lane changing are assessed in this model development process. Once the macroscopic lane changing model has been developed, the disruptive effects of the lane changes from the mainline through lane to the exit lane are analyzed and presented (Chapter 7). The disruptive behavior studied occurs at the same location and time as the data used to build the lane changing model.

The lane-changing model is only extensible between the mainline through lane and congested ramp lane over the observed length of the study corridor. Drivers making these lane changes are also making other lane changes in preparation to move into the exit lane further upstream of the location where they move into the exit lane. However, there is currently no way to track these drivers through the entire corridor and compare lane changing behavior of drivers with different destinations. The RFID tag-reader system, exclusive to the study corridor, can be used to estimate their origin and destination, and to some extent assess their lane choice behavior (the distance between general purpose lane tag readers ranges from 1.5 to 5 miles). Hence, there are some limitations to using the RFID data. Nevertheless, the study results and discussions (Chapter 8) lend further insight on driver lane choice behavior.

Chapter 9 outlines steps to be undertaken for future model development, and conclusions, discussion of the limitations of the current research, techniques for improving data quality, and directions for future research are presented in Chapter 10.

CHAPTER 2: LITERATURE REVIEW

According to the Highway Capacity Manual (2000), weaving is defined as the crossing of two or more traffic streams traveling in the same general direction along a significant length of highway without the aid of traffic control devices. The literature review will begin by describing the location of the corridor and its fundamental operation. This is followed by a review of academic research in the following areas related to the research objectives:

- Reasons why drivers weave
- Relationship between weaving and capacity
- How car-following behavior changes in the presence of weaving vehicles
- Lane-changing models
- Off-ramp bottlenecks

Corridor Description

The portion of the I-85 corridor converted from an HOV lane to an HOT lane is 14.3 miles long, stretching between I-285 and just past the SR-316 split north of Atlanta (Guensler, et al., 2013) (see Figure 3). Within the extents of the project corridor, a painted boundary exists between the managed lane and the general purpose lanes in both directions. For the majority of the HOT conversion corridor, lane changing is not allowed between the general purpose lanes and the carpool lane. However, there are several locations where drivers are allowed to enter and depart the managed lane. This lane boundary configuration is designed purposefully to increase capacity when weaving is not allowed, but also allows drivers to access the managed facility at certain locations. In its current configuration, there are ten legal weaving access points (five northbound, five southbound)

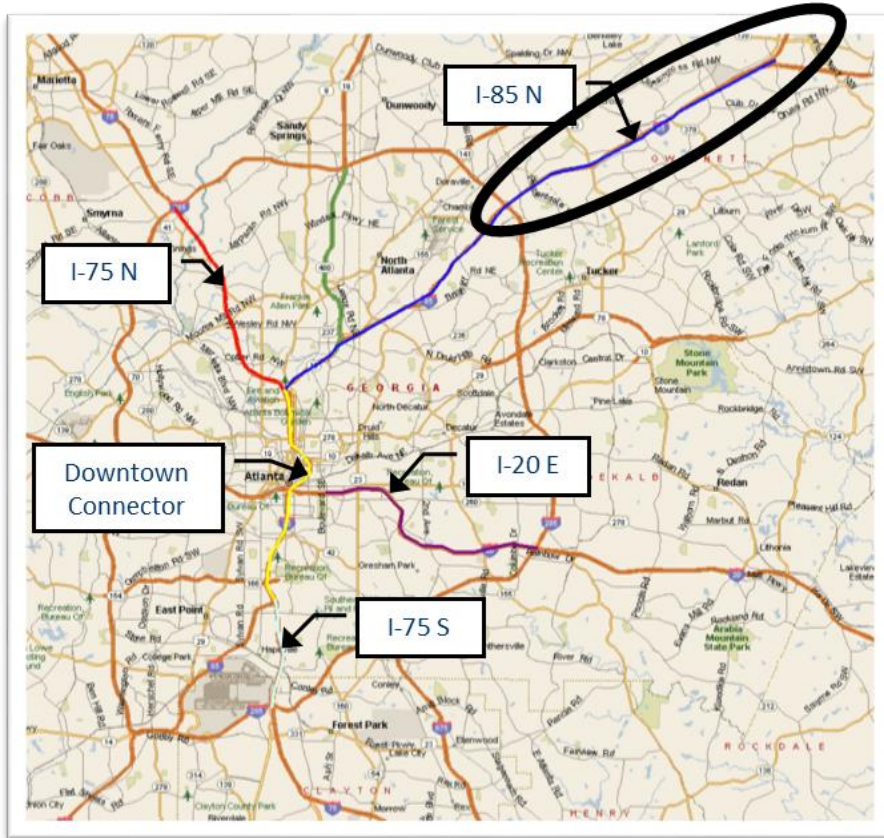


Figure 3: HOV/HOT Study Corridor

Between Chamblee-Tucker Road and the northern extents of the HOT corridor, 13 cross-streets and highways have access to I-85 via interchanges. To provide access to these cross-streets, there are 11 off-ramps and 10 on-ramps in the northbound direction, and 10 off-ramps and 11 on-ramps in the southbound direction. Because all of the exits are on the right-side of the roadway, overhead signs direct drivers in the managed lane when to leave the managed lane and begin moving over to reach an exit in time (except for the SR-316 left-hand direct access ramp for the managed lane users).

Reasons for Weaving

There are many reasons why drivers may choose to weave from lane to lane along the study corridor. Understanding why drivers make weaving decisions is useful in identifying which sections of freeway should be studied. In deciding whether or not to make a lane change, a driver must decide whether it is necessary to change lanes, whether changing lanes is desirable, and whether changing lanes is possible.

There are also several behavior factors that influence a driver's decision to change lanes. Among them are whether it is physically possible and safe to change lanes, the location of permanent obstructions, the presence of transit lines, the drivers intended turning movement, the presence of heavy vehicles, and speed (Gipps, 1986).

While Gipps' (1986) paper is focused more on lane-changing in an urban environment, a majority of the principles can also be applied to freeways. Transit lines are not generally an obstacle on freeways. Turning movements instead become entering and exiting the freeway at designated ramps. The presence of heavy vehicles, such as trucks and buses, is still relevant because they accelerate more slowly during stop-and-go conditions, and changing lanes to increase speed also remains relevant when projecting these principles onto a freeway setting.

A research study on uncongested freeway lane changing uses regression analysis to indicate that the distribution of headways and speed ratios, and density ratios most significantly affect lane changing behavior (Chang, 1990). Results of the Chang (1990) study are based off one hour of initial lane choice, test location entrance time, test location exit time, and lane change information collected from each of two sites in the Dallas-Fort Worth area. The fraction of vehicles changing lanes decreases as the average

headway increases, and as the ratio of flows between the initial lane and target lane increases, the fraction of vehicles changing lanes increases. Such behavior for preferred lane choice is of interest, although such findings may not be relevant in a mandatory, congested-flow lane changing situation.

Lane changes can further be broken down into three types: mandatory, preemptive, and discretionary (Gipps 1986).

Mandatory Lane Changing

There are several reasons as to why a driver may need to make a mandatory lane change. This happens in the case where the driver must change lanes to stay on his route (the case where if the lane change is not made, a driver will not be able to continue on his/her desired route), or if the current lane is closed ahead or if the current lane of travel drops and merges with an adjacent lane.

Preemptive Lane Changing

Preemptive lane changes describe a lane change that a driver makes to get into the correct lane in advance. The driver's motivation to change lanes is not as strong as a mandatory lane change or in the case of avoiding potential delay. Furthermore, preemptive lane changes can be broken down into four sub-cases.

- Low-density – both lanes in free-flow
- From a low to high density lane
 - e.g. HOT lane into congested traffic, or
 - uncongested through lane into a congested exit lane
- From a high to low density lane
 - e.g. congested traffic into less-congested HOT
- High density – no speed advantage

In the study area analyzed in this dissertation, there are instances where vehicles must merge across several lanes of traffic to exit, so they must start changing lanes in advance to make sure they have time to complete the maneuver. In some cases, the lane markings (that display where drivers are legally allowed to switch into and out of the managed lane cause multiple lane changes to be made in a short amount of time, resulting in drivers making more aggressive maneuvers to exit. The contrary is also true. There are locations where traffic entering the freeway from an on-ramp will make multiple lane changes to the left to enter the managed lane. Based on these facts, it is hypothesized that drivers making multiple lane changes to the right or left are making preemptive and mandatory maneuvers.

Discretionary Lane Changing

Discretionary lane changes are made to pass slower moving vehicles and reduce the driver's potential delay (Heng, et al, 2000). In the case of this study area, some drivers use the managed lane to pass slower drivers in the leftmost general purpose lane.

First-hand observations reveal this type of weaving is being done along sections of the freeway where weaving is legal and illegal.

The motive for different types of lane changes is also found in other studies (Ahmed, et al., 1996; Ben-Akiva, Choudhury, and Toledo, 2006). Because there are a wide variety of reasons for drivers to change lanes, it is expected that drivers will exhibit different types of behavior. Depending on the reason for changing lanes, the speed differential between any two lanes of a lane change may vary widely. It will be important to differentiate between lane changes made to a ramp (mandatory) and other lane changes (discretionary). It is expected that each of these types of lane changes may affect the effective capacity of the facility differently. An expected increase in the weaving intensity around the managed lane access points will provide an opportunity to measure and compare the effects of all types of weaving.

Relationship to Capacity

One factor that significantly affects effective capacity is lane changing. Capacity is affected in two fundamental ways. First, lane changing creates voids in the traffic stream of each lane; these voids reduce density of traffic for a given speed and thereby reduce the traffic flow (vehicles/lane/hour). When a driver makes a lane change, the following drivers in the target lane may have to slow down to avoid colliding with the lane-changing driver. Thus, a gap is created in front of the lane-changing driver, resulting in a temporary capacity drop. In addition, a lane change may leave gaps in the original lane. This lane change has the potential to cause following drivers to make subsequent

lane changes into newly created gaps, resulting in a further drop in capacity (Laval and Daganzo, 2005). The study considers freeway sections away from diverges, where the main incentive to change lanes is increasing speed. This dissertation focuses on interactions of vehicles making mandatory lane changes to an off-ramp, at times in the presence of off-ramp queues. The concept of capacity drops resulting from lane changes will be of interest when examining the causes of the lateral propagation of congestion.

In the case where an HOV lane is present (lane changes are restricted), the potential for reaching a higher capacity may exist (Laval and Daganzo, 2005). Also, the limited ability of vehicles to accelerate during stop-and-go waves creates voids and causes disruptive effects in the traffic stream (Laval and Daganzo, 2004). In the study, it will be important to differentiate between capacity drops that result from lane changing and capacity drops that occur due to acceleration limits or slow driver reaction time. It is expected that drivers making mandatory lane changes anticipate gaps created from slowly-accelerating drivers, or slow reaction times.

Theoretical analysis indicates that HOV lanes can affect the capacity of freeway bottlenecks through both an under-utilization effect and a disruption effect through lane changes (Menendez and Daganzo, 2006). However, empirical loop detector data suggests that the lane-changing effect of an HOV lane on the GP lanes should not be drastic, and its effect on capacity should be small. A simulation study (based on empirical data) was carried out to model how HOV lanes affect the performance of adjacent GP lanes and nearby bottlenecks. The results indicate that non-separated HOV facilities do not significantly affect the capacity of GP lanes and that if properly engineered they do not

hinder bottleneck outputs. Field tests are still needed to verify the results of the simulation (Menendez and Daganzo, 2006).

One major admission of the Menendez-Daganzo study is that an off-ramp diverge governed the flow of the freeway at the data collection location. Data from the bottleneck were not available to estimate the effect of the HOV lane on the bottleneck in the study. Empirical evidence from this study indicates that capacity did not drop at the beginning of the HOV restriction, when weaving is expected to increase. A drop to mainline speed is noticed when an off-ramp bottleneck propagates back through the system. However, the empirical evidence analysis does not mention the magnitude of weaving rates into or out of the HOV lane. Simulations built on data that do not consider a wide range of weaving intensities will not likely reproduce the effects of variable amounts of weaving, especially at high weaving intensities, when its effects on capacity are likely to arise. While the Menendez simulation may perform well on the segment analyzed, the results may be challenged under increased weaving intensities. In addition, the Menendez simulation only uses count and speed data from a single location, and does not consider all behavior exhibited between the HOV lane and the ramp. Observations from video data collected along Atlanta's managed lane freeways suggest that under the right conditions, HOT weaving sections do impact mainline flow.

Theoretical analysis compares the performance of multi-ramp freeways under two policy scenarios – an HOV scenario with an HOV lane and a general purpose scenario without one – fully recognizing storage effects (Daganzo and Cassidy, 2008). HOV lanes are effective with open-ended queues because the HOV lane space wasted by underutilization is compensated by uncongested freeway space available upstream – in

essence, the freeway can store the same number of vehicles in both scenarios. However, for closed-ended queues (ie. beltway), an underutilized HOV lane reduces the outflows that can be sustained with the same beltway accumulation. The effect is undesirable because it would extend the length of the congested period, negatively affecting all vehicles and lengthening on-ramp queues (Daganzo and Cassidy, 2008).

Complex traffic screams cannot be simply explained using the kinematic wave model applied with a triangular fundamental diagram, and are more accurately explained by a multilane hybrid theory that combines the kinematic wave model with discrete lane changes modeled as moving bottlenecks (Laval, Cassidy, and Daganzo, 2007). Traffic behavior at merges can be explained by the theory. A recurrent bottleneck, formed by a merge from a metered on-ramp, was used for collecting data for this study. Ten morning rush periods were observed, data from two dates were selected for analysis. Detailed traffic data (ramp queues and flow) were manually extracted from videos. Data examination reveals that capacity drop occurs simultaneously with an increase in lane-changing counts and shoulder lane vehicle accumulation. The simulation accurately predicts the cumulative count curves at all locations. However, discrepancies exist between the predicted and observed curves of shoulder lane accumulations and cumulative lane changes.

Modeling relationships between lane-changing and delay on the freeway, it was found that for every vehicle entering the traffic stream, vehicle delay increases from between 1.44 to 2.19 seconds, and vehicle delay is reduced by between 0.61 and 0.84 seconds for every vehicles that exits the traffic stream (Coifman, 2006). Because of the difference in delay caused by entering and exiting vehicles, it is not appropriate to use net

lane changes as a variable. Only 30 minutes of vehicle time-space data on a single-lane of a freeway just upstream of an off-ramp was used in the Coifman (2006) study.

Observations at upstream and downstream stations is estimated through simulation.

A friction factor between two lanes also affects the performance of adjacent lanes (Guin, Hunter, and Guensler, 2008). While the study only considers the relationship between traffic states on a limited-access managed lane and general purpose lane, it is expected the same principles will apply between general purpose lanes. As described, the friction factor only addresses speed differential safety concerns of drivers, and does not account for lane changing activity that may actually be responsible for the lateral propagation of congestion.

Effect of Weaving on Car-Following Behavior

When a driver makes a lane-change, there is a discontinuity between the traffic states in the initial and target lanes. Given the speed of the traffic stream in the target lane, the following distance of a lane-changing driver may be uncomfortably short compared to typical following behavior. Traffic competing for space in the weaving section will influence traffic flow in the upstream and downstream freeway lanes at the start and end of the weaving section (Sarvi, Eitemai, and Zavabeti, 2011). It is expected that a driver is willing to accept smaller-than-average spacing when making a lane-change in congested conditions.

The relaxation phenomenon was first observed by Smith (1985), who noted that vehicles changing lanes accept short spacing during the first 20 or 30 seconds, gradually attaining a more comfortable spacing. More recently, this was also observed in the

NGSIM dataset by Laval and Leclercq (2008), who also proposed a model for its simulation. This model was verified with additional data (Leclercq et al, 2008)

A macroscopic lane-changing model can be used to improve a microscopic lane-changing model. Laval and Leclercq (2008) use the macroscopic model developed by Laval and Daganzo (2006) to estimate lane changing rates as a function of initial and target lane density. Once the lane change is made, some drivers may increase the spacing between himself and the leading vehicle (by either slowing down or accelerating at a slower pace than the leading driver) until he is at a normal (comfortable) following distance (Laval and Leclercq, 2008). Oppositely, when there is a larger gap and a large speed differential between lanes, the lane changing driver may need to catch up to the leading driver in the target lane. In this case, the driver may increase his speed relative to the leading vehicle, decreasing the spacing until he reaches the equilibrium following distance.

Hidas (2005) found similar equilibrium following distance results while using the traffic simulator ARTEMiS, which was calibrated using microscopic characteristics of lane changes recorded from the field. Although the spacing of lane changing vehicles was accurately reproduced, the outputs of such a model will reflect the calibration and assumptions of the model. Other means of validating the model such as macroscopic speed-space relationships are used, but ideally, the model can be validated using additional lane change data.

Another study indicates that Newell's car following model is representative when lane changes are not present (Ma and Ahn, 2008). NGSIM data was used to conduct this research, from two sites for 45 minutes. Lane changing activities were grouped into

accelerators and non-accelerators, and accelerators were further categorized into discretionary and forced maneuvers. When the driver accelerates during the lane change, a linear regression analysis of the relationship between speed and spacing over the course of the lane change indicates that their following behavior deviates away from normal (Newell) behavior before returning back to the equilibrium relationship. Speed-spacing relationships between the mandatory and discretionary lane changes were not statistically significant. Non-accelerating vehicles exhibited large variations in speed-spacing relations. Because of the small sample size, it not known whether this variation is due to behavior differences between different types of lane-changing. In addition, anticipation and relaxation periods were estimated for the lane-changing vehicle, the initial following vehicle, and the new following vehicle. The anticipation and relaxation period for the following vehicle in the target lane is much longer than that of the lane-changing vehicle or the following vehicle in the initial lane. However, given that NGSIM data is limited, it is difficult that such a small dataset can lead to conclusive results.

Lane-Changing Models

Ahmed (1999) proposes that the decision to change lanes takes place in three steps. First, the decision to consider a lane change is made. Then a target lane is chosen based off that decision, and once an acceptable gap is available in the lane chosen, the lane change is made. The lane changing model structure is shown in the figure below.

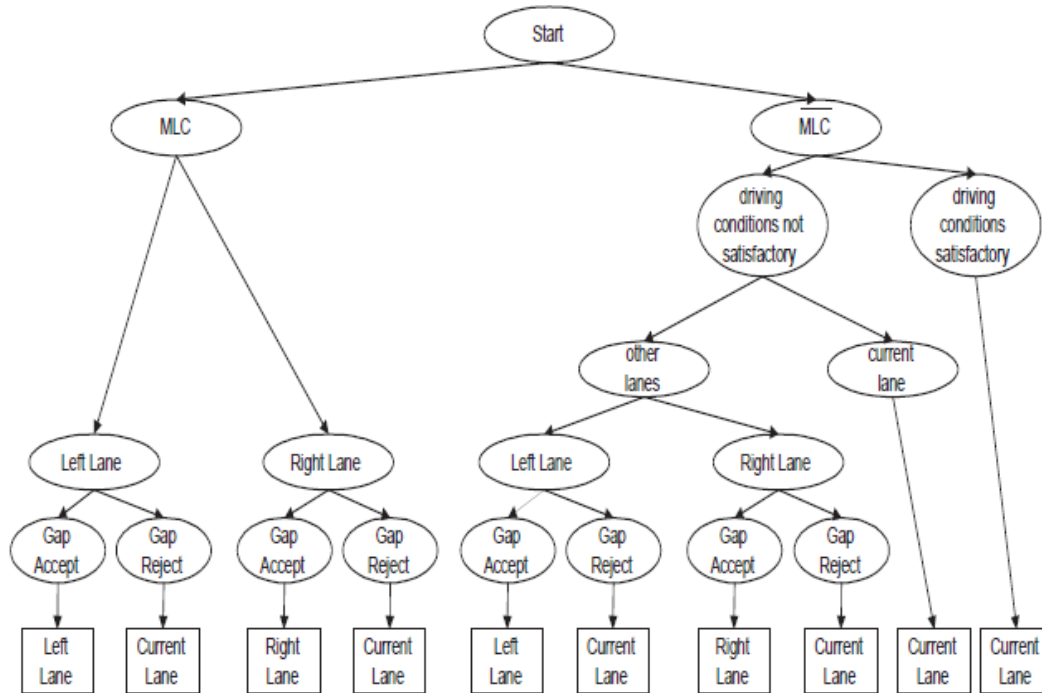


Figure 4: Lane Changing Model Structure (Ahmed, 1999)

The gap acceptance model recognizes that both the lead and lag gaps must be acceptable for a lane change to occur, and mandatory lane changes are expected to be more aggressive than discretionary lane changes. The model allows different parameters for each type of lane change.

When a vehicle makes a lane change, there may be a distinct reduction in spacing between its leader and follower vehicles in the target lane (Hidas, 2005) Using Newell's car-following model, this would cause all vehicles to decelerate urgently, resulting in a shock wave which propagates upstream. However, it is known that drivers are willing to accept closer spacing when they are able to anticipate the actions of other drivers. The relaxation period for increasing the spacing back to equilibrium takes 5 to 10 seconds (Hidas, 2005). Prevailing speed and spacing of a lane-changing vehicle's potential leader

and follower are used to assess lane change feasibility. Four hours of video data were analyzed over a length of 80-100 meters in an area where a large number of weaving maneuvers were expected. Microscopic details of 73 merging and weaving maneuvers were observed to separate them into one of three classifications: free, forced, and cooperative. Such a small sample may not be enough to capture variation in following behavior between drivers. A lane change is free if the relative gap between the leading and following vehicles in the target lane remains about the same before and after the lane change. A forced lane change is indicated by an increase in the spacing between leading and following vehicles in the target lane after the lane change is made. A cooperative lane change is characterized by the following vehicle in the target lane increasing its spacing to allow the lane-changing vehicle to move in front of it. The following figure shows simulated results for forced and cooperative lane changes.

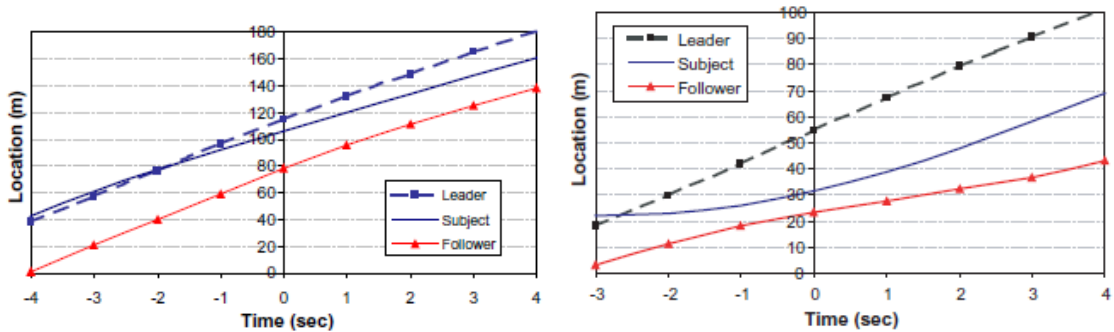


Figure 5: Time-Space Diagram for Forced and Cooperative of Lane Changes (Hidas, 2005)

The model reproduces observed behavior of individual vehicles in terms of speed, gap acceptance, and conflict resolution across all three types of lane change maneuvers. This is expected, as results of a model are expected to be a function of its input and

assumptions. Macroscopic results reveal that the speed-flow relationship is close to the expected average although further tests are needed to fine-tune the numerical parameters of the model. The car-following relationships presented by Hidas (2005) are a topic of interest for understanding the decision processes that are made by drivers under different lane changing conditions.

Many of the earlier lane-changing models only consider lanes adjacent to the current lane of travel for any vehicle and do not take in to account that a driver may wish to move over multiple lanes to reach his/her desired lane. A single driver in an HOV or HOT lane can often be observed making multiple lane changes between the managed lane to an exit ramp, especially if the managed lane offers a speed advantage. A study by Choudhury (2005) develops a framework for modeling lane-changing behavior in the presence of exclusive lanes, such as HOV and HOT lanes. The model consists selecting a target lane and gap acceptance, each of which is modeled by a random utility. An additional driver specific random term is also used to account for correlations between choices a driver makes. Lane choice is affected by speed and density of the target lane and other variables that relate to the path plan. Compared to previous lane-change models that only consider adjacent lanes for changing lanes, the proposed model performed better on the basis that it better predicts the number of lane changes and fraction of vehicles using the HOV lane. A few issues are present with regard to the data that was collected. First, detailed trajectory data from sites with exclusive lanes was not available. Another major issue with this study is that it does not account for the interaction between the lane-changing and acceleration behavior of the driver (Choudhury, 2005).

Toledo (2005) also explains sequences of lane changes (over multiple lanes) that occur which are not as well predicted using the earlier models. In this model, a likelihood function is generated to evaluate the desired target lane and gap acceptances. Results from this experiment indicate that the rightmost lane is undesirable, and that lanes to the left are more desirable. Lanes with higher average speed and lower densities were more likely to be chosen as the desired target lane. Gap acceptance models indicate that the relative speed between the lane-changing vehicle and the leading and following vehicles in the target lane correlate with the lead and lag critical gaps. The absolute speed of the subject does not significantly affect the critical gap, though more variability in speed data may lead to more conclusive results. Model validation tests indicate model improvements over previous models that only consider adjacent lanes in the lane-choice decision. The Toledo (2005) model uses over 20 variables to evaluate the target lane choice. In the presence of a high-demand off-ramp (on the right side of the freeway) and mandatory lane changes, the rightmost lane becomes very desirable, and a driver must balance the advantage of moving faster in the left lanes of a freeway against the disadvantage of making mandatory lane changes over a shorter distance. In addition, the use of so many variables may be over-fitting the data, leading to a model that may have a better fit at the expense of its transferability.

Menendez and Daganzo (2006) use empirical data to model the effects of HOV lanes on bottlenecks. One merit of this model is that it studies the interaction between the HOV lane and the general purpose lanes, mainly lane changes. In the case of lane changing between general purpose and HOV lanes, both a bound on the vehicle's acceleration and deceleration should be included, as opposed to the model proposed by

Laval (2007) which only includes acceleration in a more general lane-changing model. In addition, the Menendez-Daganzo model uses few parameters – the vehicles position is estimated by the car-following model which is constrained by safety, driver’s comfort, and the acceleration/deceleration capabilities of the vehicle. When a lane change is made, the driver comfort parameter is ignored. The simulation is time-discrete and continuous in space. Simulation results using ramp and mainline freeway volumes accurately describe discharge flows within 3 percent and lane changing rates within 4 percent (Menendez and Daganzo, 2006)

Lee (2008) extends the Menendez lane-changing model in his dissertation. The Menendez (2006) model was not designed for weaving sections and develops a model based on mandatory lane changes occurring in a certain area (a fixed cone). Lee instead uses a logit model mandatory lane changes in a given simulation interval, assuming that drivers independently re-evaluate traffic conditions at each time interval.

$$P_{MLC} = \frac{1}{1 + \exp(-\beta_0 - \beta_1 x_1 - \beta_2 x_2 - \beta_3 x_3)}$$

Each beta represents parameter estimates. x_1 is a proxy for the difference in densities between a driver’s current lane of travel and the right-most lane (exit lane) measured over a 100 meter stretch extending forward from the driver’s position. x_2 is the length of the weaving section divided by the driver’s remaining distance to the diverge. This allows the beta-parameter to be generalized across sites. x_3 is the number of lanes between the driver’s current lane and the exit lane. If a driver has decided to perform a mandatory lane change, and after a certain amount of time is not able to execute the lane

change, that driver will begin to slow down, or a vehicle in the target lane may co-operate with the lane changing-driver, to assist in the lane-changing process.

Lee collected video data from overpasses on two weaving sites and measured outflow and extracted time-space information for vehicles in the weaving lanes for a 60 minutes at one site and 80 minutes at the other site. The simulation model replicated the activation of the bottleneck, the changes in discharge flows, and the cumulative distributions of lane changes over space. The two weaving sites that Lee studied show that excessive freeway-to-ramp lane changes cause bottlenecks on the freeway. As the spatial distribution of freeway-to-ramp lane changes varies, so does the bottleneck flow rate. As more vehicles change lane closer to the off-ramp, the lower the flow rate. Traffic conditions in the auxiliary lane (typically generated by on-ramp flows) play a role in the spatial distribution of lane changes for freeway-to-ramp maneuvers. Given a limited of on-ramp flows studied, Lee found that disruptive lane changes during high ramp-to-freeway demand periods are correlated with a reduction in throughput.

However, off-ramp bottlenecks are not included as a part of Lee's study. In the following section, the correlation between off-ramp bottlenecks and freeway capacity is discussed. In addition, Lee's (2008) research focuses on a weaving section between ramps using an auxiliary lane for entering and exiting vehicles to share. In many cases of freeway-to-freeway ramps, ramp lanes are often a transition from mainline lanes when the previous freeway entrance point is far upstream. It is unknown whether a model such as this would correctly be able to estimate car-following and lane-changing behavior on such a section.

Off-ramp Bottlenecks

When off-ramp traffic backs up onto the mainline of a freeway, the mainline flow can be significantly affected. It has been observed that ramp backups are often correlated with lower flows on the freeway mainline, and when the bottleneck on the ramp is removed and the backup clears, mainline flows drastically increase (Cassidy, Annai, and Haigwood, 2002).

Flows in lanes adjacent to the off-ramp lanes gradually decrease after off-ramp queues begin to form (Munoz 2000). Count data and speed conditions were collected on I-880 before the I-238 off-ramp for a period of six hours in the afternoon peak. The queue propagated across all lanes over a 45 minute period, and the queue in the leftmost lane ends 2700 meters upstream of the off-ramp. All lanes upstream of this point exhibit similar traffic state characteristics. Evidence suggests that the location where the queue ends for each lane may be dependent on the number of lanes away it is from the exit lane. Other major findings indicate that a change in the changes in the freeway/off-ramp splits and volume can drastically affect mainline flow without any effect on the off-ramp (Munoz 2000). Upstream of the diverge, different lanes may exhibit queued and unqueued states (semi-congested). Weaving from an HOV lane in the vicinity of the off-ramp may also have interfered with the mainline discharge flow.

Off-ramp queues have been observed as sources of congestion for freeways. Given that most ramps are on the right side of the freeway, the mechanism by which ramp lane congestion propagates to other freeway lanes warrants further attention.

Literature Review Summary

Most of the research conducted to date has identified that one of the major problems is the lack of available data. Aside from a few studies that rely on small amounts of empirical data, there have not been many new empirical datasets since the NGSIM datasets were generated in 2005. Without adequate empirical data, it is difficult to conclude without any certainty whether or not any of the proposed models are representative or describe the effects of off-ramp queues accurately.

Though much of the literature made references to queues propagating into other lanes, the possible causes of this propagation are not considered. Literature that focuses on lane changing models does not assess the macroscopic effects of lane changing on the initial and target lanes (especially in the vicinity of an off-ramp). The cumulative count of lane changes is one metric used to verify output from some of the lane changing models. However, this metric is simply a function of following behavior and off-ramp demand/capacity. A more rigorous metric is needed to validate the result of lane changing models. While the count of lane changes is important, how those lane changes are distributed with respect to distance upstream of a ramp and the speed of the ramp lane should be considered. Elaboration on the macroscopic lane changing model could provide improvements to microscopic lane changing models, as evidenced by Laval and Lecelrcq (2008). There is also very limited work on the effects of HOT-to-ramp maneuvers, and the impact these drivers have on the mainline capacity.

Many of the ideas presented in previous research are noteworthy, and are definitely worth considering when determining how off-ramp queues affect mainline capacity, under what conditions drivers change lanes, and constructing macroscopic lane-

changing models. This research will address some of the data needs of previous research by collecting a large amount of data required to assess statistical relationships. A majority of the papers consider off-ramps that lead to non-freeway roads (i.e., an off-ramp with a traffic signal at its end). This may often lead to either a stopped or free-flow condition in the exit lane. Freeway-to-freeway ramps may allow more intermediate flow rates (between stopped or free-flow) to be attained, which would allow a more comprehensive study to be performed. Additionally, more lane changes are expected due to the high-demand nature of freeway-to-freeway ramps. Thus, it will be important to select a data collection site that exhibits intermediate flow rates and has high demand. The following section will outline further site selection criteria and identify sites that will be used for data collection.

CHAPTER 3 CASE STUDY SITE SELECTION

Current literature either uses NGSIM data, a large detailed vehicle trajectory dataset or small empirical datasets, which in many cases leads to limited or potentially non-extensible conclusions. A need has been identified for the collection of new large amounts of data. Research objectives include the formation of a macroscopic lane changing model, the causes of lateral propagation of congestion, and lane choice and lane changing behavior of exiting vehicles. For the purpose of establishing a lane change model, being able to monitor freeway speeds, lane changes, and other driver behavior will be necessary. Thus, selecting a site where these operational characteristics can be monitored will be of utmost importance. Equally as important is the availability of infrastructure to collect the data needed to produce adequate results.

First and foremost, a section of freeway was chosen where vehicles can be found weaving between the HOT lane and the general purpose lanes to exit at a downstream ramp. Queues from the ramp must back up onto the mainline of the freeway. A significant length of freeway is needed to monitor all of this activity. It is of interest to study the effects of weaving under both free-flow and congested conditions, as speed is expected to play a significant role in all research specified in the research objectives. Thus, sections of freeway with varying traffic conditions will be chosen. To identify impacts of weaving on traffic flow, it is important to note that the freeway section should be void of natural bottlenecks (i.e., queues building due to lane drops and unusual horizontal/vertical geometries).

As with many other locations along Atlanta's freeways, the PTZ cameras are all located along the southbound side of the freeway along the study corridor (Guensler, et al., 2013). Due to objects that occlude the view of the northbound side of the roadway, and the inability of the vehicle tracking software (described in chapter 5) to effectively handle these occlusions, only sites on the southbound side of the freeway will be considered.

Based on RFID readings from SRTA toll gantries, weaving is most intense between the weaving section south of Jimmy Carter Boulevard and the I-285 ramp in the southbound direction during the AM peak. This weaving is more intense than any other weaving section at any other time of day. Camera view availability also plays a role in determining which sections can be monitored – several GDOT PTZ cameras have views of the aforementioned weaving section.

Use of the I-85-southbound-to-I-285-westbound ramps is typically in high demand during the morning peak. Figure 7 shows the number of Peach Pass vehicles exiting the corridor in October 2012. According to SRTA Peach Pass data, up to 30 percent of traffic on the I-85 southbound Peach Pass drivers m exiting at this location. This typically results in queues forming from the off-ramp back onto the mainline. The duration and length of the queue is exacerbated due to congestion on I-285.

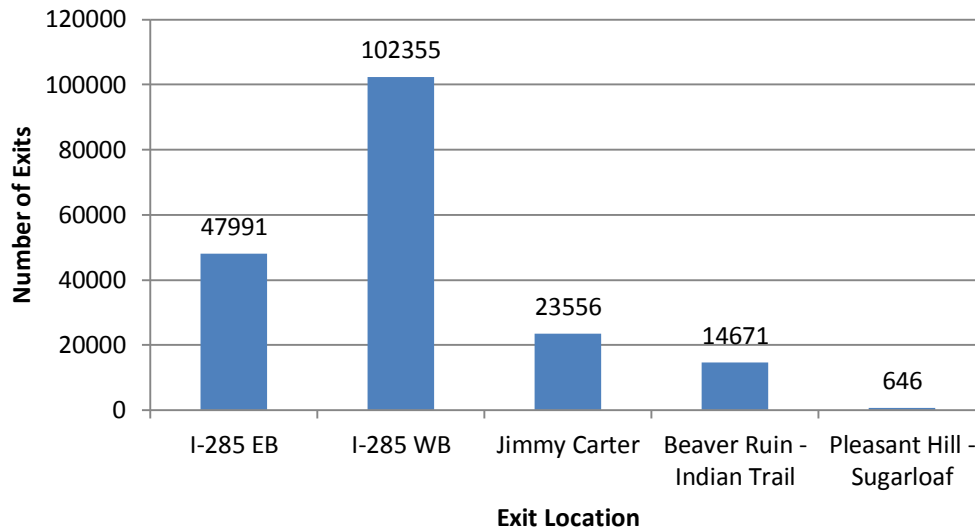


Figure 6: Number of Peach Pass Drivers Exiting I-85 Southbound (October 2012)

Site

The section of freeway monitored is the weaving section on I-85 southbound, south of Jimmy Carter Blvd to the I-285 ramps. The first reason why this segment was chosen is that the ramp to I-285 consistently backs up and causes queues to spill back onto the I-85 mainline. Also, there is a large number of weaving maneuvers observed between the HOT weaving section and the I-285 ramps. More cross-highway weaving maneuvers are seen at this segment than at any other segment on the corridor.

Of the 122,563 Peach Pass vehicles that enter the weaving section from the HOT lane in October 2012, 26,978 (32%) vehicles exit to I-285 westbound, accounting for at least 161,868 lane changes between the weaving section and the ramp. An additional 23,768 (19%) of the Peach Pass vehicles leave the HOT lane to continue past the I-285 westbound ramps, accounting for an additional 66,493 lane changes between the weaving

section and the ramp. These maneuvers are occurring predominately during weekday mornings, 6:00-10:00am.

The length of the weaving section is about 3000 feet, and the length between the beginning of the weaving section and the I-285 westbound ramp is 9000 feet. An advantage of this site is that it limits confounding factors. There is a low-demand exit ramp to Buford Highway just after the beginning of the ramp, and around 10 percent of the queued traffic remains on the mainline after the split. Other than these factors, there is no advantage to drivers being in one of the exit lanes over the other. Other factors that have the ability to majorly influence lane decision (such as a lane drop, other merging traffic, and high volume downstream exit ramps) are not present, and will not influence the results. A sitemap of the study area is shown in Figure 7. The sitemap shows overpasses, camera locations, and a sample of lane change and vehicle trajectory data captured from camera footage. Data collection and processing techniques are discussed in Chapters 4 and 5, respectively. Figure 8 shows a map of the site location.

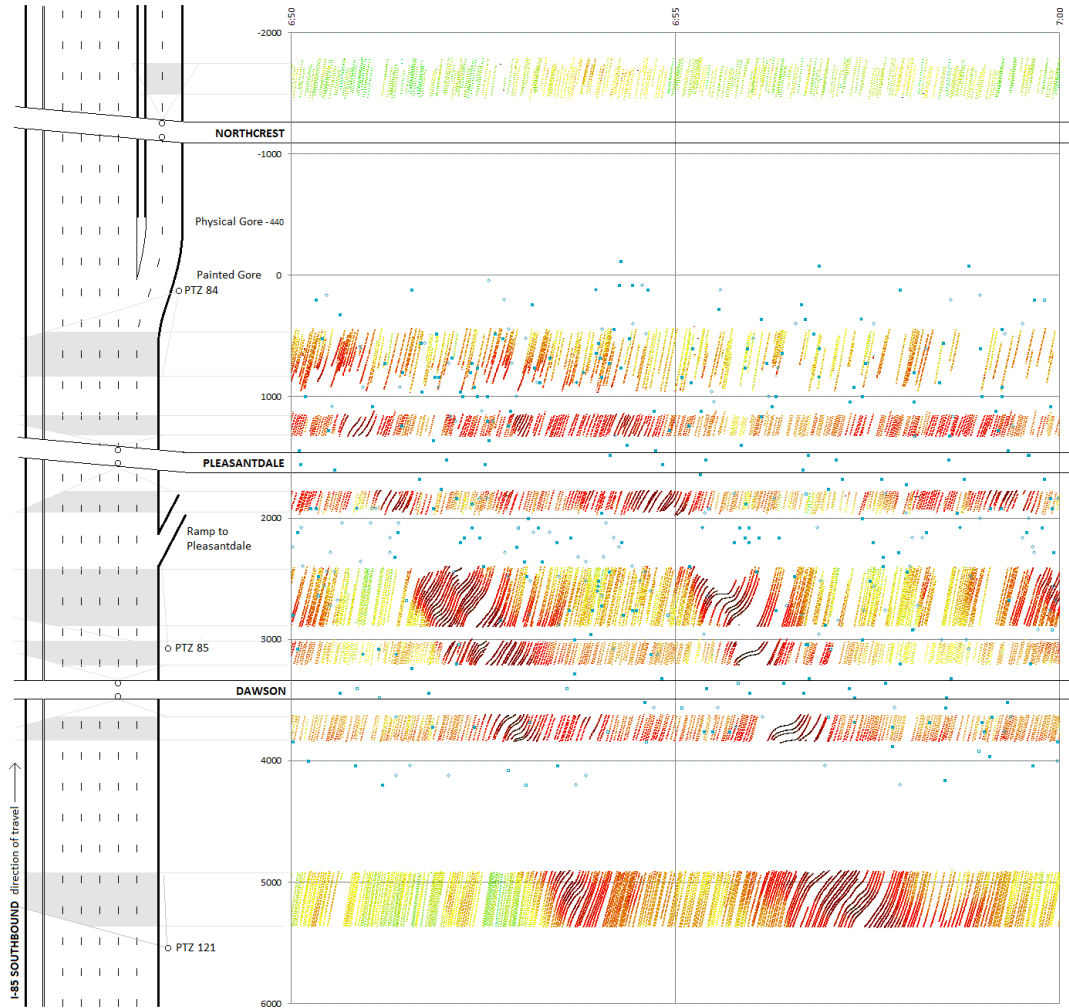


Figure 7: I-85 Site Map

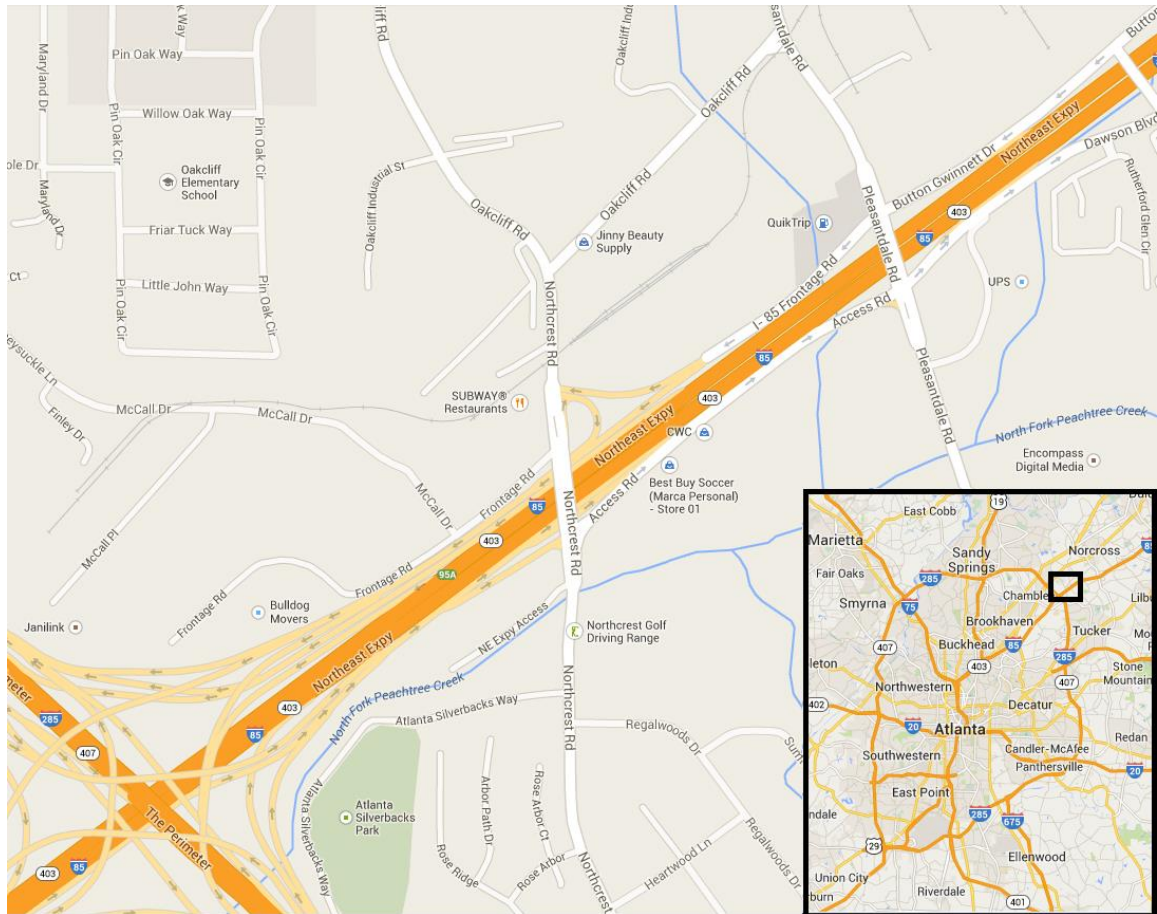


Figure 8: Site Location

In an effort to reproduce results at this site, a secondary data collection site, exhibiting similar characteristics as the I-85 site, was selected. A segment of the Buford-Spring Connector contains off-ramp queues that back up onto the mainline. This site is slightly different, in that it has only two lanes, and it has an on-ramp upstream of the ramp of interest. In later sections, the profound impacts this ramp has on the lane changing relationship will be discussed, although it does not significantly impact major findings of macroscopic lane-changing behavior researched in this paper. A site diagram

and location map of the Buford-Spring Connector site is provided in Figure 9 and Figure 10, respectively.

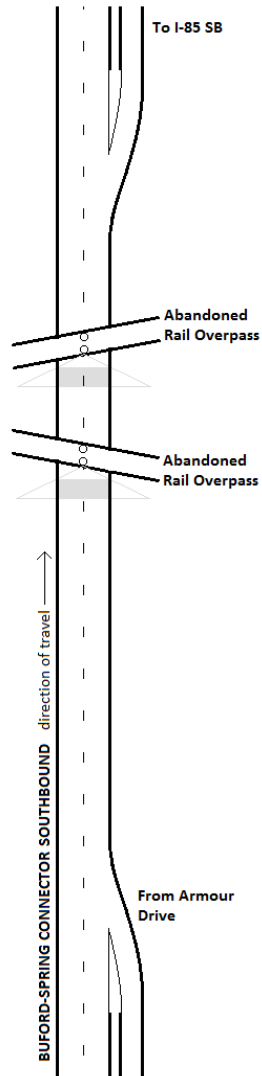


Figure 9: Buford Spring Connector Study Corridor

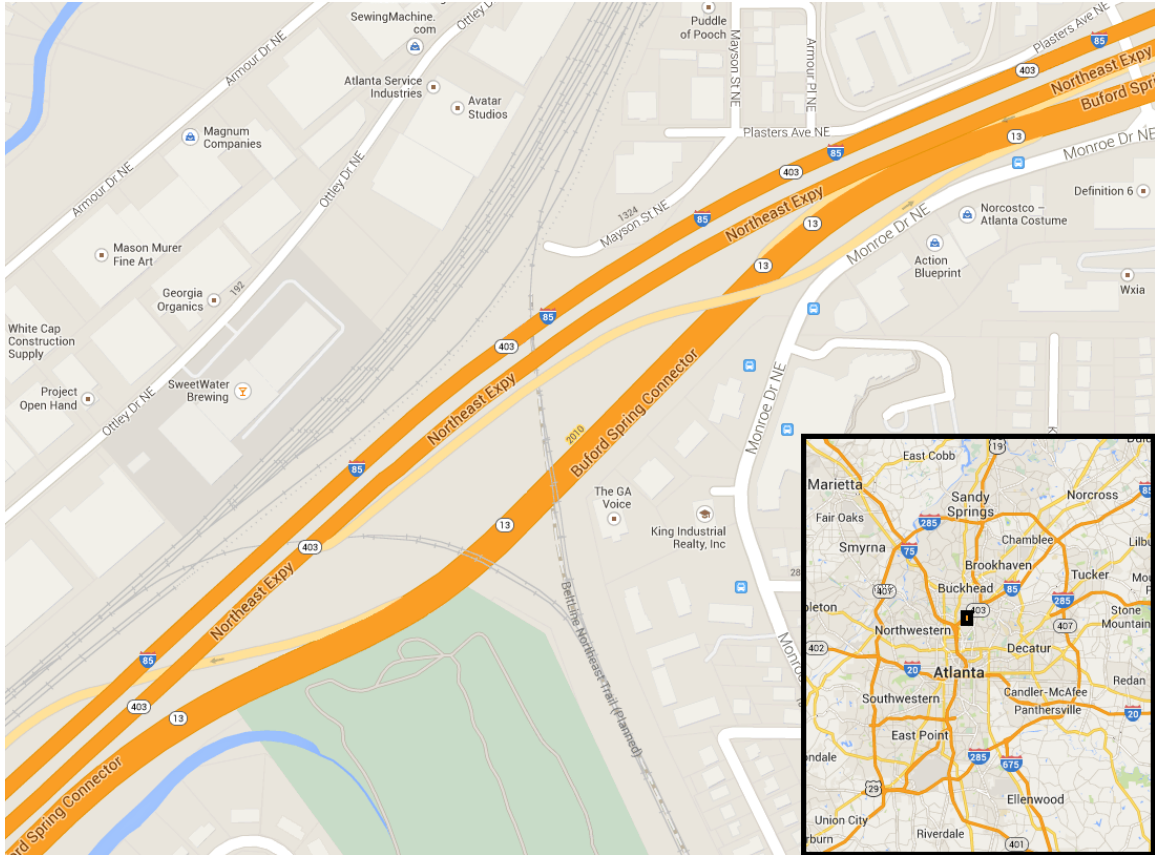


Figure 10: Site Location

Two sites, I-85 southbound upstream of the I-285 interchange, and the Buford-Spring Connector southbound upstream of the slip ramp to I-85 have been chosen as ideal sites to collect data to be used in the analysis. Both sites have overpasses for temporary video recording, and the I-85 site contains 3 PTZ cameras. Now that sites with ideal traffic conditions and ideal infrastructure to support video data collection have been identified, a methodology describing how video footage is collected and the type of data that can be extracted from the footage can be developed.

CHAPTER 4: DATA COLLECTION METHODOLOGY

Currently, there are no laser data or accurate in-road monitoring systems that can be used to collect individual vehicle speed and headway information. However, advances in computer video processing allow vehicle gaps and speeds to be extracted from a video recording (Park, 2012). A summary of the tracking method is discussed in a document provided by the developer in Appendix D. Utilization of automated tracking software is the preferred method for obtaining vehicle position and speed information. Using computer software is much less labor intensive, and will allow video data to be processed with relatively little effort.

Footage for capturing weaving events estimating speed was recorded using video cameras. From good quality video images, video processing software extracts time and space information of a subset of vehicles traveling through a camera's field of view. For this to work, the field of view must be calibrated (the scale of each pixel is a function of its angle and distance to the camera). Elevated views are preferred to avoid occlusion, and views from the side of the freeway are preferred to obtain more accurate vehicle position information. GDOT pan-tilt-zoom (PTZ) cameras located along the length of the corridor, spaced about one-third to one-half mile apart are the only elevated camera system for collecting video data. Video can also be taken from overpasses. However, overpass elevation is not as optimal for estimating speed over a long distance. Video taken from overpasses is more useful for flow and weaving counts.



Figure 11: PTZ Camera and General View

Because PTZ cameras currently installed in the field are low resolution (480x700 pixels), the length of freeway that can be analyzed with a single camera view is limited. The PTZ cameras are positioned on the side of the freeway, and in locations where the freeway has many lanes, the location of the camera can result in a narrow effective field of view. The cameras are located atop poles (approximately 75 feet in height), and provide good vertical and horizontal angles in the field of view for estimating vehicle speeds and observing disturbing lane changes over the short stretch each camera is able to monitor.

Ideally, the vehicle tracking software (described in Chapter 5) is only tracking objects represented by a minimum of 10x10 pixels. If the number of pixels representing the vehicle drops below about 100, the software may no longer be able to continue accurately tracking the selected object. This means that the lower the video resolution, the shorter the length of freeway that can be accurately analyzed. High definition cameras are preferred, but generally not available. A preliminary video analysis reveals that under optimal conditions, a single 480x700 pixel video can be used to measure vehicle gaps and

speeds for approximately 600 feet of freeway, depending on the camera height and angle. This is the area that can be covered while still ensuring that vehicles meet the minimum 10x10 pixel object size. If the camera is zoomed out, the coverage will be greater, but fewer pixels represent the vehicles in the traffic flow. Hence, as pixel scales increase, vehicle position error also increases. If the camera is zoomed in, vehicle position accuracy increases, but the amount of freeway can be monitored and analyzed decreases.

The efficient 600 foot measurement distance also assumes that vehicle occlusion does not occur. Occlusion occurs when a vehicle becomes partially or fully blocked by another physical object. Most commonly, objects that contribute to the greatest amount of occlusion include large overhead signs, or large trucks driving in lanes closest to the camera. The tracking algorithm is fairly robust, and will handle partial occlusion well, but will 'drop' vehicles that are fully or mostly occluded, resulting in a loss of data, or the inclusion of erroneous data. Other smaller objects, such as light poles or trucks not large enough to block views of other lanes can partially occlude vehicles from the camera view.

For this optimal view, the foreground edge of the camera lies around 300 feet (longitudinal) from the pole supporting the camera. Thus, given that each camera can view a maximum of 600 feet and are spaced between 1800 and 2600 feet apart, it is not possible to monitor more than one-third of the corridor at a time. The yellow circles in Figure 12 show the lengths of freeway that can be viewed by a single camera using an optimal view setting of 600 feet. This is the first limiting factor for finding locations suitable for data collection as the driver behavior on the segments that can be monitored

by the existing field cameras may not be representative of driver behavior throughout the complete length of the study section.

Approximate camera coverage for available camera views are shown in Figure 12. While it is possible to perform a study using several short unconnected segments, the results will not be as meaningful compared to a study where vehicles can be tracked through several camera frames. The inability to track individual vehicles as they move from camera to cameras through the corridor will present limitations for performing certain types of analysis for which long-distance vehicle tracking is necessary. Such barriers can be overcome with the use of properly-spaced high definition PTZ cameras, which are expected to track vehicles for approximately 1000' if mounted on similar infrastructure as existing PTZ cameras.

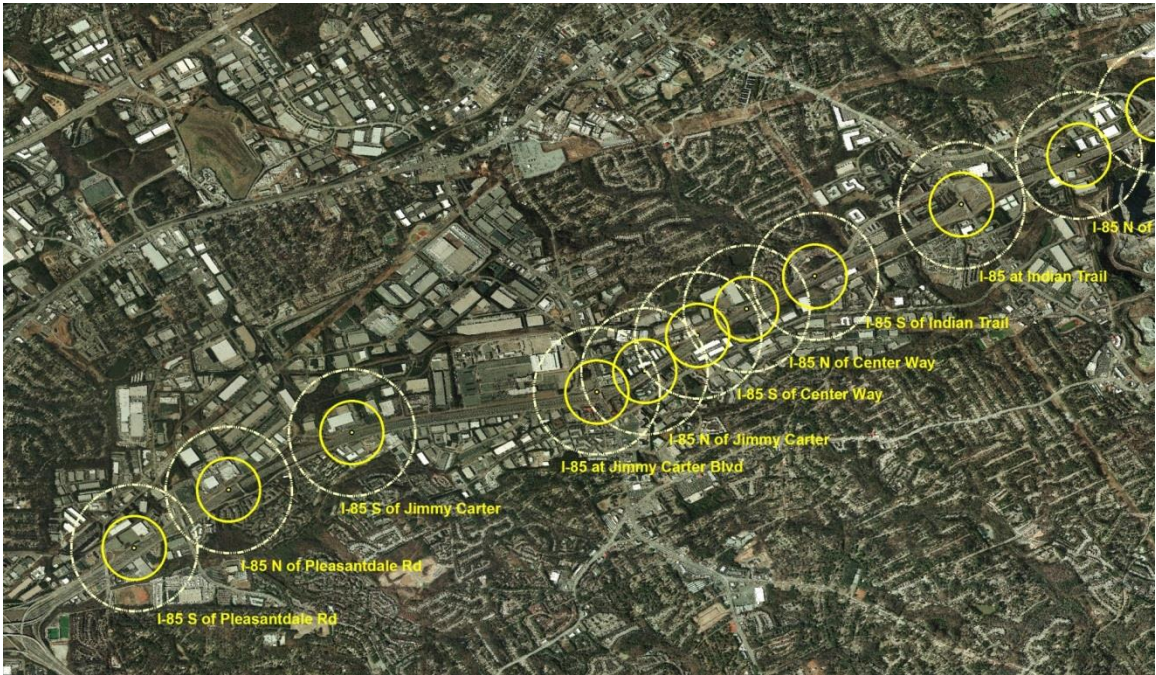


Figure 12: Camera Coverage on the Study Corridor

There are several overpasses where high-definition video cameras can be placed to collect volume and weaving count data. The increased resolution of the video image from these cameras allows a longer stretch of freeway to be analyzed. However, the fact that these locations are not as elevated as the PTZ cameras severely limits the increased data collection capabilities of these cameras. As discussed earlier, the amount of freeway that can be seen decreases as the camera elevation decreases, and the rate of occlusion increases. In the left-hand side of Figure 13 below, three highlighted vehicles in the second-right lane can easily be observed. Over the next several seconds, a semi-truck enters the camera view and occludes vehicles 2 and 3 completely from view. In this instance, vehicles 2 and 3 travelled less than 200 feet before they could no longer be tracked. Several seconds later, the semi-truck will occlude vehicle 1 from view as well.



Figure 13: Occlusion Example

From an overpass, however, the camera focuses directly linearly along the boundary between lanes. Overpass vantage points not only make lane changes easier to spot, but provide a longer field of view. However, this down-the-line view does not provide a sufficient angle for accurate measurement of vehicle headways. At smaller angles, the vehicles occlude each other, and the variability in vehicle depth as a function

of pixel distance increases, making vehicle longitudinal measurements much less accurate.

For counting weaves, the effective distance that can be accurately monitored by an elevated low resolution PTZ camera is around 600 feet (Figure 14), while the distance that can be accurately monitored from an overpass with HD camera is about 1000 feet (Figure 15). However, it is important to note that there are a limited number of overpasses along the I-85 corridor, constraining the locations where video data can be recorded. The distance between the Northcrest and Pleasantdale overpasses is 2350' and the distance between the Pleasantdale and Dawson overpasses is 1800'. Because the overpasses within the study site are a reasonable distance apart, high-definition cameras mounted on the overpasses should be able to monitor lane changes between the Northcrest, Pleasantdale, and Dawson overpasses. Additionally, lane changes can be monitored about 1000 feet upstream of the Dawson overpass (upstream-most overpass).



Figure 14: Side of Freeway View for Monitoring Lane Changes



Figure 15: Overpass View for Monitoring Lane Changes

Between the three PTZ cameras and overpass cameras upstream of the I-285 westbound ramp, vehicle trajectories can be extracted from approximately 2400 feet of freeway in the study area. Overpasses near the ramps to I-285 at Northcrest, Pleasantdale, and Dawson will be used to mount temporary HD cameras. Cameras mounted on these overpasses provide a total viewing area of about 4600 feet of freeway upstream of the physical gore of the off-ramp. Footage from these cameras was manually processed to obtain vehicle counts, lane-changing movements, and information about disruptions caused by drivers changing lanes into congested ramp lanes. Despite the low camera angle of overpass cameras, spacing of skip line striping is uniform enough to visually estimate vehicle position when lane changing is observed (discussed further in the data processing methodology chapter). Locations of the cameras and their respective camera viewing triangles are shown alongside the site map in Figure 7.

Final Camera View Selections

Because drivers may behave differently at different locations in response to different conditions, two sites with high-demand off-ramps were chosen. The first site is I-85 southbound and the ramp to I-285 westbound. The two-lane ramp at this site frequently backs up during the morning peak period, the through lanes downstream of the ramp remain in free flow, three overpasses cross the freeway between the ramp and 3200' upstream of the ramp, and there are 3 PTZ cameras up to 4800' upstream of the ramp. The second site is the Buford-Spring Connector southbound and the slip ramp to I-85 southbound. This single-lane exit ramp becomes congested during the afternoon peak period and has two abandoned rail overpasses just upstream of the ramp from where lane changes and speeds can be observed. No PTZ cameras exist along this stretch of highway. The location of the PTZ cameras and overpass-mounted cameras with respect to the I-85 and Spring-Buford corridors are shown in Figure 7 and Figure 9, respectively.

Table 1: List of Cameras Used for Data Collection

| | Camera | Location | Camera Direction |
|------------------------------|----------|------------------------|------------------|
| I-85 Site | PTZ 84 | I-85 S of Pleasantdale | N |
| | PTZ 85 | I-85 S of Pleasantdale | S |
| | PTZ 121 | I-85 S of Pleasantdale | S |
| | PTZ 86 | I-85 S of Jimmy Carter | N |
| | Overpass | Northcrest Overpass | S |
| | Overpass | Northcrest Overpass | N |
| | Overpass | Pleasantdale Overpass | S |
| | Overpass | Pleasantdale Overpass | N |
| | Overpass | Dawson Overpass | S |
| | Overpass | Dawson Overpass | N |
| Buford-Spring Connector Site | Overpass | Rail Overpass 1 | S |
| | Overpass | Rail Overpass 1 | N |
| | Overpass | Rail Overpass 2 | S |
| | Overpass | Rail Overpass 2 | N |

I-85 video was collected on February 28, May 7-9, 2013, and Buford-Spring video data was collected on October 23 and November 1, 2013. Because video for this part of the weaving study needs to be recorded from several cameras simultaneously, cameras need to remain in their designated positions for the data collected to be useful. However, the main purpose of PTZ cameras is for incident management, and from time-to-time, TMC staff members need to move PTZ cameras from the designated data collection position, resulting in less-than-ideal camera views. Protocols were developed for the movement of these cameras for data collection purposes.

Data Collection Protocols

Acquiring meaningful data requires a strategic coordination of recording periods and camera views. Working with the GDOT TMC is important, because camera views need to remain unchanged, and it will be of interest to link camera views together on certain parts of the corridor. As discussed earlier, the primary purpose of pan-tilt-zoom cameras used by GDOT TMC staff is for monitoring incidents and adverse traffic conditions throughout the corridor. Data collection via these cameras is considered a secondary priority. GDOT has allowed access of the cameras to the Georgia Tech research group for the purpose of moving cameras to collect data. Therefore, a set of protocols guide when cameras can be moved by Georgia Tech researchers so that movement will not interfere with the TMC's daily operations.

Protocols outlined in the Proposed Procedures for Changing TMC PTZ Camera Views during I-85 Video Data Collection Efforts (Appendix B) were followed for video data collection. TMC officials are notified of times, dates, and locations of data collection

efforts. The purpose of the notification is to reduce the chance that a camera view will be changed during video data collection for a non-incident related reason. In addition, Appendix B describes the procedures followed for moving camera views during video recording periods. A camera view will not be changed for the purpose of data collection when the camera is monitoring an incident or adverse traffic conditions, ten minutes after an incident or adverse traffic conditions have ended, or ten minutes after a camera has been moved by a TMC operator (i.e., cameras looking at a general view of the freeway).

The final data collection methodology involved a combination of PTZ cameras and overpass-mounted cameras for monitoring vehicles as they travel through the study corridor. The recordings were reviewed to extract important vehicle information such as speed, lane changing, and disruptive behavior. In the following chapter, the tools utilized to process the data are discussed.

CHAPTER 5: DATA COLLECTION AND PROCESSING

It is important to establish in advance the data and level of resolution required to properly analyze the impacts of lane-changing activity. Obtaining velocity and lane change information for a large subset of vehicles will be necessary for performing a thorough analysis. Data collection for this lane changing study was performed using high definition (1920x1080) video cameras temporarily mounted on overpasses and recording from permanent low-resolution (720x480) pole-mounted pan-tilt-zoom (PTZ) cameras. Recent advances in image processing allow vehicle trajectories to be extracted from an automatically detected subset of vehicles that pass through the camera's view (Palinginis et al., 2014). Such trajectory traces can be used to estimate speed. Also, a vehicle counting Android application was used to collect lane-by-lane count data from the recorded video. One benefit of using this app to collect volume data is that it allows the user to rewind the video and review counts, producing a more accurate result (Toth et. al., 2012). Lastly, lane changes are manually extracted from the video due to limitations of the image processing software. The manual identification of lane changes is a marked improvement in both detection and lane-change-location accuracy especially in the background of the image, where the pixel scale is greater.

Footage Selection

Analyzing second-by-second video data can be extremely time-consuming. Hence, it is important to select camera monitoring locations and times judiciously to ensure that the data are high quality and amenable for automated analysis. A variety of traffic conditions will be of interest for analysis. Thus, video of the study area that exhibit both free-flow and congested conditions over the course of the recording period will be needed. When examining free-flow operations, video data will have to be eliminated when queues spilling back from a downstream bottleneck on the mainline govern the flow observed in the camera view (i.e., when the capacity of the downstream bottleneck is lower than the capacity in the vicinity of the monitoring site). Because consistent driver behavior is needed to make relationships between weaving and capacity, videos containing certain conditions need to be eliminated from analysis. This includes footage collected in the absence of adverse weather conditions, low-lighting (before sunrise), and incidents that impact the flow of traffic. Future studies can explore operations under these conditions. In addition, as described earlier, the camera views can change at any time when TMC operators need to use them for incident management. Views that were disturbed to the point where meaningful data cannot be extracted will also need to be eliminated. Only footage when the camera is pointed toward the roadway is used. Footage was not processed when PTZ cameras were zoomed out by TMC operators (too few pixels to represent a vehicle) or pointed into the sun (difficult to accurately detect and track vehicles).

Vehicle Trajectories

Vehicle trajectories are extracted from the video using specialized software that track vehicle location in the field of view and transform the location on-screen into a real-world position. The tracking of the vehicles through the camera view was performed using the Gygax software developed at the Georgia Institute of Technology. Details regarding how this software works is provided in a description of the software written by the developer in Appendix D. This position can then be used to create a time-space trajectory for all vehicles that pass through the camera's view.

Useable footage is reformatted (mp4 or avi). Gygax, the vehicle tracking software, is now able to read the video, and can output time and space information for every vehicle that is detected through its automated process. The time-space data is post-processed to estimate each detected vehicle's speed. The post-process output is used to create a graphical representation of vehicle time-space data. Visual representation is useful; it easily allows the user to identify when a lane change occurs, and extract the appropriate gap and speed differential data for lane-changing vehicles. Time-space output of detected vehicles is shown in Figure 7 on the same scale as the site map. Coordinates are colored by estimated speed. From the image in Figure 7, it is also easy to see the length of freeway where time-space trajectories can be extracted is longer for the PTZ cameras than the overpass-mounted cameras – a result of more occlusion from the overpass cameras.

Verification of Image-Processing Software Data Output

Models can only be as good as the underlying data used in development. Without accurate data, it is not possible to produce a model that yields meaningful results. Given that image processing is a state-of-the-art method for extracting vehicle position, it was important to test the accuracy of the outputs.

As described previously, image processing software, Gygax is used to extract position information from every vehicle from each frame of a video recording. In the interest of creating the best possible weaving model, the accuracy of the position of these vehicles (with respect to each other) must be ensured. One of the most accurate means of obtaining vehicle position data is through laser detection. By coordinating camera views with laser gun data collection, a comparison can be made to verify the accuracy of extracted position data.

The laser gun used for data collection is the Range Finder manufactured by Laser Atlanta Optics – which measures the distance of objects with an accuracy of 6 inches. These measurements are taken approximately 77 times per second.

Next, a suitable site for taking measurements must be determined. First it must be in a location where there is PTZ camera coverage being recorded. In order to perform this test, PTZ camera footage was collected along I-85 at Beaver Ruin Road. Concurrently, from the Beaver Ruin Road overpass, a laser distance-measuring device was used to measure ground-truth positions of vehicles along the area of the freeway where the PTZ camera was focused. The clock on the laser gun was synchronized as closely as possible to the PTZ camera time so that it could more readily be compared to the video data. The data were collected near the end of the morning peak between 9:45 and 10:00am,

November 1, 2012. Conditions were sunny at the site, with the sun at an approximately 30 degree angle perpendicular to the direction of traffic. The shadows cast across lanes are not ideal for tracking. Additionally, the PTZ camera view was not optimal, having strayed from its pre-set ideal-for-tracking position. The particular site conditions, in combination with the camera angle should be a good test of the capabilities of the tracking software under non-optimal circumstances.



Figure 16: Vehicle Tracking Camera View

Traffic conditions were generally in free flow during the data collection period, with the exception of a single minute-long wave of congested traffic propagating through the observation area. Free-flow traffic is ideal for collecting laser gun data as occlusion tends to impact the continuity of measurement of leading vehicles at higher densities. More specifically, laser gun data can be collected from fewer vehicles at lower speeds due to the increased likelihood of occlusion.

Laser gun data were collected from the leftmost (HOT) and rightmost lane of the freeway for approximately equal amounts of time during the data collection period. It is of interest to make sure the tracking software is not biased with respect to the lateral position of the freeway.

Because the laser gun and tracking software produce speed readings at different frequencies, laser gun data will have to be interpolated between known time-space positions to test the accuracy of video processing results. A cubic spline effectively is able to interpolate the laser gun data (Grant, 1998). Interpolation results can be differentiated to estimate speed.

Despite non-ideal conditions for tracking, the software appears to provide reliable results. Speed comparisons were made on a frame-by-frame basis and by average vehicle speed in the camera coverage area. The frame-by-frame analysis indicates that 85% of speeds are within 5 mph of ground truth (Figure 17 and Figure 18). Furthermore, a direct comparison of the results produces a high degree of correlation, and the equation of the fit line indicates the two results are relatively unbiased. This is evidenced by a best-fit line slope of 1 and intercept of zero. Each vehicle's average speed is estimated over the duration it is tracked (typically 2-4 seconds). The average vehicle speed of the 45 tracked vehicles also appears to be unbiased, and the averaging of speeds provides a fit with even greater reliability. Approximately 60 percent of average vehicle speeds fall within 2 mph of ground truth, and all estimated average speeds fall within 4 mph of ground truth (Figure 19 and Figure 20). Figures showing the direct comparison of observed and expected values and cumulative distribution of errors are shown on the following page.

In the analysis, lane speed is estimated by averaging all observed vehicle speeds are averaged over a 30-second period, and the camera views are more ideal for tracking. Given an increased averaging period and ideal camera views, the tracking software should provide data reliable enough for estimating speed in the lane-changing analysis.

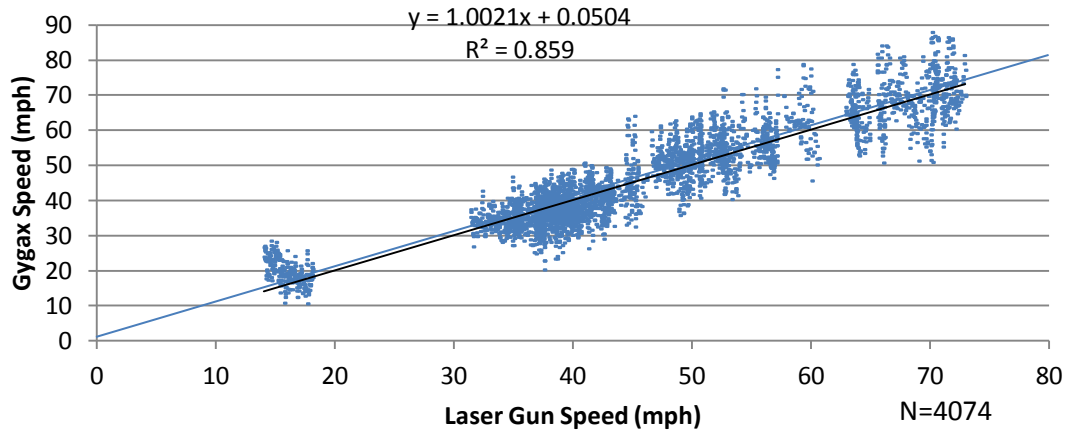


Figure 17: Frame-by-Frame Estimated Speed (Gygax) vs. Ground Truth Speed (Laser Gun)

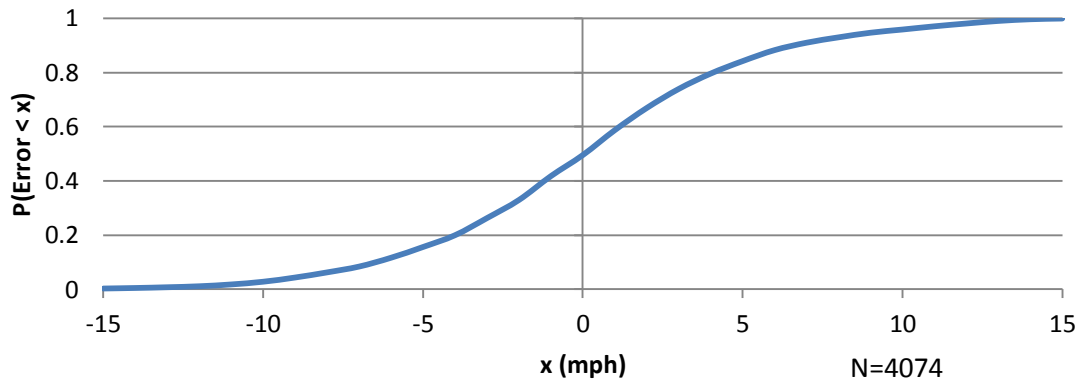


Figure 18: Cumulative Distribution of Frame-by-Frame Speed Error

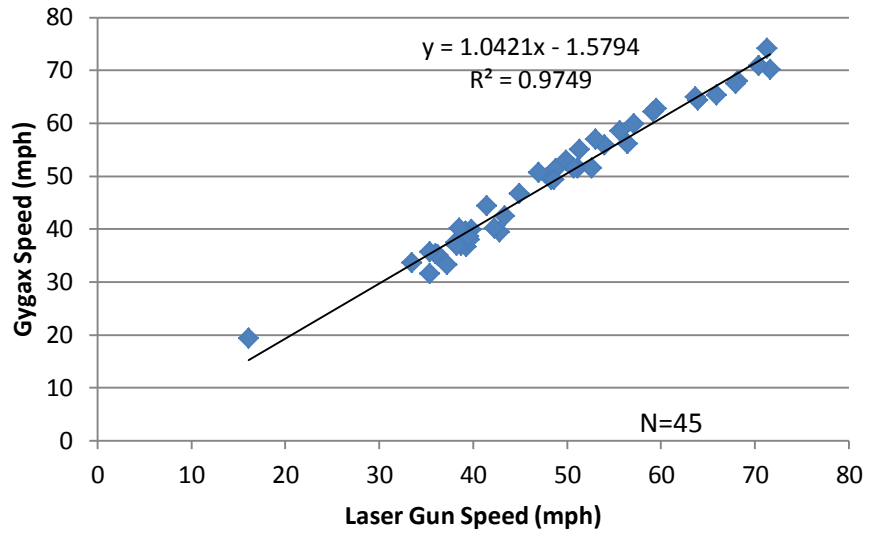


Figure 19: Vehicle-by-Vehicle Average Estimated Speed (Gygax) vs. Average Ground Truth Speed (Laser Gun)

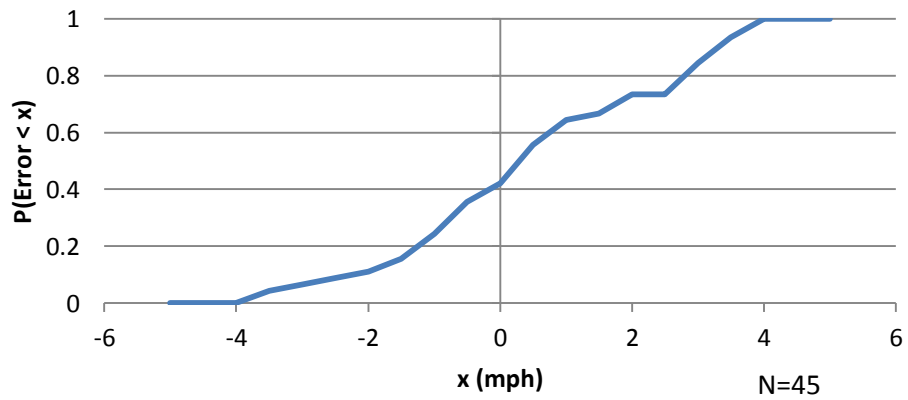


Figure 20: Cumulative Distribution of Vehicle-by-Vehicle Speed Error

Lane Change Counts

Lane change counts are manually extracted from footage taken from the overpass cameras. The surface of the freeway is not flat, and pixel scale does not vary uniformly from the foreground to the background of the image. Thus, using an automated method similar to the coordinate transformation used in the vehicle tracking software cannot be used. The lane change position is estimated by the skip-stripe location of the lane-changing vehicle's front wheel when it enters the traffic stream of the adjacent lane. Skip stripes are known to be placed in a uniform 10-30 pattern with little variance. When a lane change was observed, the time, location, initial and target lane were recorded.

At the time of initial data collection, the length of freeway beneath the overpasses could not be observed. However, because cameras are pointed off each side of the overpass, an indirect observation of lane changes was made by identifying vehicles went under the overpass in one lane, and re-emerged in the downstream camera view in a different lane. For these vehicles, the lane change location cannot be known for sure, because it was not directly observed. An illustration of the described occlusion is shown in Figure 21. In the figure, the vehicle leaves one camera view in lane 5, and is in lane 6 when it comes into the view of the camera on the opposite side of the overpass. The time-space coordinate of the lane change is currently estimated by randomly assigning a lane change position within the occluded range. Assuming the vehicle travels at a constant speed while occluded, the time the lane change is made is estimated by taking the time the vehicle becomes occluded, and adding an amount of time proportionate to the randomly assigned location divided by the entire occluded space.

$$LC_x = x_1 + U(0, 500) \quad \text{Equation 1: Occluded Lane Change Location Estimation}$$

$$LC_t = t_1 + \frac{dt(LC_x)}{500} \quad \text{Equation 2: Occluded Lane Change Time Estimation}$$

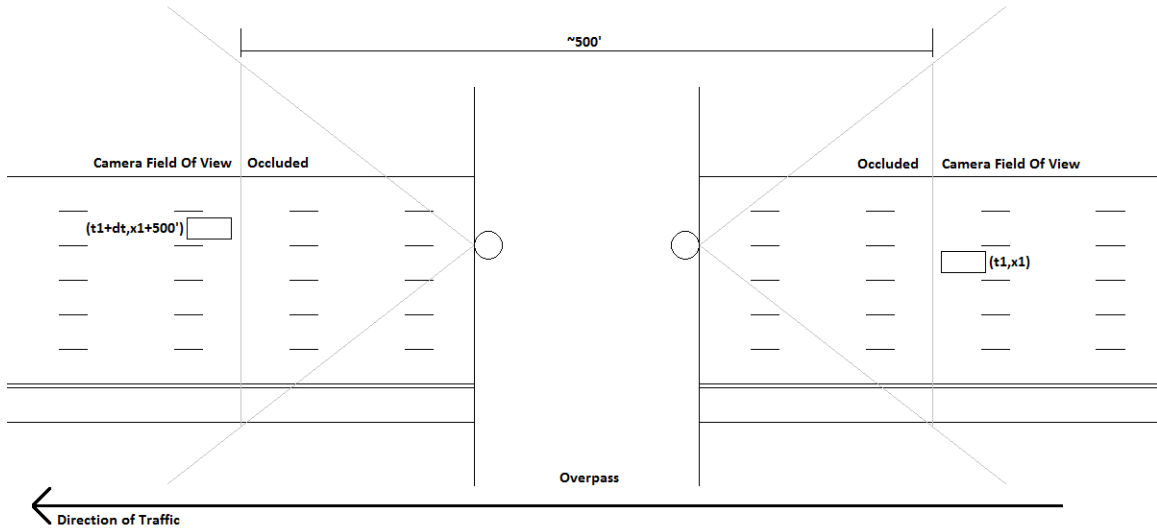


Figure 21: Underpass Occlusion

Lane Change Location Error Sensitivity

During the analysis of the data, it became apparent that certain locations in the field of view were more likely to be selected when it was difficult to ascertain in which location the lane change actually occurred. This inconsistency resulted in a few select sections containing higher numbers of lane changes, while neighboring sections containing fewer. As a result, the models fitted to this data often saw excessive error in the vicinity of the lane change locations that were more likely to be chosen. A review of the data indicated that there was a human bias in the selection of certain areas over others.

Processing of the video data required a manual identification and recording of lane changes. When the location of a lane change is partially occluded (by a larger

vehicle or another lane changing vehicle), it is not possible to tell with a high degree of confidence where the vehicle crosses the boundary between lanes. As described earlier, lane change locations are estimated by the number of skip stripes on the roadway upstream of the offramp. There are certain lane changes that occur close to the boundary of two skip-stripe locations, and the resolution of the video makes it difficult to distinguish which of the two potential locations should be selected. This is particularly true when the lane change occurs further away from the location of the camera. In situations where a lane change position had to be estimated, it was discovered upon review that locations that are a multiple of 5 skip stripes upstream of the offramp were more likely to be selected by the (human) video data processor, which created the bias.

Once the bias was identified, lane change locations were reviewed for accuracy, and the errors were corrected providing a much smoother spatial distribution of lane changes. While the shape of the resulting model did not change significantly after the bias was corrected, the error (used to validate the model) did. This shows that there is sensitivity in the data processing, and steps should be taken to avoid this type of data bias in the future.

Volume Counts

Footage from overpasses was used for the extraction of volume counts. The footage was imported into a vehicle counting app designed for Android tablets. The user is able to view the video and manually identify vehicles as they pass through detectors, also designated by the user. When a vehicle is detected, its lane and timestamp are recorded. One benefit of using this app is that it allows the user to play/pause the video and process the data at a reasonable pace (Toth et. al., 2012). The app also allows mistakes to be corrected, and allows the user to review previously processed video to assess the quality of the detections. Because of the added functionalities of this app compared to a traditional counting process, the counts are considered to be more accurate.

Peach Pass Tag Read Processing

SRTA provides a daily stream of Peach Pass tag reads from its gantries over the HOT and general purpose lanes (Guensler, et. al., 2013). Each Peach Pass has a unique identifier, which allows it to be tracked as it moves from gantry to gantry while in the system. The software assigns links for each given pair of gantries the vehicle travels between. A trip can now be described in terms of a link. This is repeated for trips made by all vehicles. Output from the software totals the number of trips between each pair of gantries, and can be joined to a GIS shapefile to graphically display the output. Each link is colored so that the reader can readily identify movements.

- Between general purpose lanes (blue)
- On the HOT lane (purple)

- Legal Weaving Maneuvers (green)
- Illegal Weaving Maneuvers (red)

In addition to displaying the number of movements on each link, the display utilizes symbology by increasing/decreasing link thickness to more easily identify links with many/few movements. A screenshot of a portion of the visualization is shown in Figure 22. These data are used to identify the lane distribution of Peach Pass vehicles, where heavy weaving occurs, and how weaving intensity changes over time.

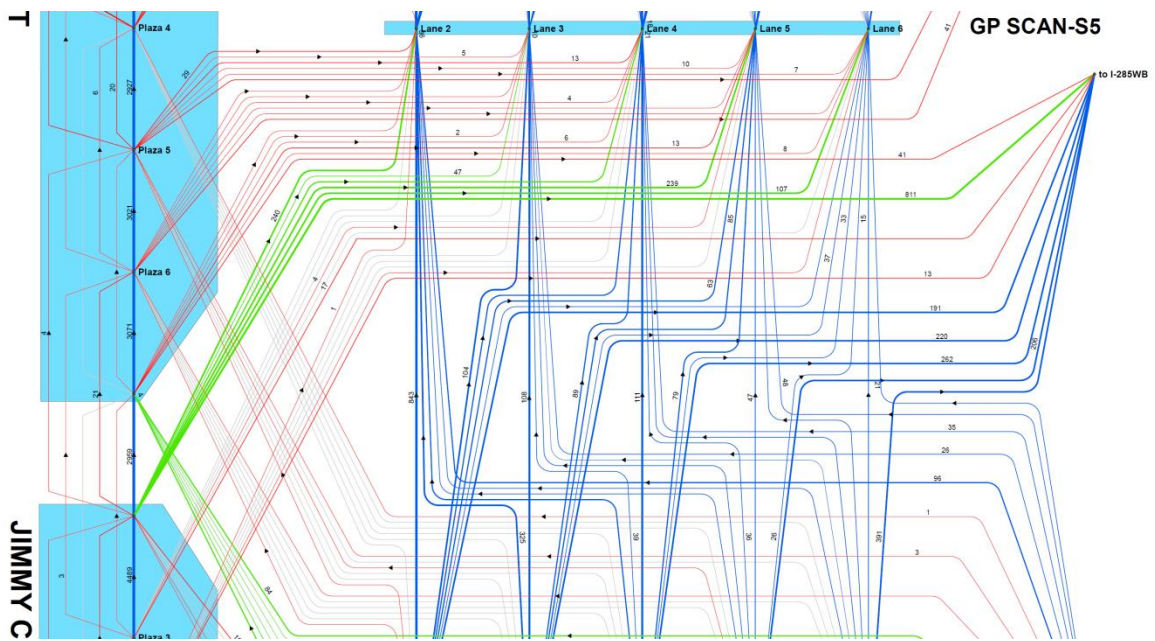


Figure 22: Partial Graphical Representation of Peach Pass Tag Read Data (10/24/12)

Video recorded from PTZ cameras in accordance with the data collection plan are each reviewed to ensure the camera was in its pre-set position. The remaining videos are again filtered only to include locations where the footage accurately represents different weaving characteristics along different parts of the study area over different times of the day.

Data Collection Summary

Video data were collected on three different days on I-85 upstream of the off-ramp to I-285 westbound, and two days on the Buford-Spring connector upstream of the slip ramp to I-85 southbound. While the start and end recording times for each camera are slightly different, there are times when all cameras were recording simultaneously. These times are listed in the table below, along with the number of lane changes and speed estimations made during each time period.

Table 2: Data Collection Summary

| | Date | 5/7/13 | 5/8/13 | 5/9/13 | 10/23/13 | 11/1/13 |
|------------------------------|------------|-------------------|-------------------|--------------------------|-------------------|-------------------|
| | Site | I-85 | I-85 | I-85 | Buford Spring | Buford Spring |
| | Time | 7:02-9:39am | 6:41-9:42am | 6:32-9:26am ^w | 3:26-5:45pm | 1:42-4:02pm |
| Lane Changes to Right | Lane 1→2 | 52 ^x | 68 ^x | 24 ^x | 814 ^y | 1415 ^y |
| | Lane 2→3 | 883 ^x | 1003 ^x | 401 ^x | - | - |
| | Lane 3→4 | 1456 ^x | 1721 ^x | 732 ^x | - | - |
| | Lane 4→5 | 1908 ^x | 2114 ^x | 914 ^x | - | - |
| | Lane 5→6 | 3639 ^y | 3958 ^y | 3644 ^y | - | - |
| | Lane 6→7 | 1557 | 1758 | 1761 | - | - |
| Lane Changes to Left | Lane 2→1 | 5 ^x | 2 ^x | 2 ^x | 334 | 586 |
| | Lane 3→2 | 550 ^x | 562 ^x | 318 ^x | - | - |
| | Lane 4→3 | 674 ^x | 778 ^x | 409 ^x | - | - |
| | Lane 5→4 | 644 ^x | 756 ^x | 427 ^x | - | - |
| | Lane 6→5 | 415 | 385 | 525 | - | - |
| | Lane 7→6 | 141 | 196 | 216 | - | - |
| | Total | 11,924 | 13,301 | 9373 | - | - |
| Speed Estimations (millions) | Lane 1 | 0.25 | 0.20 | 0.49 | 0.55 | 0.28 |
| | Lane 2 | 1.37 | 1.43 | 2.54 | 1.06 ^z | 0.80 ^z |
| | Lane 3 | 2.01 | 2.23 | 2.80 | - | - |
| | Lane 4 | 2.12 | 2.18 | 2.83 | - | - |
| | Lane 5 | 2.18 | 2.10 | 2.79 | - | - |
| | Lane 6 | 3.72 ^z | 3.03 ^z | 3.94 ^z | - | - |
| | Lane 7 | 4.08 | 2.99 | 3.81 | - | - |
| | Total | 15.72 | 14.16 | 19.21 | 1.61 | 1.08 |
| Disruption | N disrupt | 0 | 73 | 0 | 0 | 0 |
| | N t-x cord | 0 | 392 | 0 | 0 | 0 |

^w Video outage: Northcrest overpass HD camera, facing southbound, 8:25-8:48am

^x Lane changes not collected over entire study segment

^y Lane change data used in macroscopic lane changing model

^z Speed data used in macroscopic lane changing model

Table 3: Peach Pass Data Summary (October, 2012)

| | |
|-------------------------------------|------------|
| Number of weekdays of data | 20 |
| Estimated number of trips | 553,783 |
| Number of unique Peach Pass tags | 107,466 |
| Total number of tag reads processed | ~3,929,000 |

CHAPTER 6: MACROSCOPIC LANE CHANGING MODEL

An important relationship in macroscopic lane changing behavior is between the number of lane changes and the downstream speed of the target lane. From a theoretical standpoint, developing a relationship between the target lane speed and the number of lane changes is an important part of understanding the spatial distribution of traffic states in the initial and target lanes. Two factors come into play when a driver wants to make a lane change. First, the availability of gaps in the target lane must be considered. Each driver has a preferred minimum gap acceptance for making a lane changing maneuver at any given target lane speed (Gurupackiam and Jones, 2012). Thus, the distribution of gap sizes in the target lane is an important part of understanding the amount of opportunity available for lane changes to be made into the target lane. Second, the distribution of lane-changing gap acceptance preferences and the number of drivers demanding to make the lane change are essential in understanding which of the gaps available in the target lane can be filled via lane-changing maneuvers. The average gap size is directly related to the average density of traffic in the target lane.

Analogous to the fundamental diagram of traffic flow (relationship between maximum flow, density, and speed), there is an expected relationship between the number of lane changes at a given location and the speed and density of the target lane. Given that speed and density, and therefore gaps, are correlated during congested conditions, only the relationship between speed and the number of lane changes is studied in this paper. We do not have observed density or distribution of gap sizes, but speed should be sufficient for capturing the effects of these variables on a macroscopic scale.

Lane changes into a ramp lane are typically referred to as mandatory lane changes. Because the lane changes being studied are between a through lane and a choice lane, where drivers have a choice to stay on the mainline or exit, they are technically not mandatory. However, studies indicate that lane changes to the left and right are motivated by different incentives (Zheng, Suzuki, and Fujita, 2012). The behavior exhibited by these lane changing drivers, regardless of whether they intend to exit or not, is assumed to be mandatory, due to the fact they all must contend with the conditions of the congested exit lanes. From this point forward, all lane changes between the rightmost-through-only lane and the choice lane will be described as mandatory.

One of the most important factors that influences the number of lane changes that can occur into any one lane over a period of time is the speed of the target lane. At low target lane speeds, the average traffic density is very high, providing fewer opportunities for traffic in the initial lane to enter. The expected number and the maximum number of lane changes permitted into the target lanes decreases as the target lane speed decreases. As speed in the target lane increases, and density decreases, the distribution of available gaps in the target lane will change. Both the expected and maximum amount of lane changing is expected to increase. As speed of the target lane increases into the free-flow regime, it is expected that the amount of lane changing may become more variable, as the number of vehicle changing lanes is mostly dependent of the fraction of vehicles in the initial lane that must make a mandatory lane change to exit. While it may possible to achieve even higher lane changing rates as speeds increase, it is important to consider that target lane speeds may be correlated with initial lane speeds in the free-flow regime. While there are more opportunities for vehicles to make lane changes at higher exit lane

speeds, there are naturally lower volumes and less exit lane demand from the rightmost through lane (provided correlation between the initial lane and target lane speed).

Correlation between initial and target lane speed may also assist in explaining why the maximum amount of lane changing is expected to occur somewhere between a free-flow and stopped target lane state.

Preliminary Data Assessment

To estimate the speed of the target lane for a given lane change, the speed of vehicles at the downstream-most available point along a wave is used. Congested traffic states propagate upstream through the system at the wave speed. Thus, conditions experienced by lane changing drivers are expected to be the same for all drivers making a lane change into the same wave. Speeds (traffic states) between downstream and upstream locations were most highly correlated when using a wave speed of 14 mph; a typical, if not slightly below average wave speed. The speed of traffic closest to the lane change is not used because it is believed that other lane changes may cause irregularities in following behavior, influencing the speed of the traffic state in the wave. Figure 23 shows the unprocessed relationship between the location and target lane speed for each lane change. Figure 24 rasterizes the data, showing that more lane changes were observed at speeds between 30 and 40 mph and locations 1000 to 2000 feet upstream of the ramp. The data in this format do not take into account the observation frequency of each ramp speed. Data in disaggregated form do not provide many clues as to the underlying distribution from which the data is derived. The following sections in this chapter will discuss the relationship between speed and the spatial distribution of lane changes as well

as the relationship between speed and the number of lane changes, to formulate a relationship between all three variables. The spatial relationship of lane changes from the exit lane to the mainline through lanes is briefly discussed at the end of the chapter.

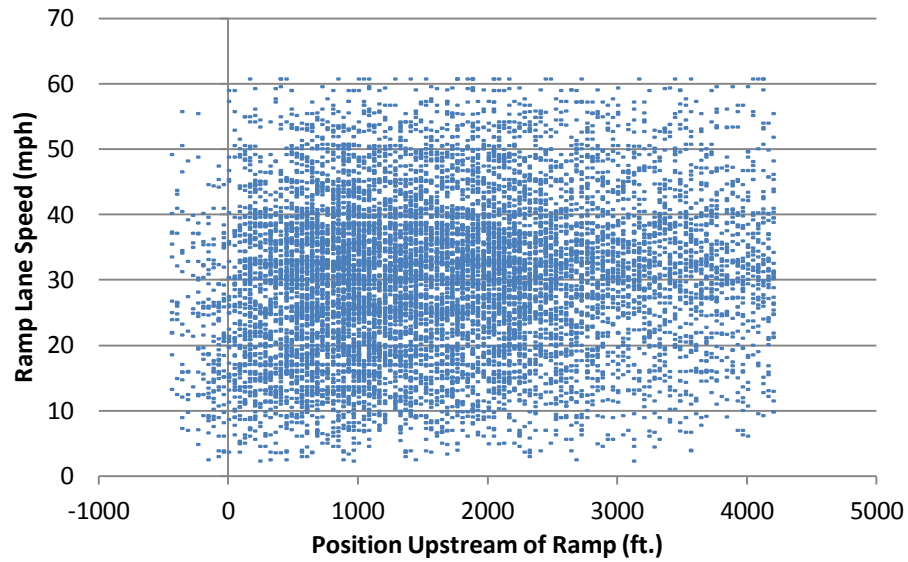


Figure 23: Speed-Space Distribution of Observed Lane Changes

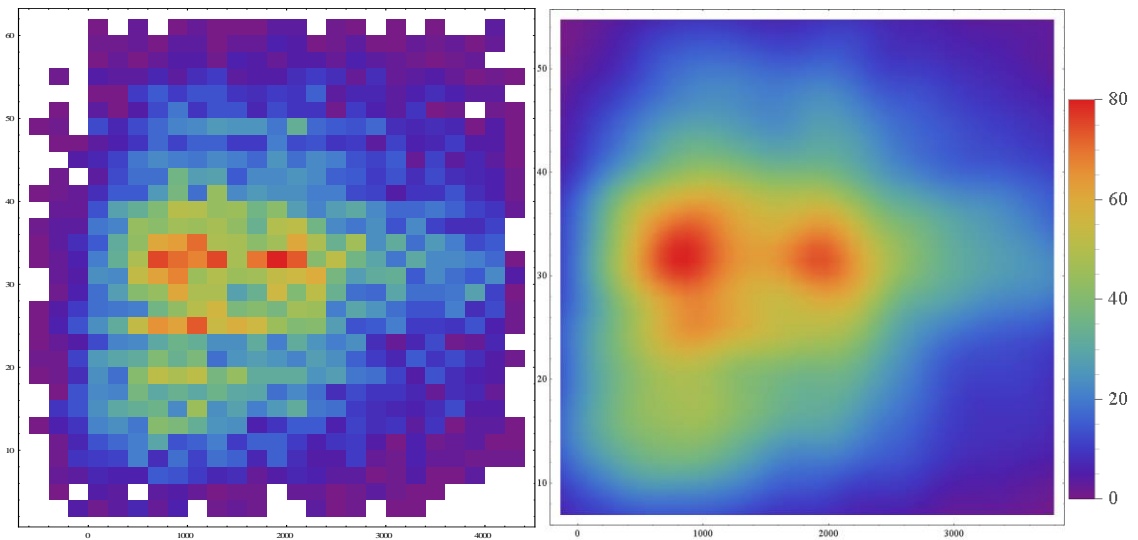


Figure 24: Density Histograms of Observed Lane Change Data

Spatial Distribution of Lane Changes

The spatial distribution of lane changes is an important part of macroscopic lane changing theory. An understanding of the factors that influence the location where a driver will change lanes will assist in improving freeway design and allows for the development of a metric against which to compare the macroscopic results of microscopic lane-changing models. On an individual level, the occurrence of lane changes appears disorderly, but aggregating by location, patterns begin to emerge. In addition, the speed of the target lane in which lane changes occur will be considered as an aggregation variable.

The spatial distribution of all lane changes into a ramp lane, upstream of the ramp split from the mainline, follows a fairly orderly pattern. Close to the physical barrier, the number of lane changes into the ramp lane is quite small. Moving upstream from the ramp, the number of lane changes observed increases dramatically, until about 1200 feet upstream of the ramp. Upstream of this point, the number of lane changes slowly decreases. The described spatial distribution of lane changes is shown on the following page in Figure 25. Upon observation, the shape of the distribution resembles a gamma distribution. As mentioned in the data collection section, lane changes that occurred under two overpasses upstream of the ramp were occluded, and an indirect observation was made and the lane change was assigned beneath the ramp. The time and location of these lane changes was estimated, resulting in some uncertainty regarding the shape of the distribution under the overpasses.

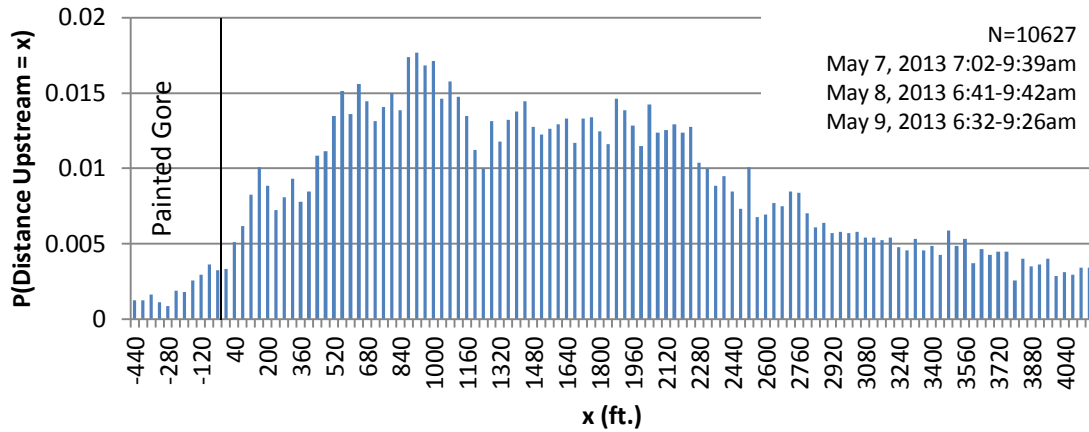


Figure 25: Spatial Distribution of All Observed Lane Changes

The speed of traffic upstream in the ramp lane is expected to play an important role in the distribution of lane changes. The logic behind this hypothesis stems from the fact that fewer gaps are available when the ramp lane is at lower speeds. This means that as ramp lane speeds decrease, the number of lane changes is expected to decrease. More importantly, fewer available gaps are more likely to be filled at a position further downstream, closer to the origin of the wave, resulting in the closure of gaps in the ramp lane further upstream. Thus, it will be important to make sure the analysis of spatial distributions of lane changes from the mainline into the ramp lane is conducted across different speed cutpoints.

Figure 26 on the following page shows the spatial distributions of lane changes aggregated by speed of the ramp lane in 10 mph bins. As the ramp speed increases, the average and median of the lane change location appear to move further upstream of the off-ramp. Table 4 presents the average and median lane change position for each of the 10 mph bins. Confidence intervals on the average lane change location are displayed in

Figure 27. Given that a lane change occurs within the study section, an assessment of the descriptive statistics of the lane change data indicates that the average and median lane change position is closer to the ramp at lower speeds and further away from the ramp at higher speeds.

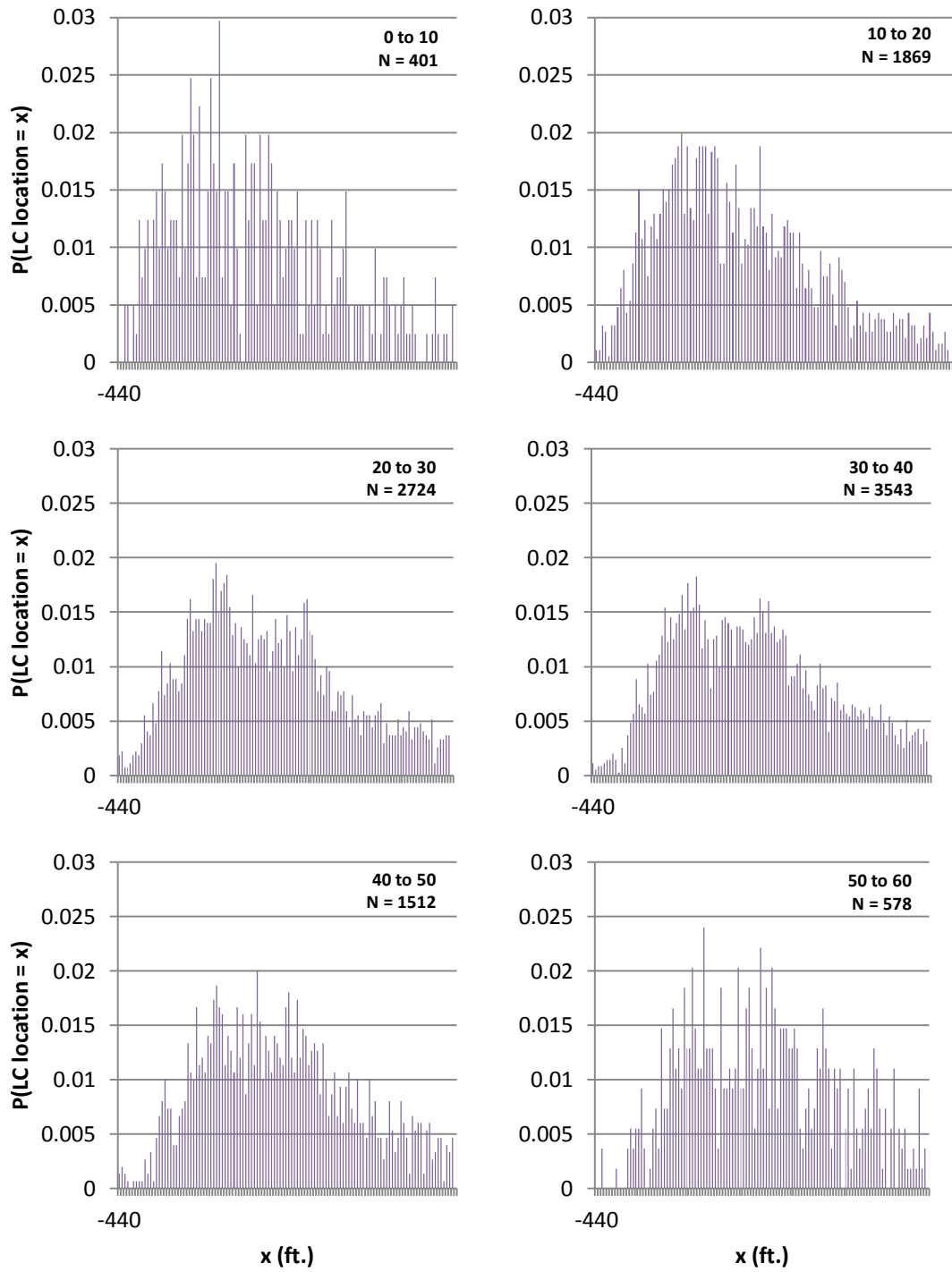


Figure 26: Spatial PDF by Speed

Table 4: Statistical Summary of Lane Change Position

| | 0to10 | 10to20 | 20to30 | 30to40 | 40to50 | 50to60 | All |
|---------------|-------|--------|--------|--------|--------|--------|-------|
| Average | 1867 | 1918 | 2130 | 2227 | 2283 | 2370 | 2150 |
| 95% median | 104.8 | 46.8 | 39.6 | 34.5 | 52.5 | 85.7 | 20.1 |
| N | 401 | 1869 | 2724 | 3543 | 1512 | 578 | 10627 |

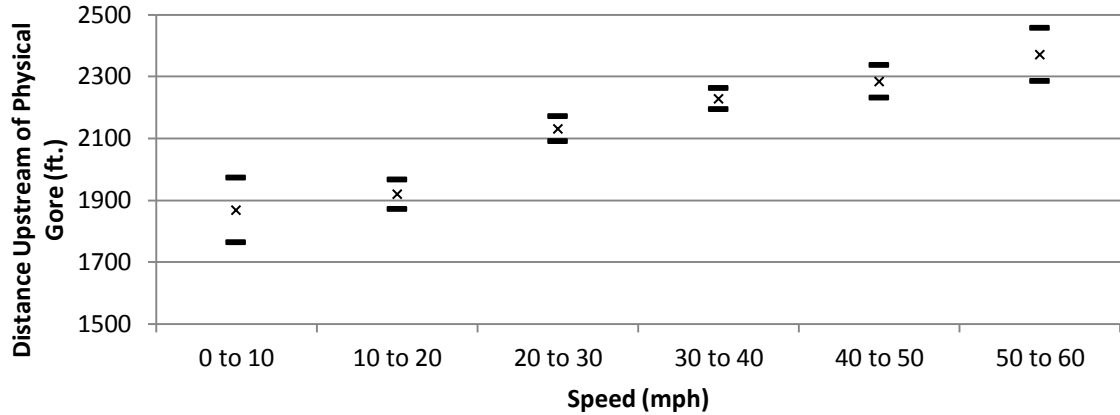


Figure 27: Average Lane Change Position Given Exit Lane Speed

Statistical Testing

A Kolmogorov-Smirnov (KS) test can be used to compare the spatial lane change distributions at different exit lane speeds. The KS tests for a significant difference between two probability distributions. The comparison can be between observed data and a known distribution, or between two samples of data with an unknown parent distribution. The KS test requires both distributions to be continuous, which is the case with the data at hand.

The KS test statistic is the supremum between the CDFs of the two distributions. The number of data points plays a role in estimating significance. As the number of observations increases, the test expects the maximum difference between the CDFs of the distribution to decrease. The significance of the test, α , is estimated by evaluating the

Komolgorov distribution at the critical value $d_{\alpha}(N)$, given the number of observations where N is the sample size (Massey, 1951). A lower percentage test statistic indicates a greater likelihood that the two tested distributions are not derived from different parent distributions.

The equation showing the relationship between the significance, critical value, and the number of observations is shown below. This is also the evaluation of the cumulative distribution function of the Kolmogorov Distribution.

Equation 3: Significance Level:
$$P(d_{\alpha} < x) = 1 - \alpha = 1 - 2 \sum_{i=1}^{\infty} (-1)^{i-1} e^{-2(i*x)^2}$$

Equation 4: Test Statistic Single Sample:
$$d_{\alpha} = \sup_x |F_N(x) - F(x)|\sqrt{N}$$

Equation 5: Test Statistic Two Sample:
$$d_{\alpha} = \sup_x |F_{1,N_1}(x) - F_{2,N_2}(x)|\sqrt{\frac{N_1N_2}{N_1+N_2}}$$

An alternative way of interpreting the critical value is to say that for a random sample of size N , the likelihood of the test statistic exceeding the critical value is α . The value of d decreases as α and N increase. If the test statistic is less than the critical value, it is accepted at significance level α , that the empirical data was not derived from a different hypothesized distribution (single sample), or that the two empirical distributions are not derived from a different parent distribution (two sample). Higher significance levels indicate increasing similarity between distributions (Massey, 1951). It is also important to address that one of the limitations of the KS test is that it is not as sensitive near the tails of the distribution. As a general practice, 5% significance minimum is expected for indicating similarity between distributions. Results displayed in this text will indicate the significance level of the critical value that matches the test statistic. Figure 28 shows the observed cumulative spatial distribution for each 10 mph speed bin. Over a

majority of the distribution, the cumulative spatial distribution of lane changes is greater at a given distance for lower speeds. A two-sample Komolgorov-Smirnov (KS) test can be performed to indicate at what level of significance the spatial distributions of lane changes are different between different target lane speeds (Efron and Tibshirani,1993; Grant, 1998). Results from this test are shown in Table 5, which shows the KS test statistic (D), and confidence interval (alpha) for each speed bin spatial distribution comparison.

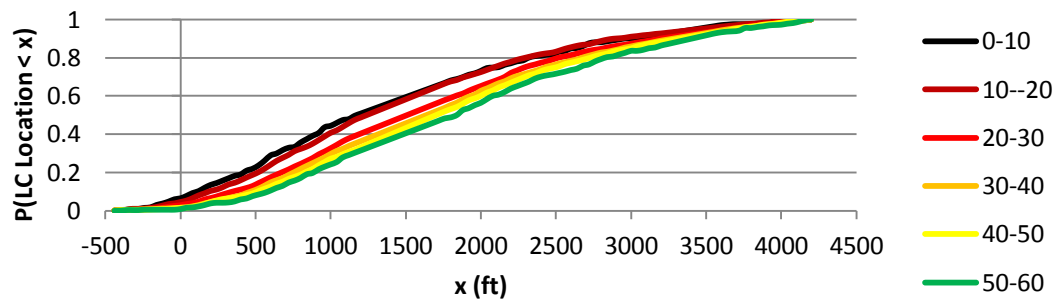


Figure 28: Cumulative Distribution Function of Lane Changes from Lane 5 to Lane 6 Given Exit Lane Speed

Table 5: Kolmogorov-Smirnov Test Results –
Comparison of Distributions with Different Exit lane speeds

| Speed (mph) | | | 10-20 | 20-30 | 30-40 | 40-50 | 50-60 |
|-------------|------|-------|--------|----------|----------|----------|----------|
| | N | | 1869 | 2724 | 3543 | 1512 | 578 |
| 0-10 | 401 | D | 0.0490 | 0.1269 | 0.1613 | 0.1891 | 0.2139 |
| | | alpha | 0.4051 | 2.56E-05 | 1.43E-08 | 2.85E-10 | 7.7E-10 |
| 10-20 | 1869 | D | | 0.0979 | 0.1312 | 0.1591 | 0.1895 |
| | | alpha | | 1.18E-09 | 1.02E-18 | 8.59E-18 | 3.41E-14 |
| 20-30 | 2724 | D | | | 0.0416 | 0.0725 | 0.1024 |
| | | alpha | | | 0.0097 | 7.32E-05 | 9.04E-05 |
| 30-40 | 3543 | D | | | | 0.0327 | 0.0648 |
| | | alpha | | | | 0.2069 | 0.0309 |
| 40-50 | 1512 | D | | | | | 0.0432 |
| | | alpha | | | | | 0.4162 |

*Shaded areas indicate distributions are not statistically significantly different at the 5% level.

The two-sample KS test indicates spatial distributions of lane changes for certain neighboring speed bins may not be derived from different distributions. This is particularly true for comparisons between the 0-10 and 10-20, 30-40 and 40-50, and 40-50 and 50-60 speed bins. The chances that two distributions are the same are increasingly less likely as the difference between exit lane speeds increases.

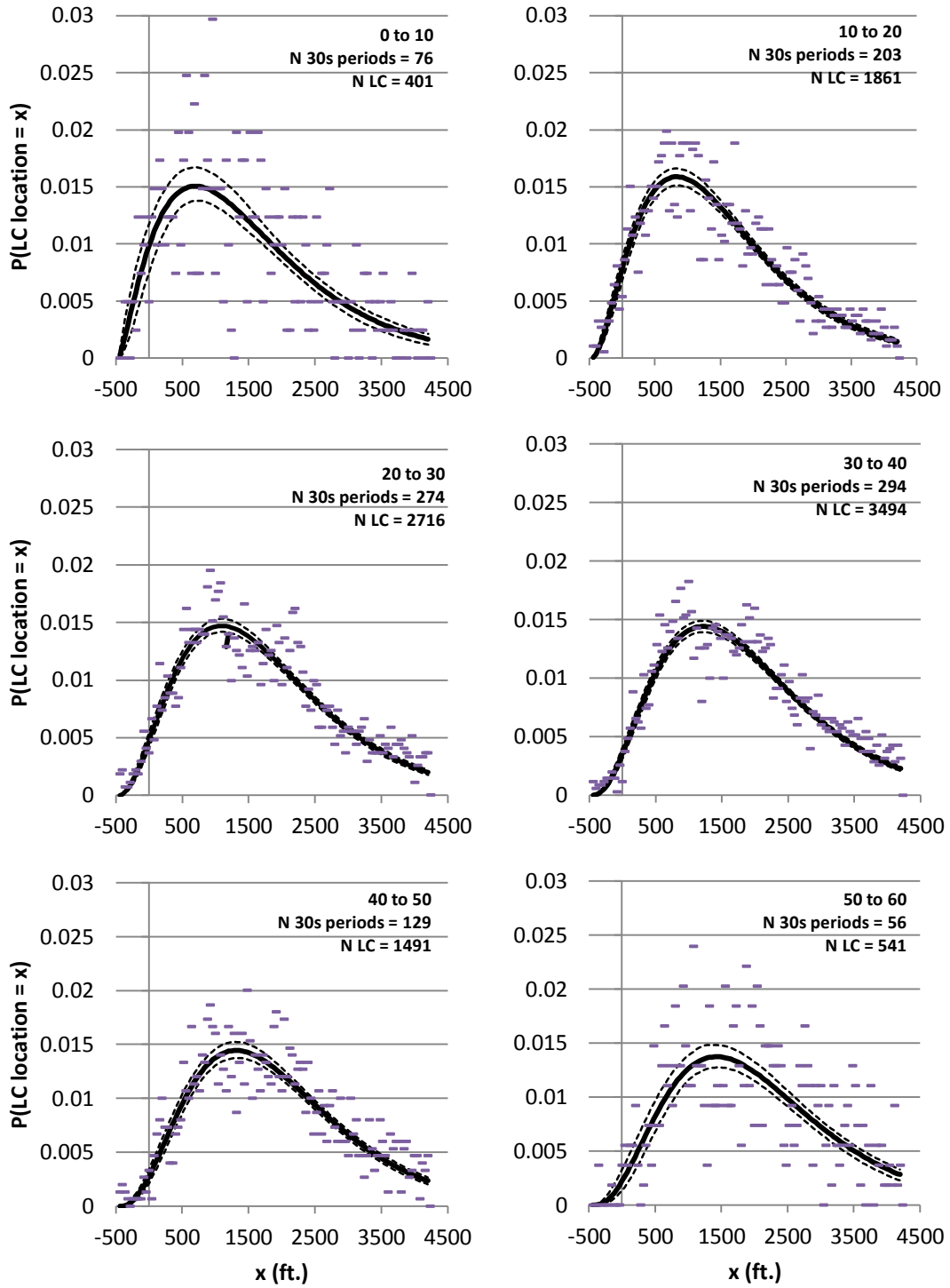
The spatial distribution of lane changes, by observation, appears to follow a gamma distribution. To test this hypothesis, bootstrap methods can be used to approximate the parent distribution from which the observed lane changes may have derived (Efron and Tibshirani, 1993). Bootstrap methods of rank-order fitting, and adaptive estimation are used in this analysis, and explained in detail below.

The bootstrap analysis allows a sampling distribution (with unknown parameters) to be fit to a subset of observed data. The algorithm resamples the observed dataset and fits the sampling distribution parameter(s) based on a least-squares fit. The resampling/fit process is typically repeated 1000 times or more.

In total, 1000 bootstrap distributions are generated, and their best-fit gamma parameters estimated. Next, the probability space is divided into 40' bins, the same resolution as the observed data. Location probability is evaluated within each 40' bin for all of the 1000 bootstrap distributions. The median probability of the 1000 bootstrap distributions from each bin is determined (50 percentile, rank 500), as well as the 95 percent confidence interval (2.5 and 97.5 percentile, rank 25 and 975). One last best-fit gamma distribution is applied to the median probabilities from each bin.

Output from the bootstrap analysis not only provides the best-fit parameters of the sampling distribution, it also provides the confidence interval of the parameter estimate. If the observed data is not representative of the sampling function, the fitted parameters will not conform well to the data and the confidence intervals increase. Small data sets may also lead to wider confidence intervals. Results of the bootstrap process for estimating the shape of the lane change spatial distribution are shown in Figure 29. The bootstrap best-fit curve, confidence interval of the fit, and the observed data (from which the bootstrap estimates are derived) are shown in the figure.

An observation of the bootstrap best-fit gamma distribution indicates the average and median lane change location appears to increase as the ramp speed increases. Furthermore, the number of 30-second observations and number of lane changes that occurred within the 30-second observations are listed for each speed bin. Speed bins with fewer observations tend to show wider confidence intervals, indicating more uncertainty in the shape of the spatial distribution of lane changes. Greater amounts of uncertainty are expected for distribution derived from less data.



Best-Fit — **2.5/97.5 percentile** ···· **Observed** - -

Figure 29: Bootstrap Best-Fit Gamma Distribution

The narrow width of the confidence interval provides evidence that the observed lane change data is governed by a gamma distribution. Bootstrap methods have been used to estimate the best fit gamma distribution parameters. However, this analysis operates under the assumption that the data are gamma distributed, and its results alone do not guarantee that this assumption is correct. Further tests are needed to indicate the initial assumption is correct.

If the observed distribution is indeed gamma distributed, the statistical properties of the observed distribution should closely match the statistical properties of the best-fit distribution. The mean, standard deviation, and median of the observed and best-fit spatial lane change distribution can be compared for each speed bin. A comparison of statistics (Table 6) between the observed and best-fit distributions indicates that the best-fit tends to underestimate the expected position of the lane change for any given speed bin. In all cases, the difference in the average lane change location between the observed and best-fit gamma distribution is less than one percent (less than 40 feet, or one skip line) of the sample space. The median lane change position of the best-fit gamma distribution is also within 40 feet of the observed median for all speed bins excluding the 50 to 60 mph bin, where fewer lane changes were observed.. A comparison of gamma parameters against the freeway speed indicates a negative correlation between the first gamma parameter and exit lane speed, and a positive correlation between the second gamma parameter and exit lane speed. This relationship will be important in developing the lane changing model later in this chapter.

Table 6: Comparison of Statistics – Observed versus Bootstrap Best-Fit

| | | Exit Lane Speed (mph) | | | | | |
|----------|---------------|-----------------------|-------------|-------------|-------------|-------------|-------------|
| | | 0 to 10 | 10 to 20 | 20 to 30 | 30 to 40 | 40 to 50 | 50 to 60 |
| | N | 401 | 1861 | 2705 | 3494 | 1491 | 541 |
| Observed | Average μ | 1867 | 1918 | 2130 | 2227 | 2283 | 2370 |
| | s | 1072 | 1032 | 1055 | 1048 | 1042 | 1052 |
| | Median | 1680 | 1720 | 2000 | 2120 | 2200 | 2360 |
| Best-Fit | Gamma Param | 824 | 698 | 705 | 682 | 665 | 684 |
| | Gamma Param | 2.37 | 2.84 | 3.20 | 3.44 | 3.66 | 3.71 |
| | E[x] | 1824 | 1891 | 2105 | 2183 | 2256 | 2322 |
| | σ [x] | 1032 | 994 | 1013 | 1008 | 1004 | 1011 |
| | Median | 1640 | 1720 | 1960 | 2080 | 2160 | 2240 |

A KS test can be performed to indicate the significance of each speed bin fit.

Table 5 shows the KS test statistic (D), and significance (alpha) for each comparison of best-fit and observed lane change distributions. Results indicate at the 5% significance level that observed data for five of the six speed bins are not derived from a distribution different from the derived bootstrap best-fit distribution (the 30 to 40 mph bin did not pass).

Table 7: KS Test Results – Comparison of Observed vs. Bootstrap Best-Fit

| Speed (mph) | 0 to 10 | 10 to 20 | 20 to 30 | 30 to 40 | 40 to 50 | 50 to 60 |
|-------------|---------|----------|----------|----------|----------|----------|
| N | 401 | 1861 | 2705 | 3494 | 1491 | 541 |
| D | 0.0300 | 0.0193 | 0.0242 | 0.0307 | 0.0250 | 0.0405 |
| alpha | 0.8621 | 0.4908 | 0.0820 | 0.0026 | 0.3024 | 0.2981 |

*Shaded areas indicate distributions are not statistically significantly different at the 5% level.

Results from the KS test indicate the gamma distribution provides a reasonable fit for the spatial distribution of lane changes when the ramp speeds are below 30 miles per hour. However, the goodness of fit decreases for speeds greater than 30 mph, as indicated by the significance level. This is especially true for the 30 to 40 mph speed bin, which contain the largest number of data points of all the speed bins. This is not very surprising, considering it is easier to identify a statistically significant difference between two datasets with more data. Whether or not this difference is meaningful cannot be

ascertained without a further consideration of factors that may be affecting the shape of the lane changing distributions.

For the 30 to 40 mph range, the bootstrap best-fit spatial distribution of lane changes, when compared against the observed data used to derive the bootstrap best-fit distribution, yields a KS statistic which indicates the observed data is likely not derived from the bootstrap-best-fit hypothesized distribution. There are currently two hypotheses that may explain this observation. The first hypothesis proposes that vehicles moving from lane 7 to the Pleasantdale Road exit ramp are creating gaps in lane 7 which provides opportunities for lane changing from lane 6 to lane 7. In effect, gaps in lane 6 provide additional opportunities for lane changing from lane 5 to lane 6. These secondary and tertiary lane changing effects may be responsible for the influx of vehicles downstream of the Pleasantdale off-ramp. Also this hypothesis is supported by the fact that the supremum of the difference between the CDF of the empirical distribution and the bootstrap-generated distribution (location of the KS test statistic) falls ~900' downstream of the ramp to Pleasantdale.

A general influx is expected as discretionary lane changes from 6 to 7 results in gaps in lane 6. To test if there is an influx of vehicles moving from lane 5 to lane 6 due to vehicles moving from lane 6 to lane 7, a look-back can be performed on each lane change. If a vehicle moving from lane 5 to lane is filling in a gap left by a vehicle moving from lane 6 to lane 7, the two lane changes should be within a certain time space area of each other. Given that the lane change from 5 to 6 should occur later in time and space than the lane change from 6 to 7, a look-back (within a certain time-space region) can be used to find potential lane-change pairs.

Preliminary results using this technique (looking back a maximum of 15 seconds and 1200') indicate that a larger proportion of the lane changes from 5 to 6 just upstream of the off-ramp to Pleasantdale Road are a result of gaps opening from lane changes from 6 to 7. Up to 50 percent of lane changes directly upstream of the ramp appear to be filling gaps that have opening up, while for the remainder of the distribution the fraction is between 10 and 25 percent. The spatial distribution of the remainder of lane changes (not paired with another lane change) lacks the influx of vehicles just upstream of the ramp, a further indication that the influx of lane changes in this area is a result of exiting vehicles, and that the physical layout of the infrastructure may play an important role in systems operations on the macroscopic level.

The second hypothesis proposes that a decrease in the number of lane changes occurs under the Pleasantdale Road overpass. Support for this hypothesis is compromised when comparing the number of indirectly observed lane changes under the Dawson Blvd. overpass to directly observed lane changes on either side of the Dawson Blvd. overpass. There does not seem to be a decrease in the number of lane changes under the Dawson Blvd. overpass. Thus, the first hypothesis appears more credible – there is not a decrease in the number of lane changes under the Pleasantdale overpass, but rather an influx of lane changes due to traffic exiting at the Pleasantdale Road off-ramp. The influx of lane changing activity is discussed in Appendix C.

A comparison of spatial distributions of lane changes across days will indicate whether or not macroscopic lane-changing behavior remains consistent given an upstream ramp speed. Despite dissimilar ramp speed distributions between days, the lane-changing distribution is expected to remain consistent across days. The comparison is

between two observed data sets; thus, a two-sample KS test will be used to test lane-changing distributions between days. For each speed bin, three comparisons are made – May 7 vs. May 8, May 8 vs. May 9, and May 7 vs. May 9. The number of observations for the compared datasets (N_1 , N_2), the KS test statistic (D), and confidence interval (α) for each speed bin spatial distribution comparison are shown. The test results overwhelmingly indicate that at a given ramp speed, the distribution of lane changes remains consistent from day-to-day. This is evidenced by a significance level (α) greater than 5 percent for all day-to-day speed bin comparisons.

Table 8: KS Test Results – Comparison of Observed Data Between Days

| | | Exit Lane Speed (mph) | | | | | |
|-------------------------|-------|-----------------------|----------|----------|----------|----------|----------|
| | | 0 to 10 | 10 to 20 | 20 to 30 | 30 to 40 | 40 to 50 | 50 to 60 |
| 5/7/13 vs. 5/8/13 | N1 | 166 | 591 | 863 | 1237 | 347 | 90 |
| | N2 | 146 | 642 | 924 | 1413 | 612 | 94 |
| | D | 0.1443 | 0.0526 | 0.0247 | 0.0413 | 0.0513 | 0.0627 |
| | alpha | 0.0804 | 0.3563 | 0.9470 | 0.2091 | 0.5993 | 0.9942 |
| 5/8/13 vs. 5/9/13 | N1 | 146 | 642 | 924 | 1413 | 612 | 94 |
| | N2 | 92 | 626 | 929 | 856 | 540 | 359 |
| | D | 0.0887 | 0.0304 | 0.0606 | 0.0177 | 0.0226 | 0.1065 |
| | alpha | 0.7595 | 0.9319 | 0.0667 | 0.9455 | 0.9984 | 0.3395 |
| 5/7/13 vs. 5/9/13 | N1 | 166 | 591 | 863 | 1237 | 347 | 90 |
| | N2 | 92 | 626 | 929 | 856 | 540 | 359 |
| | D | 0.1318 | 0.0365 | 0.0517 | 0.0372 | 0.0460 | 0.1199 |
| | alpha | 0.2646 | 0.8094 | 0.1789 | 0.2150 | 0.7541 | 0.2667 |

*Shaded areas indicate distributions are not statistically significantly different at the 5% level.

Given an exit lane speed, a reliable estimate can be made as to where vehicles will change lanes to enter the exit lane, without necessarily needing to know the decisions drivers are making on a microscopic level. The Pleasantdale Road off-ramp impacts the spatial distribution of lane changes in its vicinity, and thus, this particular result cannot be directly applied to another site. Other sites are expected to exhibit similar consistency in lane changing distributions from day-to-day given a static infrastructure and consistent travel demand (origin-destination pairs) by time of day. Hence, it may be possible to calibrate such relationships throughout the system and even develop relationships between predicted changes in demand and system performance. However, conclusions regarding these relationships cannot be made at this time, and are left as a topic for future research once more data becomes available.

Number of Lane Changes vs. Speed

To study the relationship between target lane speed and the number of lane changes, a multivariate histogram of the two variables can be generated. The number of

lane changes is a discrete variable, and will remain that way in the histogram. Speed is a continuous variable, and must be placed into bins of equal size. Figure 30 below, shows the frequency of the number of lane changes in a 30-second wave, given the speed of the exit lane. It appears more lane changing is likely to occur and there also seems to be increased variability in the number of observed lane changes, at middle speeds. This does not take the distribution of exit lane speeds into effect.

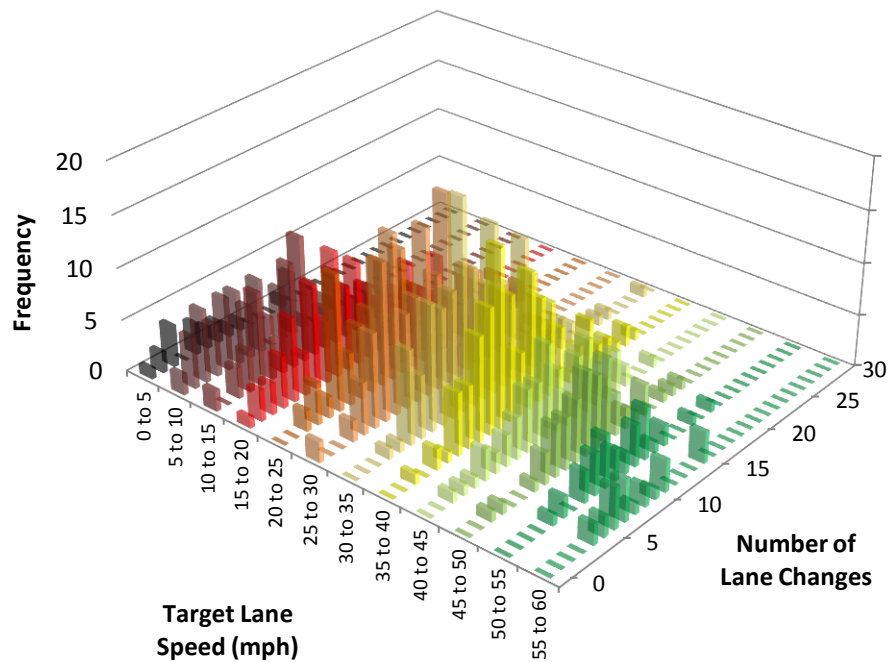


Figure 30: Histogram of Number of LC Versus target Lane Speed (5mph bins)

Next, it will be of interest to condition the histogram by speed of the exit (target) lane. The resulting function will be the probability density of the number of lane changes along a wave given a target lane speed. The conditional PDF represents a saddle-type shape. When target lane speeds are very slow, the probability of zero or one lane change is very high, and as speed increases, the most likely number of lane changes increases.

However, the variability of the number of lane changes also increases. This means that the probability space is spread over a larger number of lane change possibilities, causing the probability of the mode to decrease as target lane speeds decrease. As target lane speeds increase over 30 mph, the likelihood of fewer lane changes again increases, and the variability decreases resulting in the value of the mode to increase again, resulting in the saddle shape of the conditional PDF.

It is important to note that a high degree of correlation is found between the initial and ramp lane speeds at greater ramp lane speeds, and thus, may be driving the shape of the distribution at higher speeds. Under the right conditions, it seems reasonable that higher amounts of lane changing are possible when the initial and target lanes are both in free flow, but the initial lane has a much greater density compared to the target lane. Under such conditions, it may be possible for a large number of vehicles to move into the target lane, although they all do not necessarily make this maneuver within the same wave. However, such conditions that may cause more weaving at higher speeds were not noted during the study period.

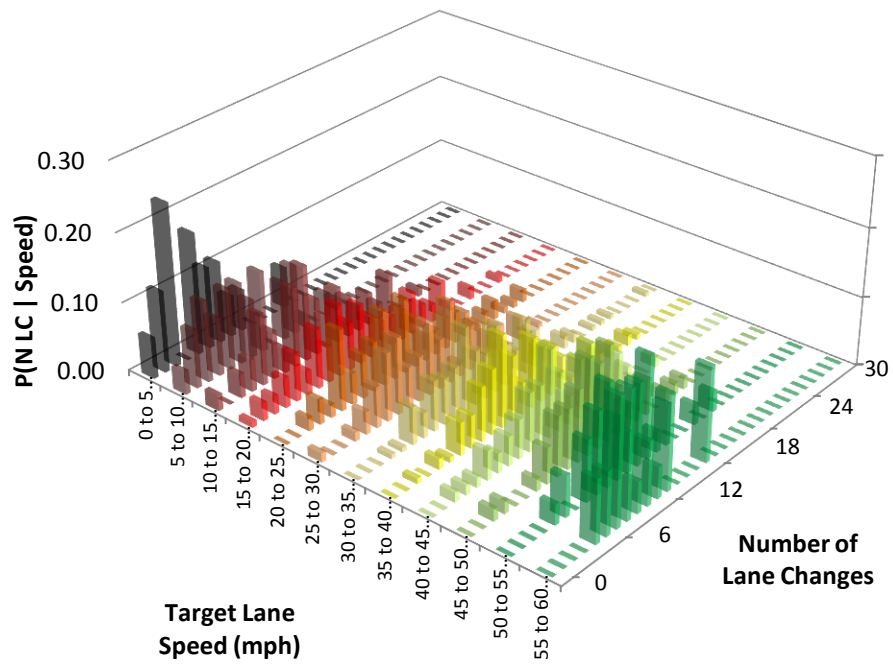


Figure 31: PDF of Number of Lane Changes Conditioned by Speed (5 mph bins)

The average and the 95% confidence interval of the number of lane changes given a target lane speed are shown in Figure 32. A second-order polynomial is fit to each average to indicate trends in the average number of lane changes as speed changes.

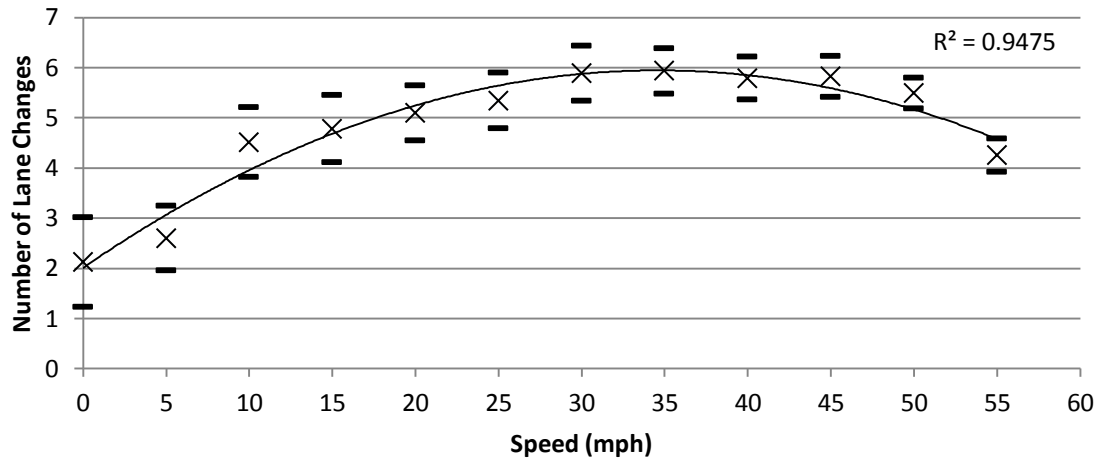


Figure 32: Target Lane Speed vs. Average Number of Lane Changes

Statistical Testing

As with the spatial data, a bootstrap analysis can be performed to estimate the parameter of the Poisson distribution for each given target lane speed range. Figure 33 on the following page shows the results of the Poisson bootstrap analysis and the data for the observed number of lane changes. As expected, the speed bins containing more observational data tend to show better fit and tighter confidence intervals. Given that there tends to be overlap between the median bootstrap sample and the best-fit Poisson distribution, the Poisson distribution is also a candidate distribution for describing the relationship between exit lane speed and the number of lane changes. One exception is in the 55 to 60 mph range; a small number of observations and large variance in the observed number of lane changes leads to a large amount of uncertainty in the model. However, high variability in the lane change position is not surprising in a free-flow state, where the distribution is driven by individual driver preference. Given varying densities at free flow speeds, the number of vehicles that will make lane changes is also expected

to vary widely. Additionally, there appears to be a parabolic relationship between speed and the best-fit Poisson parameter.

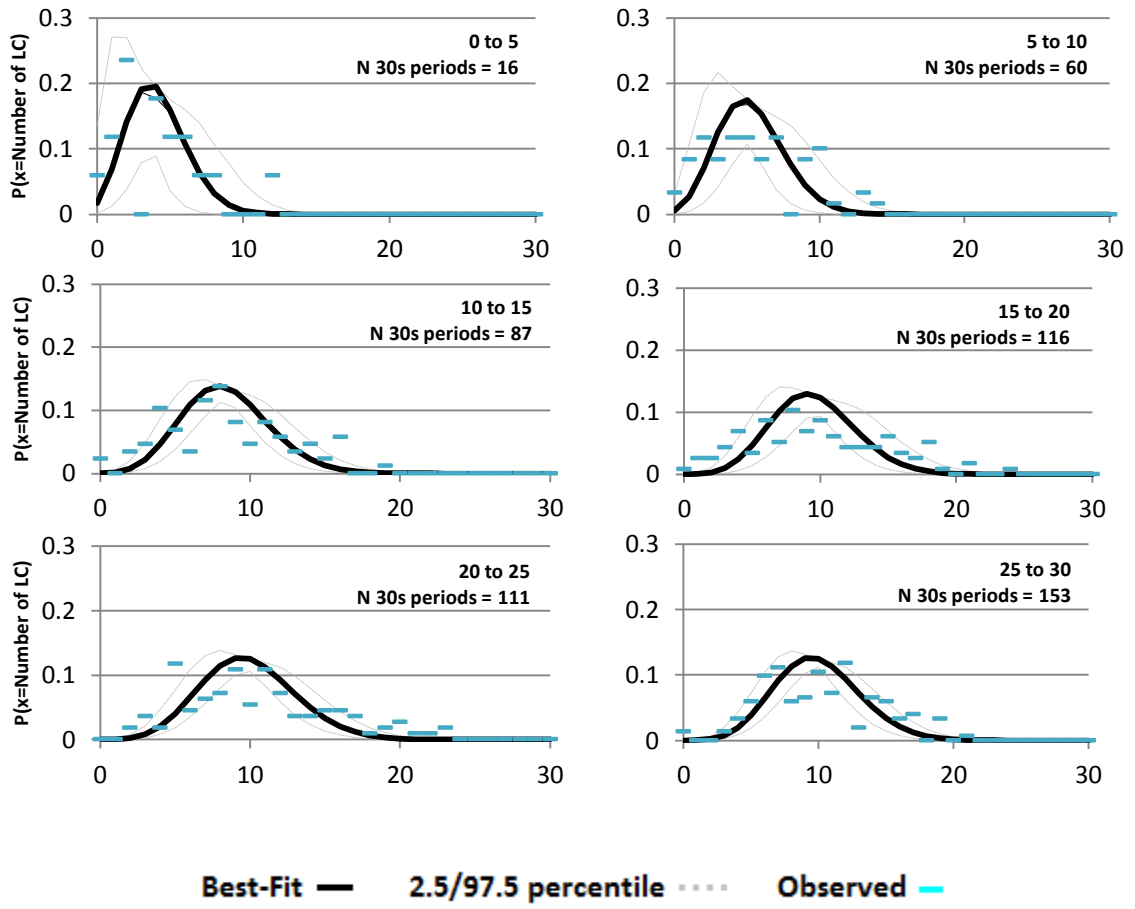


Figure 33: Bootstrap Best-Fit Poisson Distribution

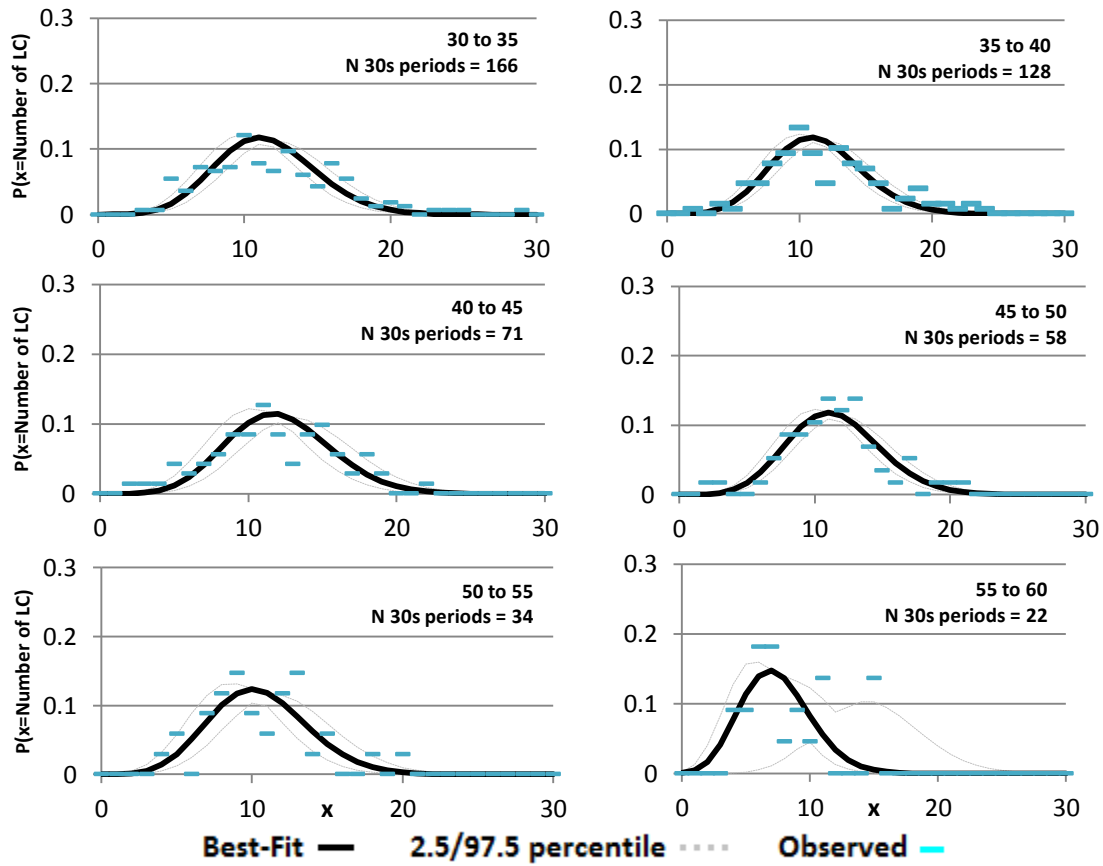


Figure 33 (continued): Bootstrap Best-Fit Poisson Distribution

Final Model Selection

The next objective of this dissertation is to ascertain the relationship between the distribution of the number of lane changes, given location and target lane speed. Up to this point, the spatial distribution of lane changes and the expected number of lane changes given a target lane speed have been discussed. Findings from the bootstrap analysis thus far indicate a parabolic relationship between the ramp speed and the

expected number of lane changes, while the number of lane changes given the ramp speed follows a Poisson distribution, and the spatial distribution of lane changes is roughly gamma-distributed. It is hypothesized that the shape of the curve relating the parameter of the Poisson distribution to position and speed of the target lane is an intersection of the functions.

Several different fitting functions were used to estimate the relationship between the number of lane changes, target lane speed, and lane change location. These fitting functions used polynomial relationships that allow interaction between the location and speed terms with varying orders. The goal of such an equation form is to fit the data as well as possible. Equation 6 displays the described fitting equation in matrix-form.

$$\begin{bmatrix} a_{00} & a_{01} & a_{02} & \dots \\ a_{10} & a_{11} & a_{12} & \\ a_{20} & a_{21} & a_{22} & \\ \vdots & & & \ddots \end{bmatrix} \begin{bmatrix} 1 \\ v \\ v^2 \\ \vdots \end{bmatrix} [1 \quad x \quad x^2 \quad \dots] = \lambda(x, v)$$

Equation 6: Interactive Polynomial Fitting Equation

The choice of the form of the derived function fitting equation (Equation 7) was motivated by the gamma-like relationship between the likelihood of observing a lane change and the distance upstream of the ramp and the parabolic relationship between the magnitude of observed a lane change activity and target lane speed. As discussed previously, the parameters of the gamma distribution appear to be a function of the speed of the target lane, and the magnitude of the spatial distribution of lane changes appears to be correlated with speed.

The gamma distribution in the equation below represents the estimated probability of a lane change occurring at position, x, upstream of the ramp at a given exit lane speed,

v . Based on the results of the bootstrap analysis, there is an approximately linear relationship between exit lane speed and each parameter of the gamma distribution). Coefficients $a_4, a_5, a_6,$ and a_7 describe this relationship. When this gamma distribution is multiplied by a given total number of lane changes, the resulting distribution is the number of lane changes expected to occur at any location. It is known that there is a parabolic relationship between the total number of lane changes and the target lane speed. The shape of the parabolic relationship is estimated with coefficients $a_1, a_2,$ and a_3 . Thus, when the gamma distribution (evaluated at location, x , and exit lane speed, v) is multiplied by the parabola (evaluated at exit lane speed, v), the resulting value is the expected number of lane changes for a given location, x , and ramp lane speed, v .

$$\lambda(\widehat{x, v}) = \underbrace{(a_1 + a_2v + a_3v^2)}_{\text{Parabolic}} \underbrace{\frac{\exp\left(-\frac{440+x}{a_6+a_7v}\right) (440+x)^{-1+a_4v+a_5} (a_6v+a_7)^{-a_4v+a_5}}{\Gamma|a_4v+a_5|}}_{\text{Gamma Distribution}} \quad x > -320$$

Equation 7: Derived Fitting Equation for Lane Change Data

Where $\lambda(x, v)$ is the estimated number of lane changes (Poisson parameter), x is the distance upstream of the painted gore, v is the speed of the target lane, and Γ is the gamma function.

The sum of independent Poisson random variables has a Poisson distribution with a parameter equal to the sum of parameters of the summed distributions (Lehman, 1986). Thus, the total expected number of lane changes into a target lane can be estimated by integrating (adding) the Poisson parameter for all positions at the target lane's speed. The same method of summing Poisson distributions can be used to estimate the distribution of

the total number of lane changes expected for a subset of data during the observation period. Comparing the observed number of lane changes against the distribution of lane changes predicted by the model provides a metric against which the accuracy of the macroscopic lane-changing model can be tested. Performing this analysis requires the distribution of observed speeds to be known. Speeds estimated using the tracking software will be used in this analysis.

There is a small fraction (43 observed, 0.4% of total) of vehicles that wait until the last minute to move into the ramp lane. These vehicles are typically seen weaving through the gore area. For locations closer to the ramp, the likelihood of a lane change to occur estimated by the gamma distribution tends to zero. Although the likelihood of a lane change close to the ramp is close to zero, it is still positive and has the potential to cause error in a model that estimates the number of lane changes at this location to be zero. A reasonable argument can be made that the behavior exhibited by last-minute lane changers may be the result of a different decision making process, and should be modeled separately. Thus, comparison of observed data against expected data will not include lane changes within 120 feet of the physical gore for all fitting equations. A distance of 120 feet upstream of the physical gore was chosen because of large chi-square values resulting from large differences between observed and expected numbers of lane changes in this region. Lane changes in the final 120 feet are discussed in further detail in Appendix C.

Mathematica was used to perform a nonlinear maximum-likelihood fit on the lane change data using the interactive polynomial equation as well as the derived function. The Akaike information criterion (AIC), are used to estimate the likelihood that each

model minimizes error between the observed data and the generated model (Akaike, 1974). AIC measures the relative quality of different models generated from the same dataset. The purpose of the AIC is for model selection. However, it is important to note that the AIC, being a relative test statistic, does not assess quality of the model, and by itself is not useful. However, it is useful for comparing models against each other (even if all the models do not fit the data well). Supplemental tests are used to assess the quality of the model and are performed later in this section. The value of the AIC is a function of the log-likelihood of the model and the number of parameters in the model (Equation 8). Larger values of AIC indicate a lower likelihood of a model minimizing error. The AIC equation indicates penalties for additional coefficients. As the log-likelihood becomes less negative and as fewer variables are used in the model, the more likely a model will be the best model (of the given set).

Differences between the AIC of a given model and the AIC of the model with the minimum AIC are used to estimate the relative quality of each model (Table 8). The model with the lowest AIC will always have the greatest likelihood of being the highest-quality model. The equation for establishing relative likelihoods is displayed in Equation 9. The actual probability of a model minimizing the error is estimated by taking its relative likelihood divided by the sum of all model relative likelihoods (Equation 10).

Table 9: Qualitative Assessment of a Model with a Given AIC
(Burnham and Anderson, 2002)

| Difference between model AIC and minimum AIC | Level of Empirical Support |
|--|----------------------------|
| 0 to 2 | Substantial |
| 3 to 7 | Considerably Less |
| Greater than 10 | Essentially None |

$$AIC = -2 * \log(\text{maximum likelihood}) + 2k \quad \text{Equation 8: AIC Equation}$$

$$R_i = \exp\left(\frac{AIC_{min} - AIC_i}{2}\right) \quad \text{Equation 9: Relative Likelihood of a Model}$$

$$\frac{R_i}{\sum R_i} \quad \text{Equation 10: Model Likelihood}$$

Where ML_i is the maximum likelihood of model i , k is the number of parameters used to calibrate model i , n_i is the number of observations for model i , AIC_{min} is the AIC of the model with the lowest AIC, and R_i is the relative likelihood of model i .

The r-squared, AIC and model likelihood (based on the AIC) are displayed for all models in Table 10. Despite the sixth-order parabolic model exhibiting a higher r-squared value than the derived model, the number of variables used in the model raises its AIC indicating the variables may be over-fitting the model. In the case of the fitting models in this section, the AIC difference between the model with the lowest AIC (derived function) and the model with the second lowest AIC (sixth order polynomial) is greater than 30, resulting in the model likelihood of the derived function to be very close to 1 and the likelihood of choosing any of the interactive polynomial fitting equations is essentially negligible. The estimated model likelihoods are in accordance with the qualitative assessment of empirical support for a model from Table 8.

Table 10: Interactive Polynomial Fit Statistics

| Order | 0 | 1 | 2 | 3 | 4 | 5 | 6 | Derived Function* |
|------------------------|---------|---------|----------|----------|----------|----------|----------|-------------------|
| Number of Coefficients | 1 | 4 | 9 | 16 | 25 | 36 | 49 | 7 |
| R^2 | 0.07834 | 0.08183 | 0.09701 | 0.10171 | 0.10197 | 0.10224 | 0.10245 | 0.10237 |
| AIC | 53318.3 | 52866.9 | 50874.7 | 50257.1 | 50231.6 | 50206.0 | 50191.4 | 50160.2 |
| Relative prob. (AIC) | 0 | 0 | 7.1E-156 | 9.09E-22 | 3.13E-16 | 1.13E-10 | 1.68E-07 | 1 |
| Model likelihood (AIC) | 0 | 0 | 7.1E-156 | 9.09E-22 | 3.13E-16 | 1.13E-10 | 1.68E-07 | $1 - (1.7E-7)$ |

*Selected Model

Furthermore, the polynomial equation form exhibits no discernible relationship between the model coefficients and what they represent, and displays erratic, non-realistic behavior directly outside of the area of observation. Such characteristics are generally arguments against the use of an interactive polynomial model. For the purpose of curve fitting, the polynomial model is sufficient if not extending it beyond the range of observations, but causality is not inherent.

A contour plot of the final model (derived function) is displayed in the three-dimensional and two-dimensional formats in Figure 34. At lower speeds, fewer lane changes are expected, and when they do occur, they are more likely to be closer to the ramp. As speeds increase, the total amount of lane changing increases and occur further away from the ramp, on average. Above 40 mph, the total number of lane changes begins to decrease again, although the average lane change location continues to increase.

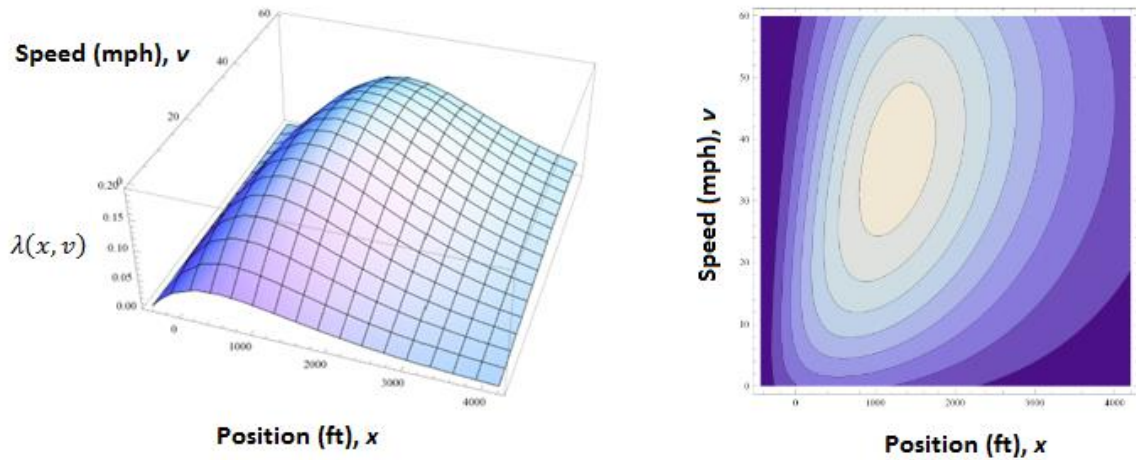


Figure 34: Three-Dimensional and Two-Dimensional Contour Plots for Best Fit Model

Now that an equation form has been selected, verification of the model can be conducted with a separate calibration and validation data sets. A subset of the data is used to calibrate the model, while the remainder will be used to validate the model. The data was collected over a period of three days, approximately for the same amount of time each day. A model can be derived from two days of data and verified with data collected from the third day. Given three days of data, there are three possible combinations of calibration/validation datasets. All three combinations of calibration/verification datasets are tested for model robustness.

It will also be of interest to make sure that the distribution of conditions is similar across the development and verification datasets. The location of infrastructure and camera setup remains consistent from day to day. The data available and distributions of ramp speeds between days are compared in Table 10. All three combinations of development and verification data sets exhibit similar ramp speed distributions. Table 10 shows that for each day of data collection, there are few 30-second observations where

low ramp speeds are observed. As ramp speed increases, so does the number of 30-second observations until ramp speeds reach 30 to 40 mph. At this point, the number of observations decreases as ramp speed increases. In addition, inter-correlation between data sets should ideally not be present. If the same drivers use the ramp and make lane changes into the exit lane from day to day, and encounter the same traffic conditions each day, the data may be inter-correlated between days. Given the data at hand, it would be very time-consuming and difficult to ascertain if the same vehicles are seen every day experiencing the same conditions. While it is expected that a considerable percentage of commuters use the corridor every day, the likelihood of these drivers experiencing the same conditions each time they drive the corridor from day-to-day is assumed to be small.

Table 11: Calibration and Verification Data Set Dates

| Calibration Data Dates | Speed Range | N 30s periods | % | Verification Data Date | Speed Range | N 30s periods | % |
|---|-------------|---------------|------|---------------------------------|-------------|---------------|------|
| 5/7/13, 5/8/13 (N 30s periods = 676) | 0 to 5 | 12 | 1.8 | 5/9/13 (N 30s periods = 346) | 0 to 5 | 4 | 1.1 |
| | 5 to 10 | 42 | 6.2 | | 5 to 10 | 18 | 5.2 |
| | 10 to 15 | 55 | 8.1 | | 10 to 15 | 32 | 9.2 |
| | 15 to 20 | 76 | 11.2 | | 15 to 20 | 40 | 11.5 |
| | 20 to 25 | 74 | 10.9 | | 20 to 25 | 37 | 10.6 |
| | 25 to 30 | 100 | 14.8 | | 25 to 30 | 53 | 15.2 |
| | 30 to 35 | 137 | 20.3 | | 30 to 35 | 29 | 8.3 |
| | 35 to 40 | 80 | 11.8 | | 35 to 40 | 48 | 13.8 |
| | 40 to 45 | 54 | 8.0 | | 40 to 45 | 17 | 4.9 |
| | 45 to 50 | 29 | 4.3 | | 45 to 50 | 29 | 8.3 |
| | 50 to 55 | 16 | 2.4 | | 50 to 55 | 18 | 5.2 |
| | 55 to 60 | 1 | 0.1 | | 55 to 60 | 21 | 6.0 |
| 5/8/13, 5/9/13 (N 30s periods = 707) | 0 to 5 | 12 | 1.7 | 5/7/13 (N 30s periods = 315) | 0 to 5 | 4 | 1.3 |
| | 5 to 10 | 37 | 5.2 | | 5 to 10 | 23 | 7.3 |
| | 10 to 15 | 60 | 8.5 | | 10 to 15 | 27 | 8.6 |
| | 15 to 20 | 81 | 11.4 | | 15 to 20 | 35 | 11.1 |
| | 20 to 25 | 76 | 10.7 | | 20 to 25 | 35 | 11.1 |
| | 25 to 30 | 101 | 14.2 | | 25 to 30 | 52 | 16.5 |
| | 30 to 35 | 99 | 14.0 | | 30 to 35 | 67 | 21.3 |
| | 35 to 40 | 94 | 13.3 | | 35 to 40 | 34 | 10.8 |
| | 40 to 45 | 54 | 7.6 | | 40 to 45 | 17 | 5.4 |
| | 45 to 50 | 46 | 6.5 | | 45 to 50 | 12 | 3.8 |
| | 50 to 55 | 26 | 3.7 | | 50 to 55 | 8 | 2.5 |
| | 55 to 60 | 21 | 3.0 | | 55 to 60 | 1 | 0.3 |
| 5/7/13, 5/9/13 (N 30s periods = 661) | 0 to 5 | 8 | 1.2 | 5/8/13 (N 30s periods = 361) | 0 to 5 | 8 | 2.2 |
| | 5 to 10 | 41 | 6.2 | | 5 to 10 | 19 | 5.3 |
| | 10 to 15 | 59 | 8.9 | | 10 to 15 | 28 | 7.8 |
| | 15 to 20 | 75 | 11.3 | | 15 to 20 | 41 | 11.4 |
| | 20 to 25 | 72 | 10.9 | | 20 to 25 | 39 | 10.8 |
| | 25 to 30 | 105 | 15.8 | | 25 to 30 | 48 | 13.3 |
| | 30 to 35 | 96 | 14.5 | | 30 to 35 | 70 | 19.4 |
| | 35 to 40 | 82 | 12.4 | | 35 to 40 | 46 | 12.7 |
| | 40 to 45 | 34 | 5.1 | | 40 to 45 | 37 | 10.2 |
| | 45 to 50 | 41 | 6.2 | | 45 to 50 | 17 | 4.7 |
| | 50 to 55 | 26 | 3.9 | | 50 to 55 | 8 | 2.2 |
| | 55 to 60 | 22 | 3.3 | | 55 to 60 | 0 | 0 |

Parameter estimates and t-values for the chosen model are displayed in Table 11.

The first three coefficients (a_1, a_2, a_3) describe the parabolic relationship between the

number of lane changes and ramp speed (the magnitude of the number of lane changes, as described previously in this chapter), and are signed as expected. Each calibration of the model estimates the maximum average lane changing rate occurs at a speed of 40.7, 37.9, and 38.8 mph, which is consistent with observation. It is important to note that correlation is expected between each of the polynomial coefficients. These coefficients will trade off with each other to minimize the sum of square errors between the expected and observed magnitude of the number of lane changes. Thus, the t-values for all three polynomial coefficients should not be rigorously interpreted.

The next four coefficients (a_4, a_5, a_6, a_7) describe the linear relationship (slopes and intercepts, as described earlier in this chapter) between speed and the gamma distribution parameters. At a speed of 0 mph, the first gamma distribution parameter is positive for all calibrations, and increases with respect to speed for all calibrations indicating this parameter is non-negative for all speeds, a requirement for gamma distribution parameters. At a speed of 0 mph, the second gamma distribution parameter begins from a large positive value for each calibration. The first calibration dataset indicates a positive relationship between speed and the second gamma parameter, and the remaining two calibration datasets indicate a negative relationship between speed and the second gamma parameter. Even at speeds in excess of 60 mph, the second parameter of the gamma distribution remains positive for all calibrations. There are limitations using the model to predict lane changes when ramp speeds are greater than 60 mph, as there is no data used to develop the model above 60 mph. Given the relationship between speed and the gamma distribution parameters, the model-estimated relationships between

average lane change position, variance of lane changing position, and speed can be assessed.

Table 12: Parameter Estimates Using Calibration and Verification Data Sets

| Verification Data Set | | 5/7/13 N = 315 | 5/8/13 N = 361 | 5/9/13 N = 346 |
|-----------------------|-------|-----------------------------|-----------------------------|-----------------------------|
| Calibration Data Set | | 5/8/13 5/9/13 N = 707 | 5/7/13 5/9/13 N = 361 | 5/7/13 5/8/13 N = 676 |
| Coefficient | a_1 | -0.24552 (-10.67) | -0.26894 (-11.19) | -0.2441 (-7.83) |
| | a_2 | 19.9945 (14.18) | 20.4001 (13.96) | 18.9585 (11.14) |
| | a_3 | 102.096 (4.97) | 112.991 (5.50) | 139.471 (6.41) |
| | a_4 | 0.00623758 (0.92) | 0.0327552 (6.18) | 0.042545 (8.30) |
| | a_5 | 2.86695 (13.01) | 2.01875 (12.56) | 1.82765 (12.41) |
| | a_6 | 4.63279 (2.08) | -4.49551 (-2.70) | -6.11689 (-3.86) |
| | a_7 | 621.753 (8.93) | 921.122 (14.83) | 935.242 (16.03) |

Parameter estimates for the calibration/observation data sets indicate many similarities between models. The signs and magnitude of most of the parameters remain the same, with the exception of the a_6 coefficient when calibrating the model with data from May 8 and 9, and validating with data from May 7. The a_4 coefficient is also much lower than usual, indicating the tradeoff between the gamma distribution parameters is different for this model calibration dataset. A comparison of average and standard deviation of the lane change locations between the days indicates that despite the different gamma parameters, all models perform relatively the same, although the coefficient tradeoffs likely indicate overfitting may be occurring. The greatest correlations are seen between the three coefficients that describe the relationship between

lane changing intensity and speed, and the four variables describing the relationship between the gamma parameters (describing spatial distribution of lane changes) and speed. Correlation between the polynomial variables is expected, and correlation between the variable that describe that parameters of the gamma distribution is also expected, as tradeoffs are expected with these variables.

Despite the tradeoff in the gamma distribution variables, all of the datasets provide relatively stable results in the estimating the average lane change position given speed (Figure 35). For each developed model, the average lane change position increases from approximately 1750 feet upstream of the ramp when the ramp is moving at 0 mph to between 2500 and 3000 feet upstream of the ramp when the ramp speed is 60 mph.

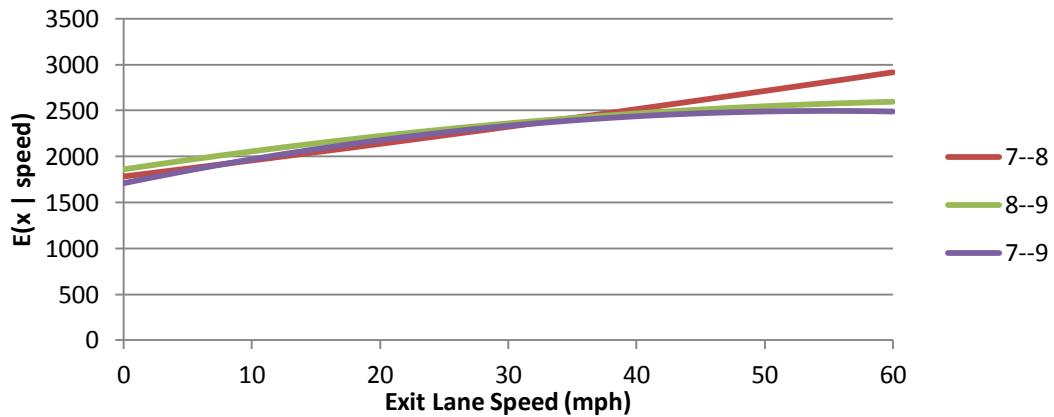


Figure 35: Average Lane Change Position Predicted by Model (I-85)

However, the variance in lane change location appears to differ between models (Figure 36). Two of the calibration datasets indicate the variance of lane change position remains relatively constant with respect to speed, while the other calibration dataset indicates variance of lane change position increases as speed increases. While an increase in variance of lane change position is logical, there is not enough evidence to

ascertain whether the variance of lane change position is constant or increasing with respect to speed.

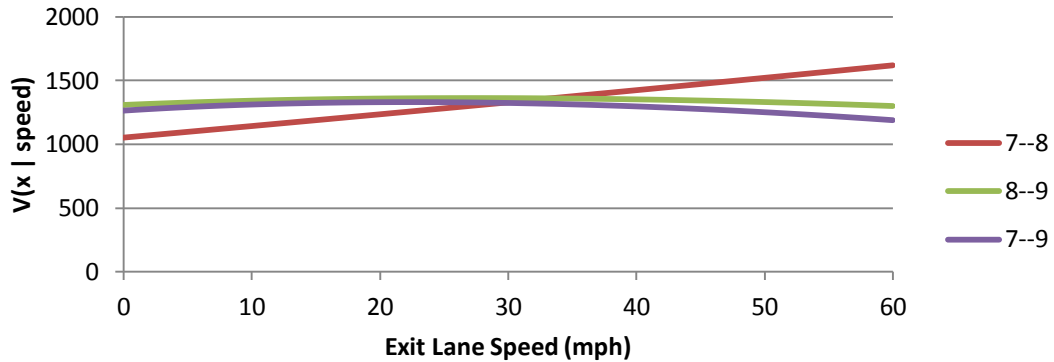


Figure 36: Model Standard Deviation Lane Change Position Predicted by Model (I-85)

A chi-square test is performed on aggregated data to ascertain how well the model performs. If the distributions of the model parameter estimates are normal, the distribution of the sum of square errors for a non-homogeneous Poisson process should approximately chi-square (Massey, 1995). Assessing where the critical value falls on the chi-square distribution (given degrees of freedom) reveals the significance of the model fit. Chi-square test results for the calibration/validation models are shown in Table 14.

The chi-square test results (Table 14) indicate that the model is performing well at low and high speeds, but at speeds between 25 and 40 mph, the model does not perform as well, although significant at the 5% level. Chi-square values for all speed bins for each verification dataset are less than the 5% significance chi-square critical value of 134.37 (109 d.o.f). Expected and observed numbers of lane changes are plotted in Figure 37, Figure 38 and Figure 39 on the following pages. The model tends to fit the data relatively well. A closer look at the observed data and best-fit estimation in Figure 37, Figure 38

and Figure 39 indicates that a consistent error is present 2000 feet upstream of the ramp in the 25 to 40 mph ramp speed range. In this location, the Pleasantdale off-ramp may play a role in the lane change distribution, and is discussed in Appendix C.

Table 13: Chi-Squared Test Results for Best-Fit Curve (I-85)

| | Speed (mph) | 0-5 | 5-10 | 10-15 | 15-20 | 20-25 | 25-30 | 30-35 | 35-40 | 40-45 | 45-50 | 50-55 | 55-60 |
|-------|-------------|-------|-------|-------|-------|-------|-------|-------|-------|-------|-------|-------|-------|
| May 7 | N (30s) | 4 | 23 | 27 | 35 | 35 | 52 | 67 | 34 | 17 | 12 | 8 | 1 |
| | Chi-sq | 102.2 | 124.2 | 112.3 | 122.3 | 94.8 | 116.7 | 114.7 | 116.6 | 111.8 | 116.3 | 114.1 | 47.1 |
| | p-val | 0.665 | 0.151 | 0.395 | 0.182 | 0.832 | 0.290 | 0.336 | 0.291 | 0.408 | 0.298 | 0.349 | 1.000 |
| May 8 | N (30s) | 8 | 19 | 28 | 41 | 39 | 48 | 70 | 46 | 37 | 17 | 8 | 0 |
| | Chi-sq | 79.8 | 99.9 | 118.6 | 117.7 | 108.4 | 122.7 | 113.7 | 113.8 | 103.7 | 105.0 | 114.8 | |
| | p-val | 0.984 | 0.723 | 0.250 | 0.268 | 0.498 | 0.175 | 0.359 | 0.359 | 0.625 | 0.591 | 0.333 | |
| May 9 | N (30s) | 4 | 18 | 32 | 40 | 37 | 53 | 29 | 48 | 17 | 29 | 18 | 21 |
| | Chi-sq | 89.1 | 112.2 | 121.6 | 121.0 | 94.9 | 99.3 | 113.9 | 118.5 | 112.2 | 121.2 | 95.2 | 120.6 |
| | p-val | 0.918 | 0.399 | 0.192 | 0.204 | 0.831 | 0.737 | 0.354 | 0.250 | 0.399 | 0.201 | 0.825 | 0.211 |

Chi-square critical value at 5% significance(109 d.o.f.): 134.37

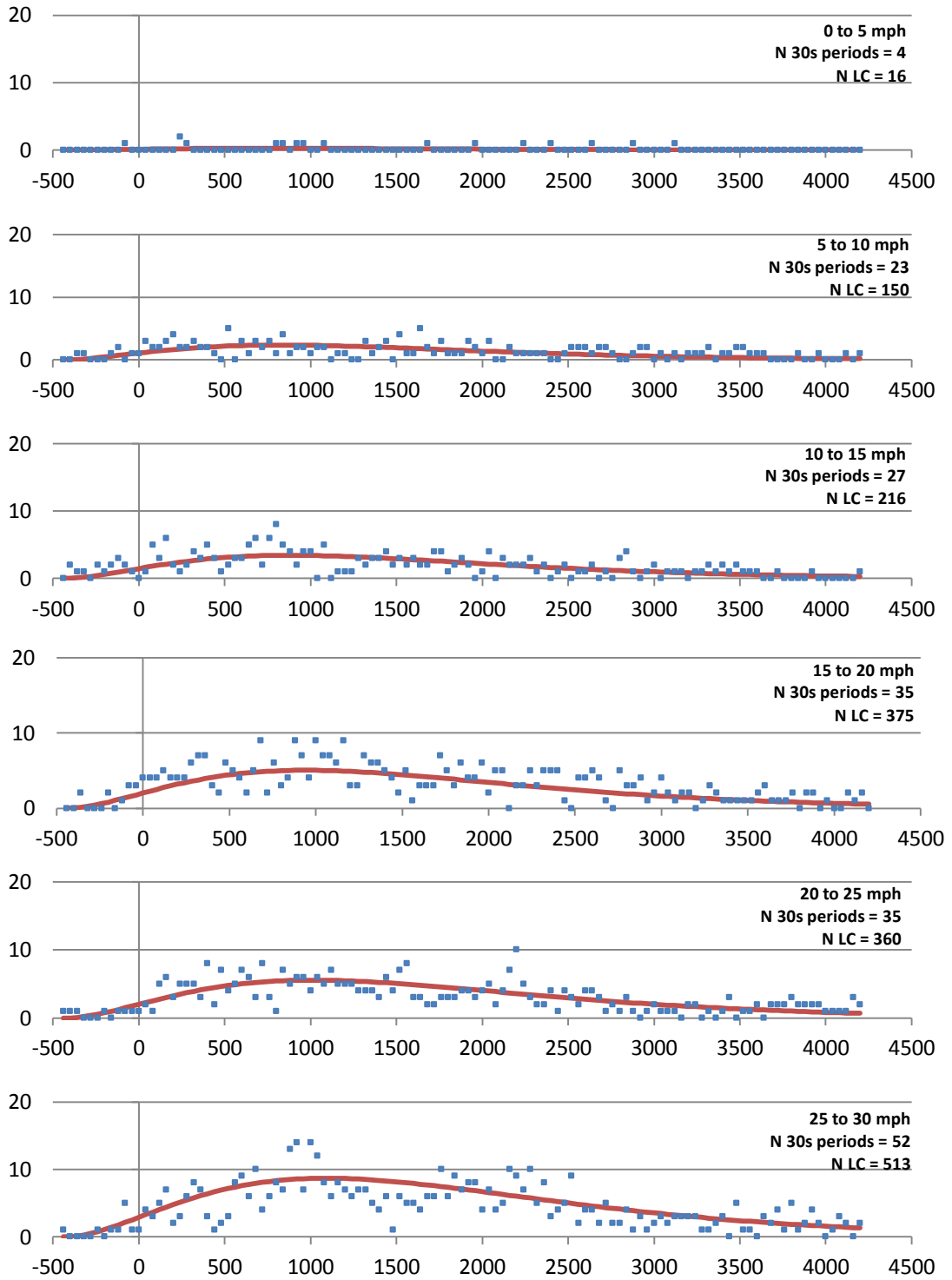


Figure 37: Observed (5/7/13) vs. Final Model

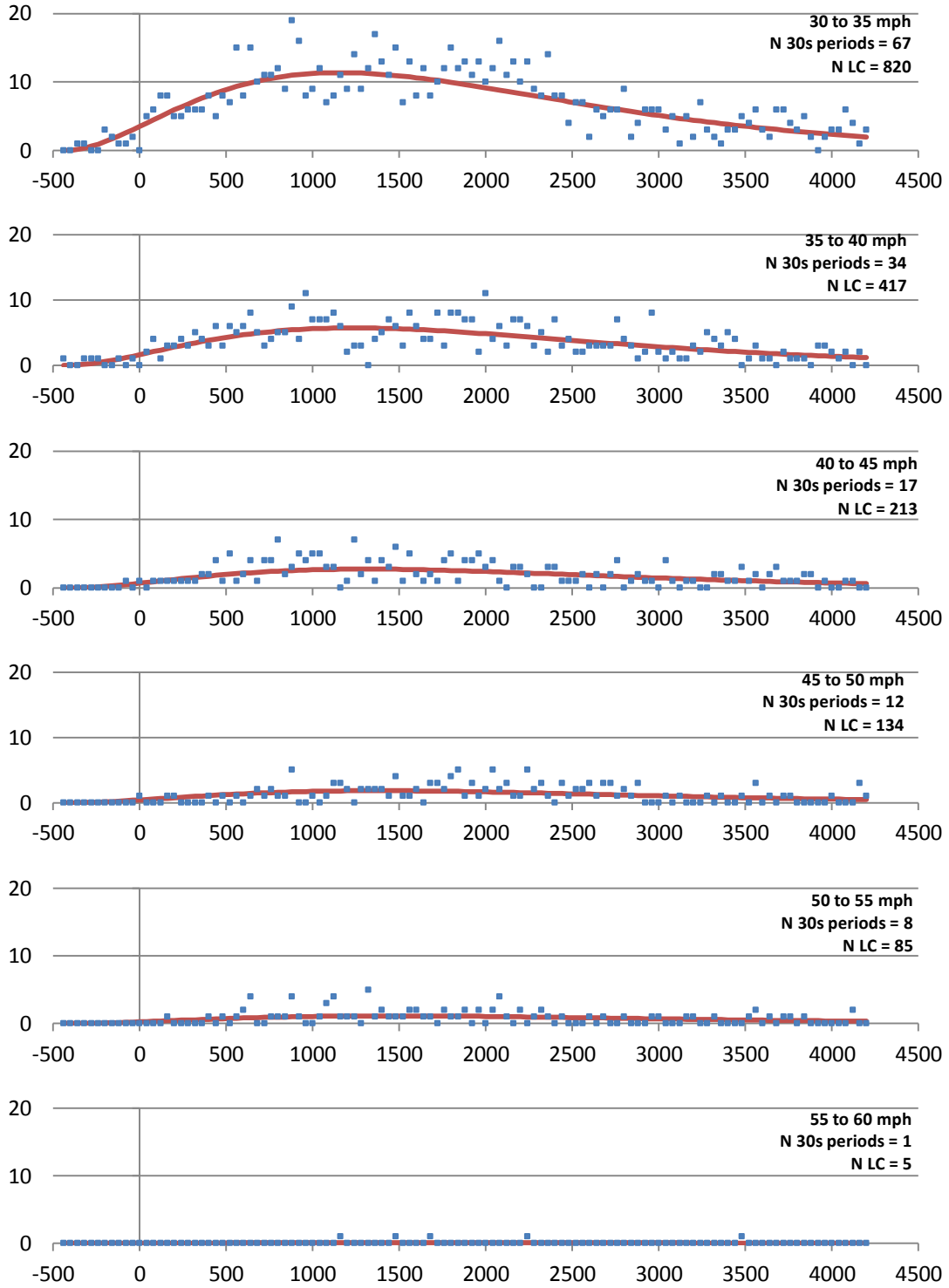


Figure 37 (continued): Observed (5/7/13) vs. Final Model

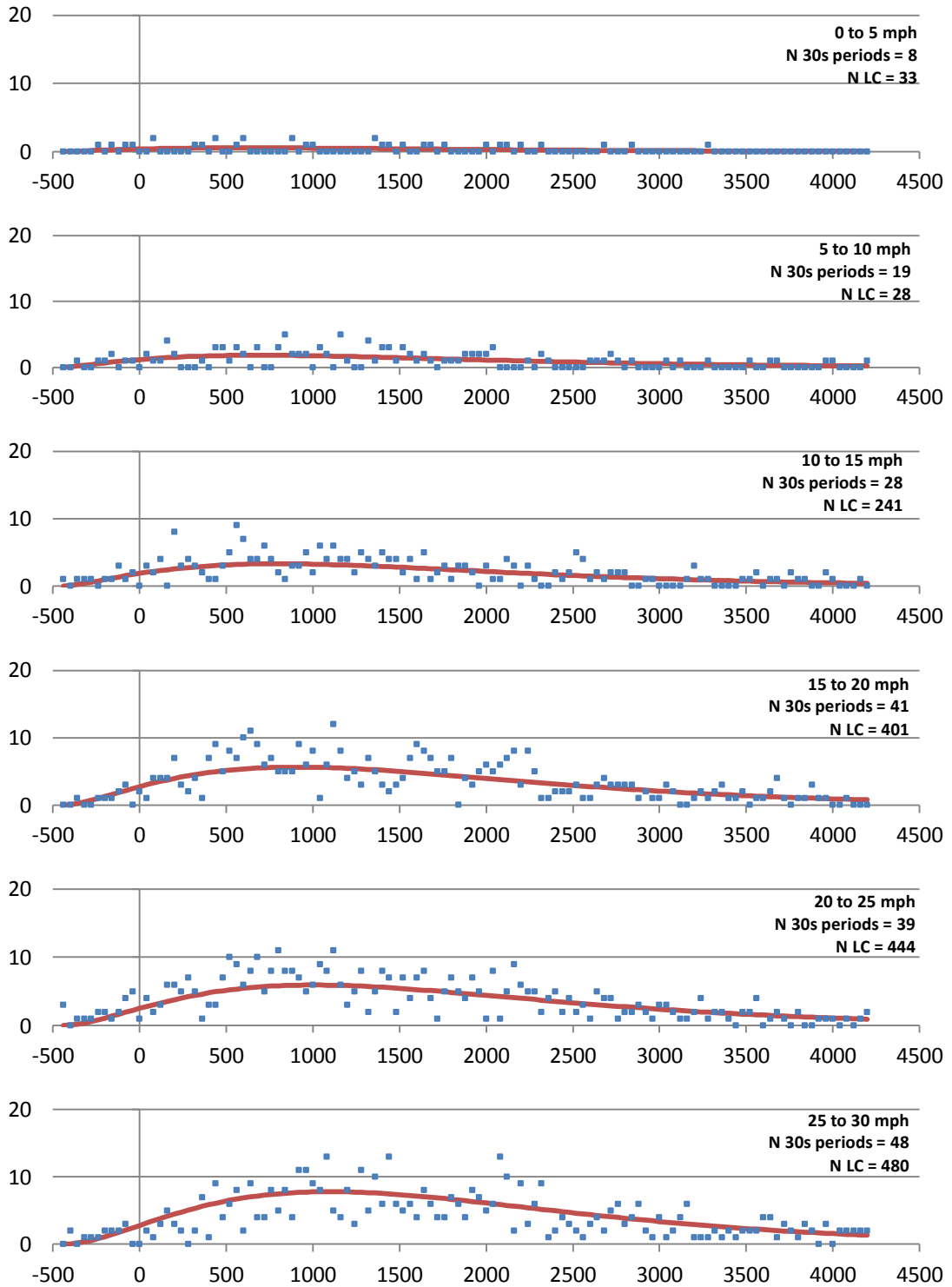


Figure 38: Observed (5/8/13) vs. Final Model

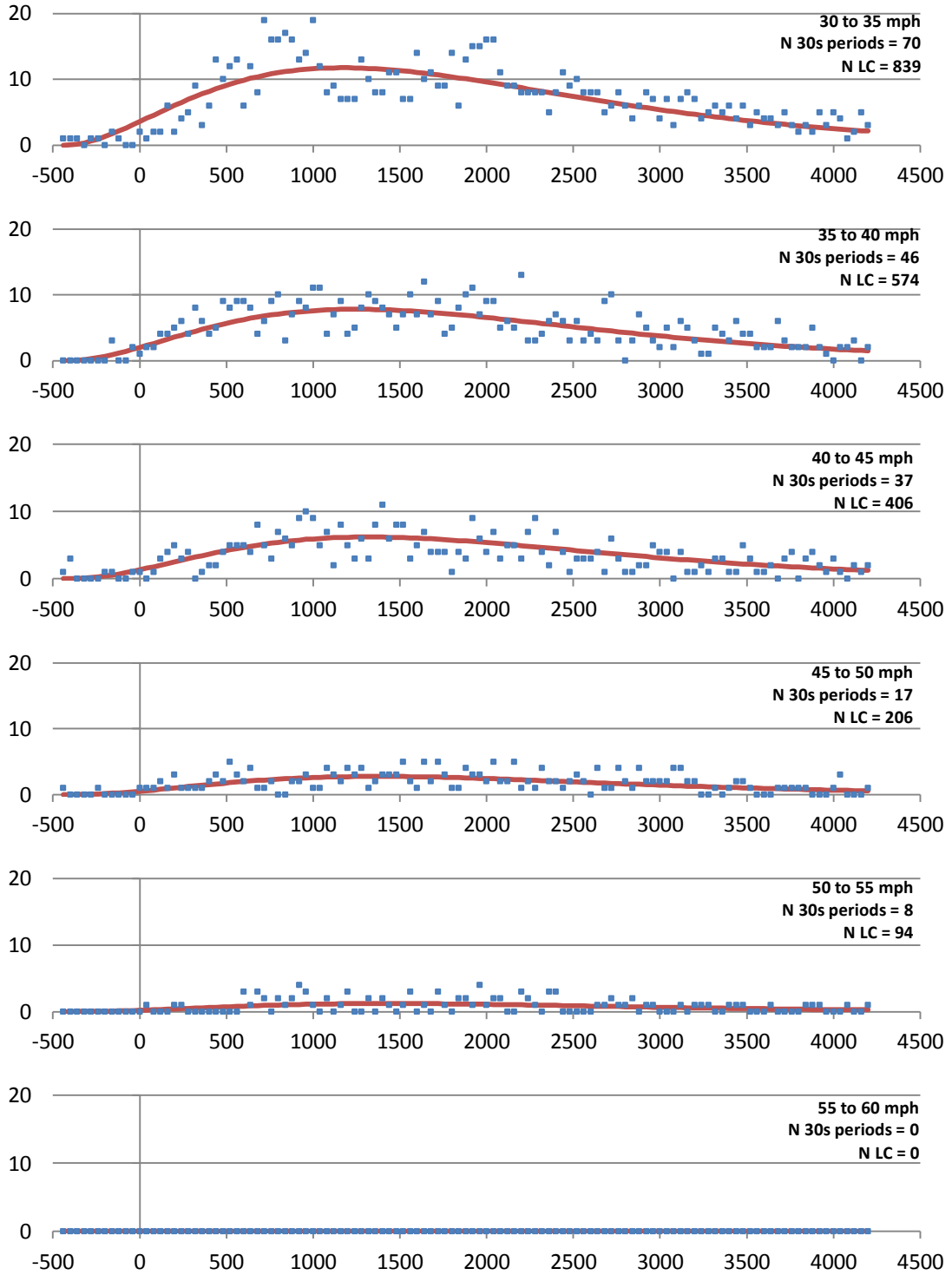


Figure 38 (continued): Observed (5/8/13) vs. Final Model

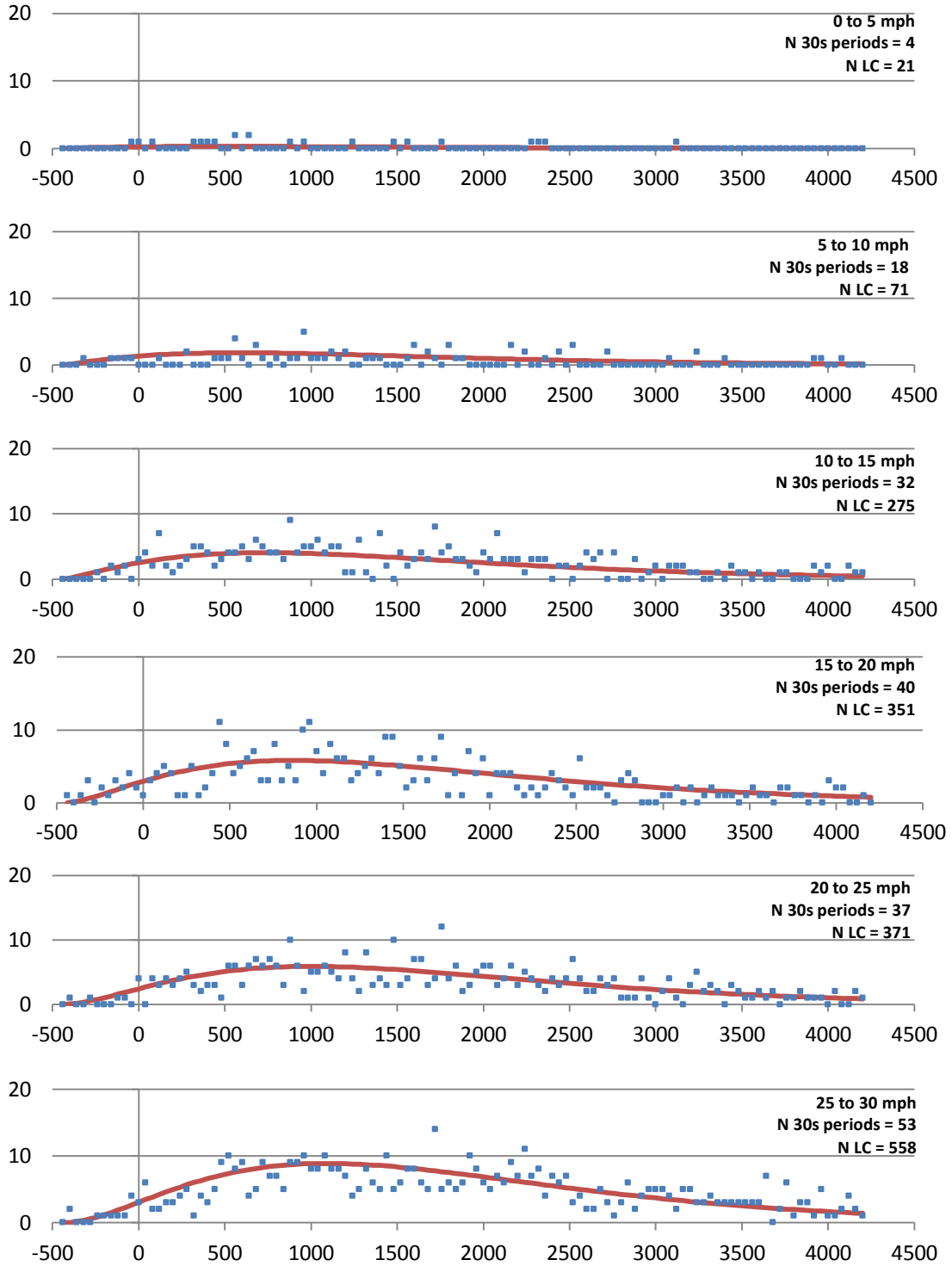


Figure 39: Observed (5/9/13) vs. Final Model

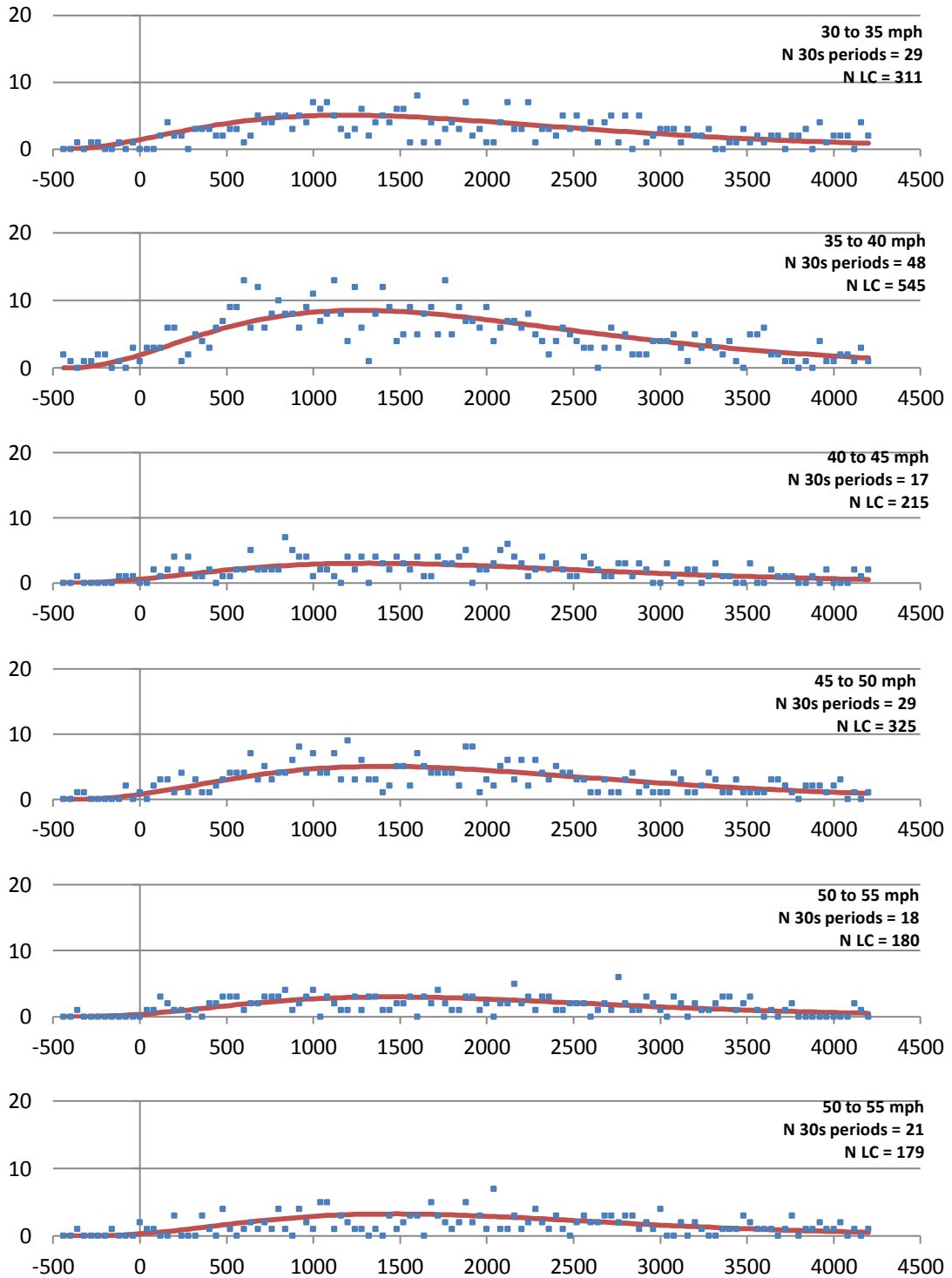


Figure 39 (continued): Observed (5/9/13) vs. Final Model

A model for the relationship between the number of lane changes, ramp lane speed, and lane change location has been developed. The model performs well when used to predict the number of lane changes for validation data sets. Despite the model performing well at low speeds and closer to the ramp, more lane change observations should be made under low-speed conditions closer to the ramp (as they occur infrequently) before the model is applied to other sites.

Secondary Site Model Verification

In an effort to further verify the fitting function, data were collected from a secondary site on October 23 and November 1, 2013. The selected site was the Spring-Buford connector southbound, upstream of the slip ramp to I-85 southbound (see Chapter 3, Figure 8). As with the I-85 site, this site contains an upstream off-ramp which appears to affect the fitting function coefficients, resulting in what seems to be a scaled down version of the lane changing model curve of the I-85 site. Despite lane changes exhibiting a more compact spatial distribution, the parameters are able to control for these changes.

While the observable portion of the segment is much shorter than the I-85 site, it is expected that part of the lane change distribution can be seen. As with the I-85 site, cameras were mounted on overpasses, to collect speed data and to manually extract lane change times and positions. No PTZ cameras were available along this stretch of freeway.

Table 14: Parameter Estimates for Best-Fit Curve (Buford-Spring Conn.)

| Coefficient | Estimate | Standard Error | t-Statistic | P-Value |
|-------------|----------|----------------|-------------|---------------------------|
| a_1 | -0.06193 | 0.020933 | -2.92416 | 0.00345692 |
| a_2 | 4.34649 | 1.02968 | 4.22005 | 0.000024509 |
| a_3 | 77.2344 | 10.2126 | 7.58558 | 3.32×10^{-14} |
| a_4 | 0.015295 | 0.0110175 | 1.6152 | 0.106257 |
| a_5 | 2.15698 | 0.190071 | 8.83421 | 1.07139×10^{-18} |
| a_6 | 3.64988 | 3.93009 | 0.892071 | 0.892071 |
| a_7 | 328.161 | 68.324 | 5.77637 | 7.72158×10^{-9} |

The parameter estimates for the relationship between speed and magnitude of lane changing activity (a_1, a_2, a_3) are similar in magnitude to the parameters found at the I-85 site. The max lane changing rate is found at 35 mph, similar to the I-85 site. The parameter estimates for the gamma distribution parameters are of the same sign as the parameters of the I-85 site, but the average and standard deviation of the lane change position are smaller. The a_4 and a_6 gamma distribution parameter coefficients are insignificant at the 5% significance level. It is not surprising that the two insignificant variables are the same as the two least significant variables when the model was run on the I-85 lane change data. Although the performance of the model is good, additional research may be needed to confirm the inclusion of these variables, or to isolate factors in addition to ramp lane speed that influence model performance.

As with the I-85 site (all data), the model calibrated using the Buford-Spring Connector data indicates the average lane change position increases with respect to speed (Figure 40). At both sites, the average lane change location upstream of the exit ramp increases with respect to speed. However, the lane change position standard deviation of the Buford-Spring model (Figure 41) increases with respect to speed, not providing any

definite evidence into the relationship between speed and standard deviation in lane change position. At the very least, it can be estimated that the variance of lane change position either remains constant or increases with respect to speed. Further research is needed to make a more conclusive statement regarding this relationship.

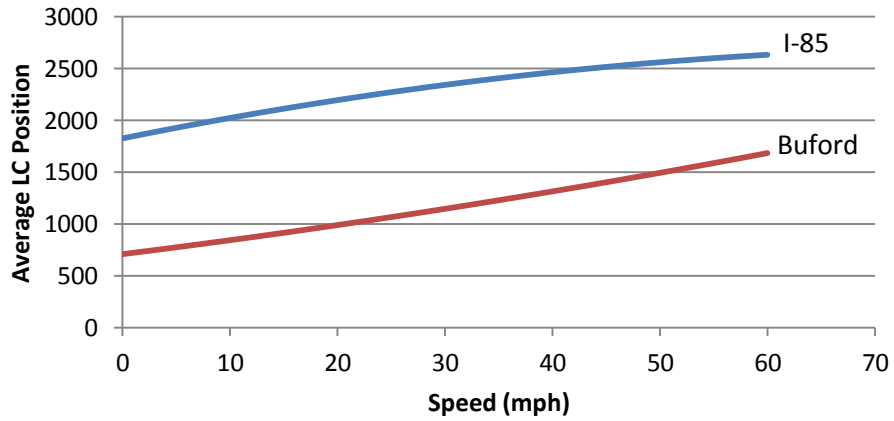


Figure 40: Average Lane Change Position

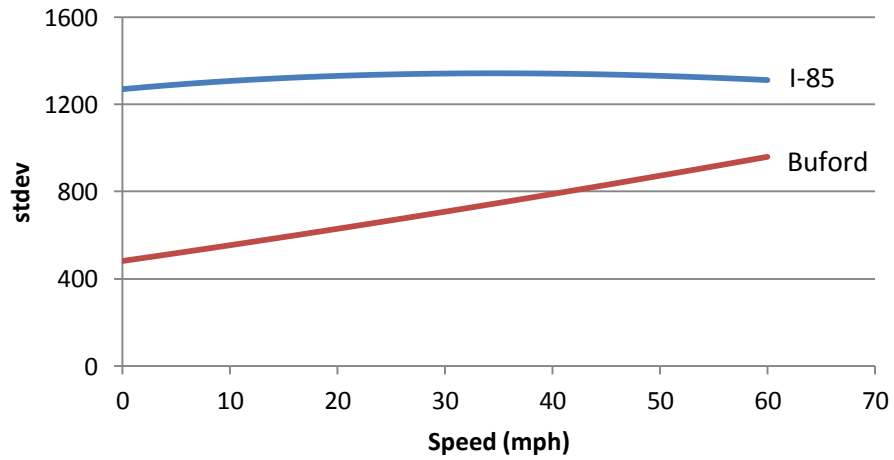


Figure 41: Standard Deviation of Lane Change Position

Inspection of the fit curve (Figure 42) indicates many more of the lane changes are occurring closer to the ramp and with lower spatial variance compared to the I-85 site. The figure is plotted at the same scale as the I-85 site for reference. Curve fit beyond 1600 feet should not be interpreted, as there is no data in this region, and the shape of the distribution beyond 1600 feet is purely speculative. As with the I-85 site, this site contains physical infrastructure which appears to affect the coefficients of fitting function. Despite a lane change spatial distribution exhibiting lower average and standard deviation, the fitted parameters are able to control for these differences between the I-85 site and the Buford-Spring site. However, the relationship between site characteristics and the model parameters are left as a topic for future research. Results from a chi-square test indicating the results of the fit are displayed in Table 15. Chi-square values for all speed bins are less than the 5% significance chi-square critical value of 61.7 (47 d.o.f). As with the I-85 site, last-minute lane changing is not predicted accurately by the model. Comparisons within 120' of the physical gore are not included in the chi-square test evaluation of the model.

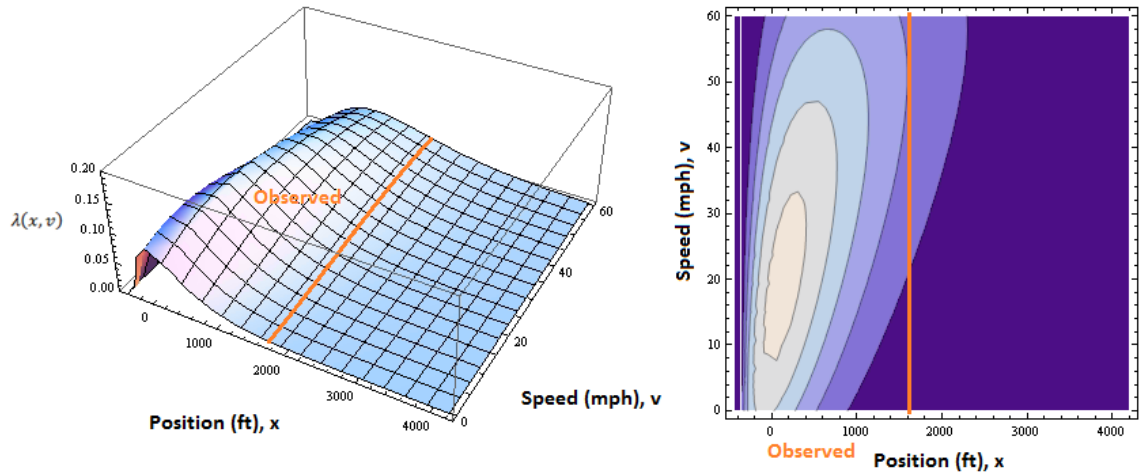


Figure 42: Three-Dimensional and Contour Plots for Best Fit Model (Spring-Buford Conn.)

Table 15: Chi-Squared Test Results for Best-Fit Curve (Buford-Spring Conn.)

| Speed (mph) | 0-5 | 5-10 | 10-15 | 15-20 | 20-25 | 25-30 | 30-35 | 35-40 | 40-45 | 45-50 | 50-55 |
|---------------|------|------|-------|-------|-------|-------|-------|-------|-------|-------|-------|
| N 30s periods | 28 | 143 | 121 | 76 | 41 | 32 | 21 | 24 | 10 | 19 | 6 |
| Chi-sq | 53.9 | 59.8 | 56.5 | 37.8 | 54.4 | 35.7 | 52.9 | 34.2 | 30.4 | 58.3 | 35.5 |
| p-value | 0.15 | 0.06 | 0.10 | 0.74 | 0.14 | 0.81 | 0.17 | 0.86 | 0.94 | 0.07 | 0.81 |

Chi-square critical value at 5% significance (47 d.o.f.): 61.7

The chi-square test results indicate the new model fits the observed data well, and the fitting equation can be calibrated to work at other sites. Comparing the model shape from the Buford-Spring site against the I-85 site, there appears to be dependence between site characteristics and the model parameters. Thus, caution should be exercised when transferring the results from one site to another. However, the fitting equation remains the same for both sites, and is a noteworthy contribution in the field of traffic operations. The data collection method can be applied and a curve can be calibrated for other off-ramp sites. As data from additional off-ramp sites become available, factors that influence the model parameters between sites can be analyzed in further detail, and more advanced

models can be derived. A discussion on expanding the model is presented in more detail in Chapter 9.

A comparison of observed and expected data from the model calibrated using the Buford-Spring Connector data is shown in Figure 43 on the following page. In the 5 to 15 mph range, the model seems to underestimate the number of lane changes around the beginning of the painted gore (0'). This is interesting considering this is the location of the maximum amounts of lane changing for this site. Such an underestimation is not noted at the I-85 site, indicating this may be an anomaly, but could also be explained by drivers insisting on moving into the ramp lane without moving through the painted gore. Aside from this speed-space region of the model, there tends not to be bias present in the residuals.

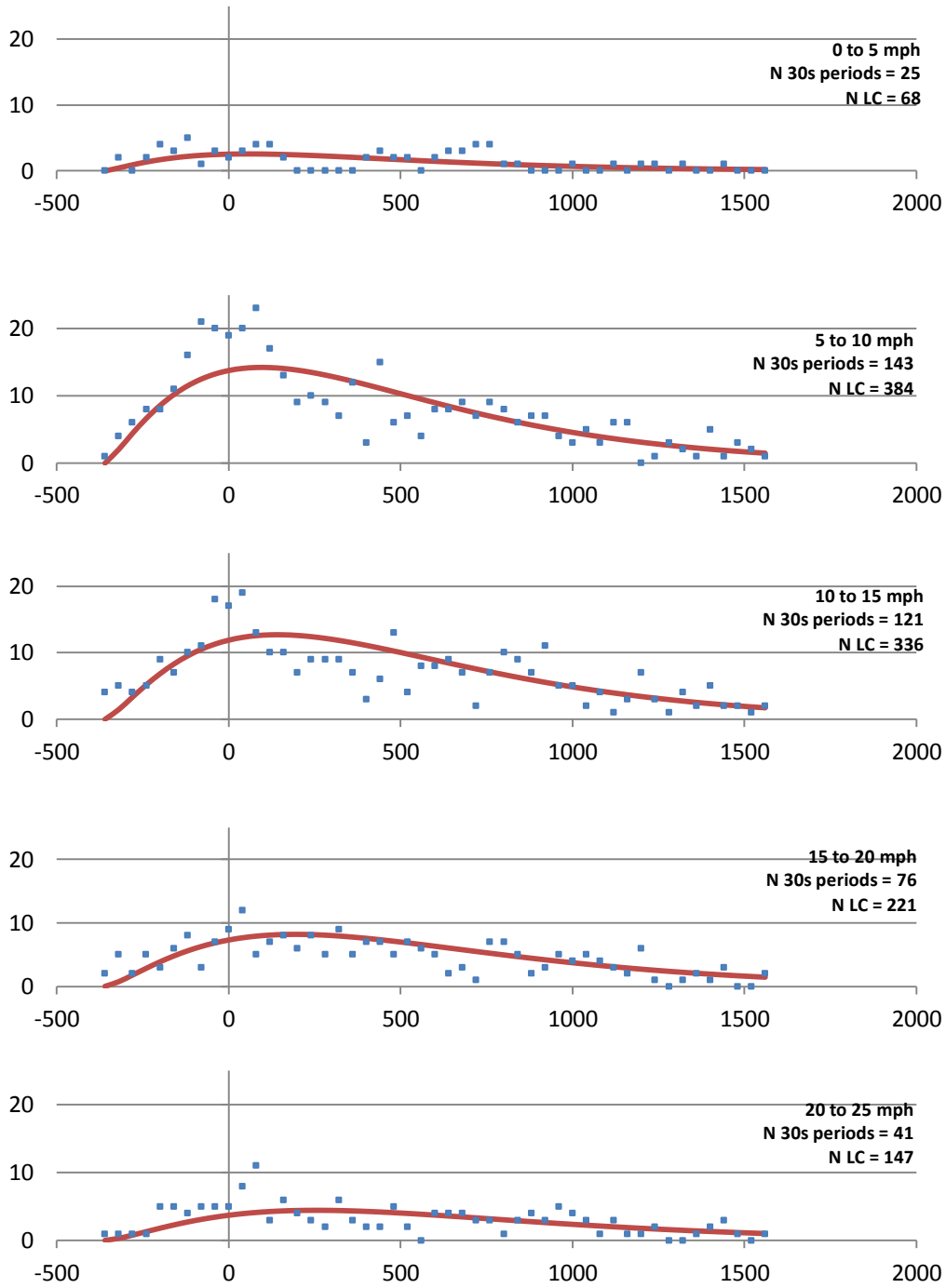


Figure 43: Observed vs. Expected Number of Lane Changes (Buford-Spring Connector)

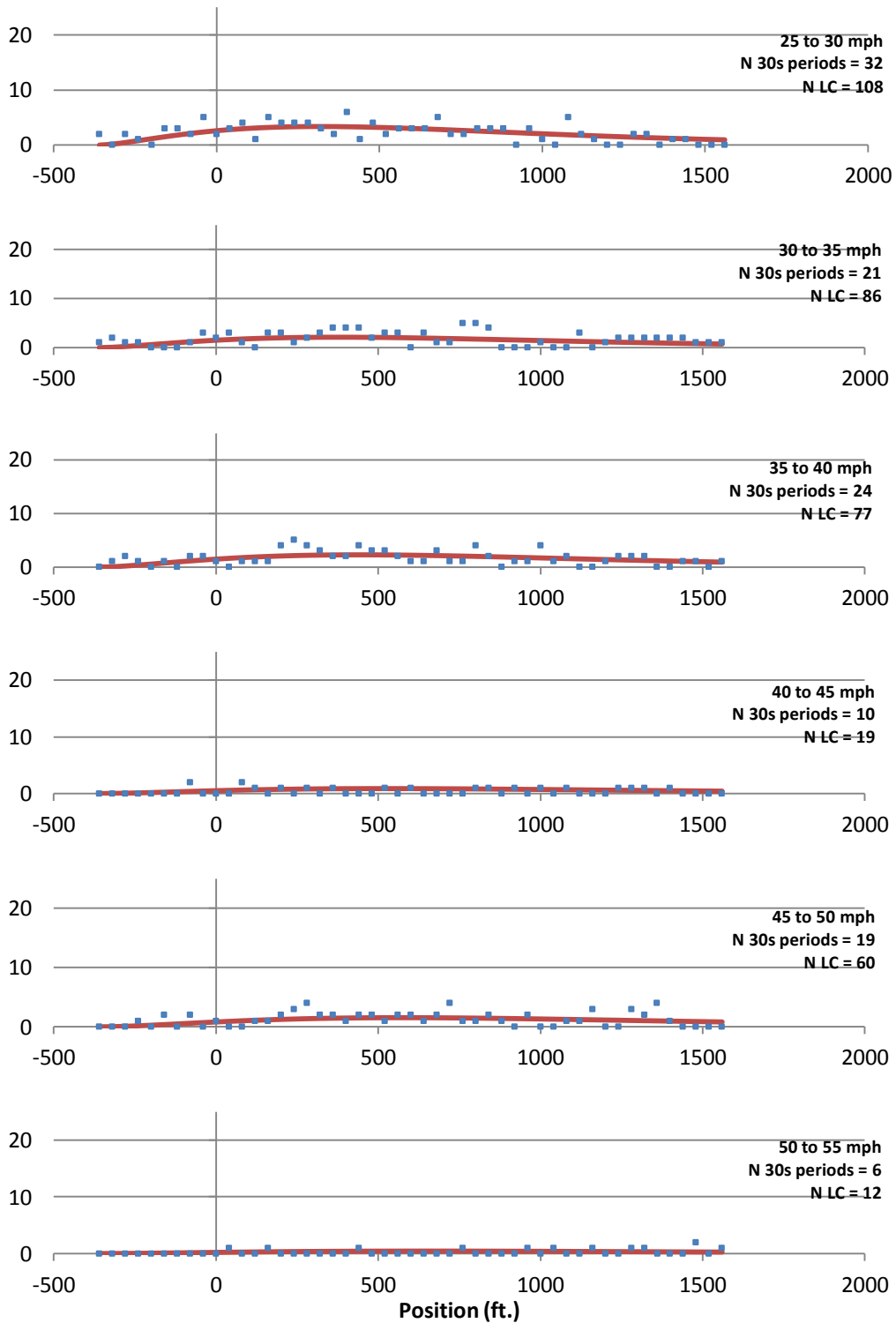


Figure 43 (continued): Observed vs. Expected Number of Lane Changes (Buford-Spring Connector)

Lane Changes out of a Ramp Lane

Movements from the ramp lane into the mainline through lanes are just as important as lane changes from a through lane to a congested ramp lane. Lane changes from the ramp lane to a through lane are also mandatory as drivers wishing to remain on the mainline must move out of the exit lanes to do so. As with mandatory lane changes into the ramp lanes, lane changes out of the ramp lane are expected to exhibit well-ordered macroscopic lane changing behavior. Shown below is the spatial distribution of all the 6 to 5 lane change data.

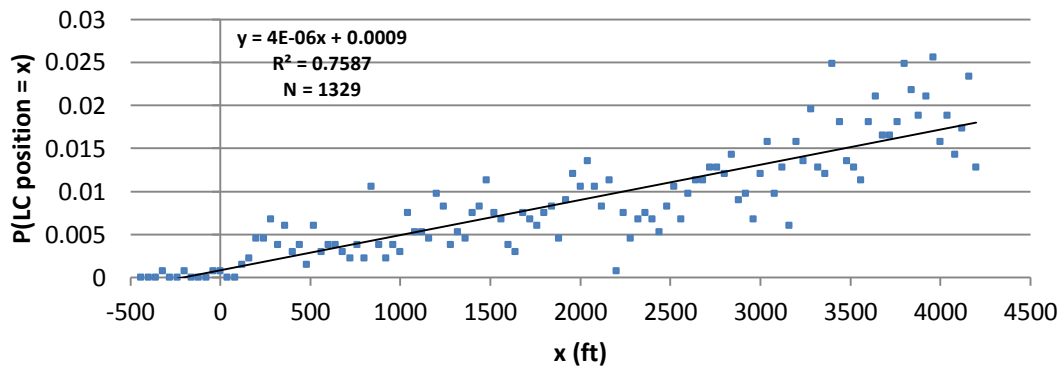


Figure 44: Spatial PDF of All Lane Changes from Lane 6 to Lane 5 (5/7/13 - 5/9/13)

The data displays an upward trend, drivers are more likely to change out of the ramp lane further upstream of the ramp. However, by observation, the shape of the spatial distribution is not obvious. A look at the cumulative distribution function (Figure 45) of this data lends further insight into the distribution from which the spatial component of these lane changes is derived.

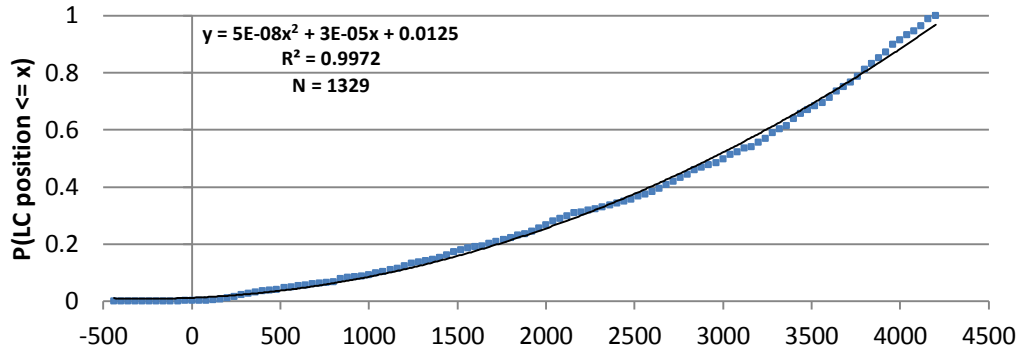


Figure 45: Cumulative Distribution Function of Lane Changes from Lane 6 to Lane 5

A best-fit second-order polynomial is fit to the data, and is able to account for over 99 percent of the variance in the data without an intercept term. The derivative of the function used to describe the CDF gives a triangular (linear) PDF. A bootstrap study to find the best fit distribution to represent lane changes out of the ramp lane should assume a triangular (linear) PDF. It is important to remember that the result of regressions that pertain to these lane changes should not be extrapolated beyond the limits of the study area. Obviously, there are limits to the amount of lane changing that can occur over a given distance over a given amount of time. Given this function cannot continue to increase indefinitely in this manner, it must also be recognized that an estimate cannot be made regarding the shape of the rest of the distribution, or the estimated portion of the entirety of the distribution that is observed in the study section. One hypothesis may be that this is the tail end of a distribution belonging to the exponential family of distributions. However, insufficient data upstream of the study site do not allow exploration of the hypothesis. The tail of the full distribution (data at hand) can at best be approximated by a triangular PDF.

When paired with lane changes across the same boundary in the opposite direction, it becomes fairly obvious that a majority of lane changes are moving into the ramp lane in the study area. However, at some point upstream of the study section, it is expected that a majority of the lane changes will be vehicles leaving the exit lane, perhaps moving over to the mainline lane after entering the freeway from the Jimmy Carter on-ramp, approximately 2.25 miles upstream of the ramp to I-285. Given this long distance between ramps, the area where the majority of lane changes switches between opposing lane change movements occurs at point in each distribution where there is not a lot of lane changing occurring. Future research could focus on the interaction of the shapes of spatial distributions of opposing lane changing movements (lane 5 to lane 6 against lane 6 to lane 5) when they are forced to interact over a shorter distance. Many such locations are available, although finding a suitable location where adequate data can be collected may be more difficult.

Furthermore, given the ideal infrastructure situation, the on-ramp from Jimmy Carter (2 miles upstream) would not exist. The presence of this on-ramp may influence, not necessarily, the shape of the spatial distribution of lane changes out of the ramp lane closer to the ramp diverge to I-285, or in the case of the study section, the data presented in this analysis.

Macroscopic Lane Changing Model Conclusion

In this chapter, a relationship between the expected number of lane changes, exit lane speed, and distance upstream of the off-ramp has been developed. The model will estimate the parameter of the Poisson distribution that corresponds to the expected

number of lane changes in a 40 foot segment over a 30 second period. Inputs to the model include the distance from the offramp to the 40 foot segment and the speed of the exit (target) lane. There is a gamma-like relationship between the location of the 40 foot segment and the expected number of lane changes. Each of the parameters of the gamma distribution is estimated as a linear function of exit lane speed. As ramp lane speed increases, the average lane change position moves further and further from the ramp. Conclusions regarding the variance of lane change location are unknown with respect to target lane speed. Furthermore, the magnitude of the gamma distribution is a parabolic function of the speed of traffic in the exit (target) lane. Lane changing intensity is lower at lower target lane speeds, increasing until target lane speeds are between 35 and 40 mph, and continually decreasing as speeds increase beyond 40 mph.

The same model equation form was fitted at a secondary site. While the same model form provided a good fit to the observed data, its parameters were quite different compared to the model developed from data from the first site. The secondary site exhibited different physical characteristics which likely resulted in different parameters. The relationship between freeway physical characteristics and the model parameters is left as a topic for future research, and is discussed in Chapter 9.

While the model does an adequate job of assessing macroscopic lane changing behavior, the impacts lane changes have on traffic flow have not yet been quantified and analyzed. The next chapter will develop the relationship between lane changing behavior (into a congested exit lane) and the lateral propagation of congestion.

CHAPTER 7: LATERAL PROPAGATION OF CONGESTION

Lane changing is expected to contribute to the lateral propagation of congestion from exit lanes to the through lanes. That is, when a ramp lane becomes congested, the congestion is likely to propagate to other lanes on the mainline (Cassidy, Jang, and Daganzo, 2001). However, the mechanism by which this propagation occurs has not been studied to date.

In the previous chapter, a preliminary model was developed for lane changing from a mainline through lane into a congested ramp lane. The model is macroscopic. It estimates the likelihood of a number of lane changes given a target lane speed and location upstream of the ramp. The effects these lane changes have on the traffic stream is not accounted for in the model. Analyses in this chapter examine the potential link the behavior of drivers making these lane changes to the lateral propagation of congestion observed in this study and other studies (Munoz and Daganzo, 2000).

Understanding the factors that contribute to the propagation of congestion should lead to a better understanding of driver behavior and freeway operations. Table 16 outlines three ways in which congestion can propagate through a freeway corridor. Each congestion propagation mechanism is considered in the analysis of freeway speed prediction, and is described in the following paragraphs.

Table 16: Mechanisms of Congestion Propagation

| Propagation Type | Direction of Propagation | Figure |
|-------------------------|---------------------------------|---------------|
| Wave | Longitudinal | Figure 46a |
| Friction Factor | Lateral | Figure 46b |
| Disruption | Lateral | Figure 46c |

Predicting upstream speed is typically accomplished by observing a downstream traffic state and propagating that condition upstream at the wave propagation speed of congestion. An example of wave propagation is shown in Figure 46a, as congestion waves propagate backward through the system at approximately the same time on both lanes. While this may provide a decent estimation in a homogeneous traffic stream, there are conditions under which the aforementioned model does not perform well. One of these cases is the presence of a congested off-ramp. If the mainline does not experience congestion downstream of the off-ramp, the simple wave-propagation model would suggest that traffic conditions in non-ramp lanes upstream of the ramp should be in free flow.

Multiple factors are considered to affect the speed differences between lanes. A friction factor may exist between lanes with a high speed differential (Guin, et al., 2008). While there are certain situations (managed lane) where the friction factor explains a speed differential between a congested and otherwise free-flowing lane, there are other situations where mechanisms other than the friction factor may be contributing to a reduction of speed in the less-congested lane. Disruptions made by lane-changing vehicles may also be responsible for the lateral propagation of congestion.

A friction factor between the mainline lanes and the congested ramp could contribute to the lateral propagation of congestion into the mainline. The friction factor

explains a decrease in speed, as drivers display more cautious behavior when traveling past slowed or stopped traffic lanes (Guin, Hunter, and Guensler, 2008). Under this assumption, lane-by-lane traffic speed would increase in mainline lanes further away from the congested ramp lanes. While this freeway operation characteristic is noted within the first mile upstream of the ramp, even further upstream, it is noted that speed across lanes is more homogeneous. This effect, which has been noted by other researchers (Cassidy, Annai, and Haigwood, 2002; Munoz and Daganzo, 2000), is only partially explained by the friction factor.

Figure 46b shows a situation where a congested off-ramp spills back onto a freeway. Not much lane changing occurs between the left and right lanes, as most of the traffic that needs to stay on the freeway is already in the left lane, and most of the traffic that needs to use the ramp is already in the right lane. However, drivers in the left lane exhibit slower speeds and increasing following (gap) distance to provide more reaction time for avoiding potential collisions with vehicles moving out of the congested lane in front of the driver. Downstream of the off-ramp, the friction factor between the two lanes is minimal, as the right lane is now in free-flow.

There is an alternative case where many drivers are making the mandatory maneuver from the left to the congested exit lane. Given potentially varying conditions in the exit lane, a fraction of lane-changing drivers decrease speed to match the speed of traffic in the ramp lane, wait for an acceptable gap, and cause following drivers to slow down to a speed below what would be predicted by the friction factor (Figure 46c). It is hypothesized that these lane-changing disruptions are partially responsible for the lateral propagation of congestion from the ramp to the mainline, and may be able to help explain

why lane-by-lane speeds become more homogeneous further upstream from the ramp. Such lane changes are disruptive to conditions in the initial lane, and are referred to as disruptive lane changes from this point forward.



a. Wave Propagation b. Friction Factor c. Lane Changing Disruption

Figure 46: Types of Congestion Propagation

The lane-to-lane progression of the lateral propagation of congestion is evident in Figure 47. Data for the figure were provided by the GDOT VDS system. Downstream of the ramp, all of the mainline lanes are in free-flow. Just upstream of the congested ramp, there are much larger speed differences between lanes. The slowest speeds are noted in the ramp lanes, and speeds continuously increase from lane to lane moving to the left. Moving further upstream, the variance in speed between lanes decreases. However, at this point, all lanes are experiencing congestion, except the HOT lane, as lane changes are prohibited into and out of the HOT lane at this location.

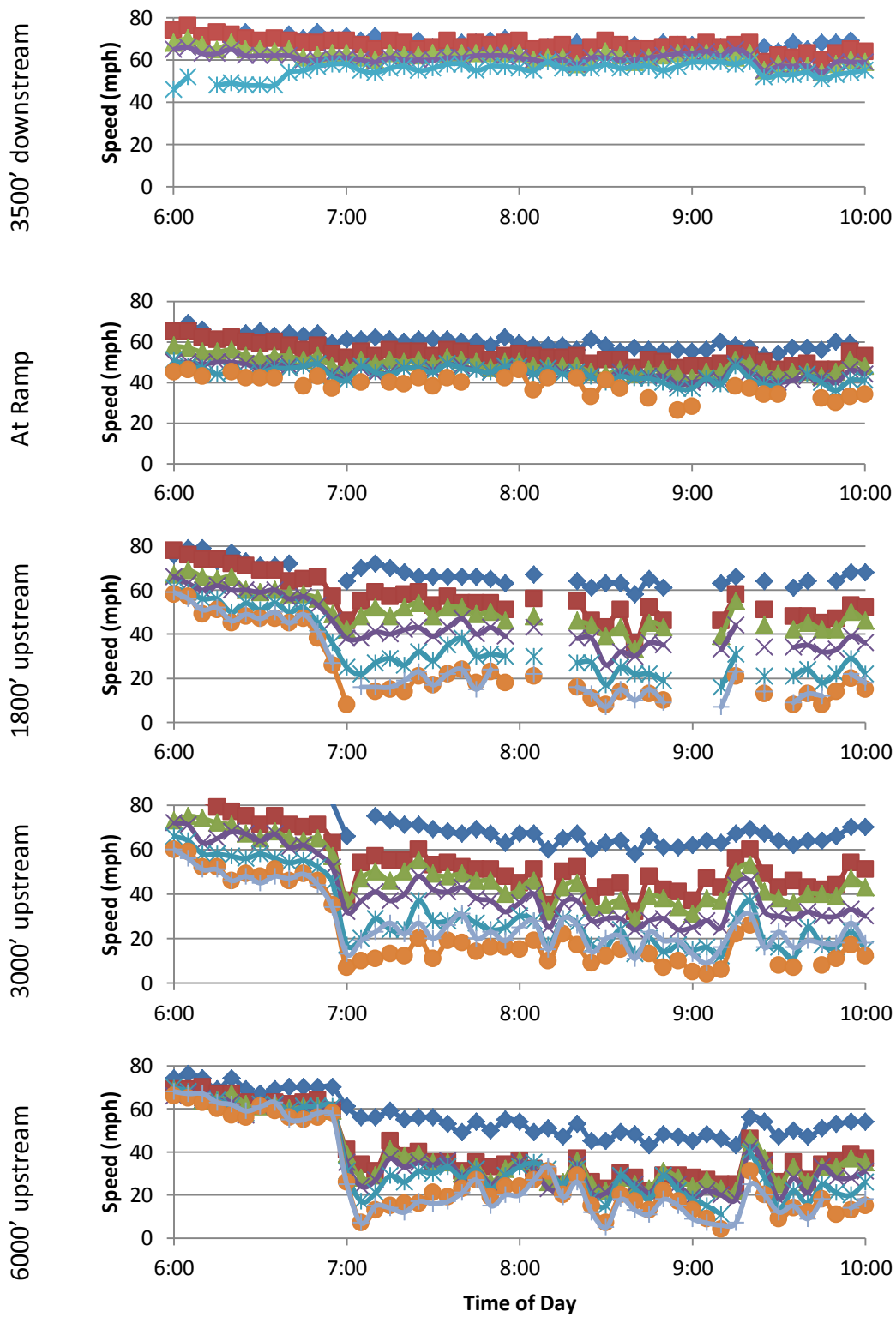


Figure 47: Lane-by-Lane VDS Speed in the Vicinity of the Ramps to I-285 WB

To test the hypothesis that disruptions impact the lateral propagation of congestion, linear regression models can be created to estimate whether speed at an upstream location is more closely correlated with the propagation of speed from a downstream location or with the speed of a disturbance given the presence of a disruption.

Certain drivers, when attempting to enter the ramp lanes, may decrease speed to match the speed of traffic in the target ramp lane. Sometimes, the lane-changing driver is able to maneuver quickly and easily into the target lane, without affecting the following behavior of proceeding drivers. Other drivers decelerate, causing the speed of the lane to drop well below speeds that appear to result from a simple friction factor between the lanes, leaving large gaps in front of them while waiting for a gap to open in the lane they are entering. Lane-changing drivers displaying this type of behavior are said to be causing a disruption on the initial lane. The impact of each disruption can vary greatly, depending on its speed and duration, and its interaction with other disruptions. Disruptions result in the formation of downstream gaps, increasing the availability of space for making lane change maneuvers downstream of the disruption.

Disruptions are not necessarily made only by lane-changing vehicles. A vehicle that slowly accelerates within the traffic stream, perhaps in cases where a driver has a slow reaction time, may also contribute to a disruption. Additionally, a disruption is not always made when the vehicle moves into the exit lane. Vehicles required to make multiple lane changes to exit have the potential to cause disruptions across all lanes between their initial lane and the exit lane. Furthermore, some drivers appear to purposefully make multiple lane changes very close to the exit ramp to avoid the slower-

moving ramp traffic in these lanes for as long as possible. Traffic attempting to exit from the HOT lane must cross multiple lanes within a short span. Disruptions tend to be more visibly noticeable when the target lane is moving slower. Frequent slow or stopped conditions in the I-85 ramp lanes to I-285 westbound provide an opportunity to observe disruptions caused by drivers moving into the ramp lane.

In certain instances, a single vehicle will create a very large disruption by coming to a stop (or near stop) for a pronounced period of time in the initial lane of a weave. In such extreme cases, it is easy to show a cause-effect relationship between the disruption and the resulting wave. However, in other cases, the formation of a wave is more subtle, resulting from several disruptions feeding off one another. One vehicle may create a small disruption to make a lane change, causing proceeding vehicles to slow down. Once that vehicle has changed lanes and the disruption has ended, vehicles queued up behind the lane changing vehicle accelerate until another vehicle waiting in the queue either accelerates slowly or remains in queue to change lanes, resulting in an extension of the original disruption. The process can be repeated resulting in longer lasting waves.

To assess the driver behavior that results in the lateral propagation of congestion, the speed of vehicles in each lane are needed, as well as the trajectories of vehicles making lane changes that are hypothesized to be responsible for creating disruptions that slow traffic down in the initial lane. The tracking software is used to extract time-space information from a subset of automatically detected vehicles from each overpass and overhead PTZ camera to estimate speed of the traffic (as described in Chapters 4 and 5). Time-space trajectories for disruptive lane-changing vehicles are manually extracted from available cameras where camera coverage is available, (PTZ cameras and overpass

cameras do not provide sufficient coverage to extract accurate automated vehicle trajectories for the entirety of the study corridor).

An example of several disruptive lane changes is presented in Figure 48. Each screenshot, taken five seconds apart, show an initial disruption due to a lane change, and an extension of the disruption due to the behavior of following lane changing drivers. In the first frame (9:35:48), a bus decreases its speed to move into a gap in the ramp lane. A large gap is left in front of the bus, the vehicles behind the bus slow down, and can be seen following each other more closely in the second frame (9:35:53). Also, in the second frame, the bus has completed its lane change, and vehicles immediately following the bus have also had time to maneuver into the ramp lane. Because of these lane changes, a vehicle moving from Lane 4 to Lane 5 takes advantage of the open space created by the lane changing vehicles. The vehicles in Lane 5 begin to accelerate in the third and fourth frames (9:35:58, 9:36:03). By the fifth frame (9:36:08), the blue van is traveling noticeably slower than it would be under typical car-following conditions. In the sixth frame (9:36:13), the blue van has not moved, a queue starts to build behind the blue van, and a white car has moved into Lane 5 from Lane 4, taking advantage of space created in front of the blue van. The blue van can be seen nudging its way into the exit lane as the queue extends in the seventh frame (9:36:18). By the eighth frame (9:36:23), the van has completed the lane changing process, and the queue of vehicles behind it can accelerate. Disruptive lane changing, as evidenced in the Figure 48 example, is more common and easily-noticeable when the exit lanes are moving at lower speeds. As exit lane speed increases, disruptive behavior and the intensity of its impact appears to diminish. Case studies of the impacts of disruptions are presented in the next section.

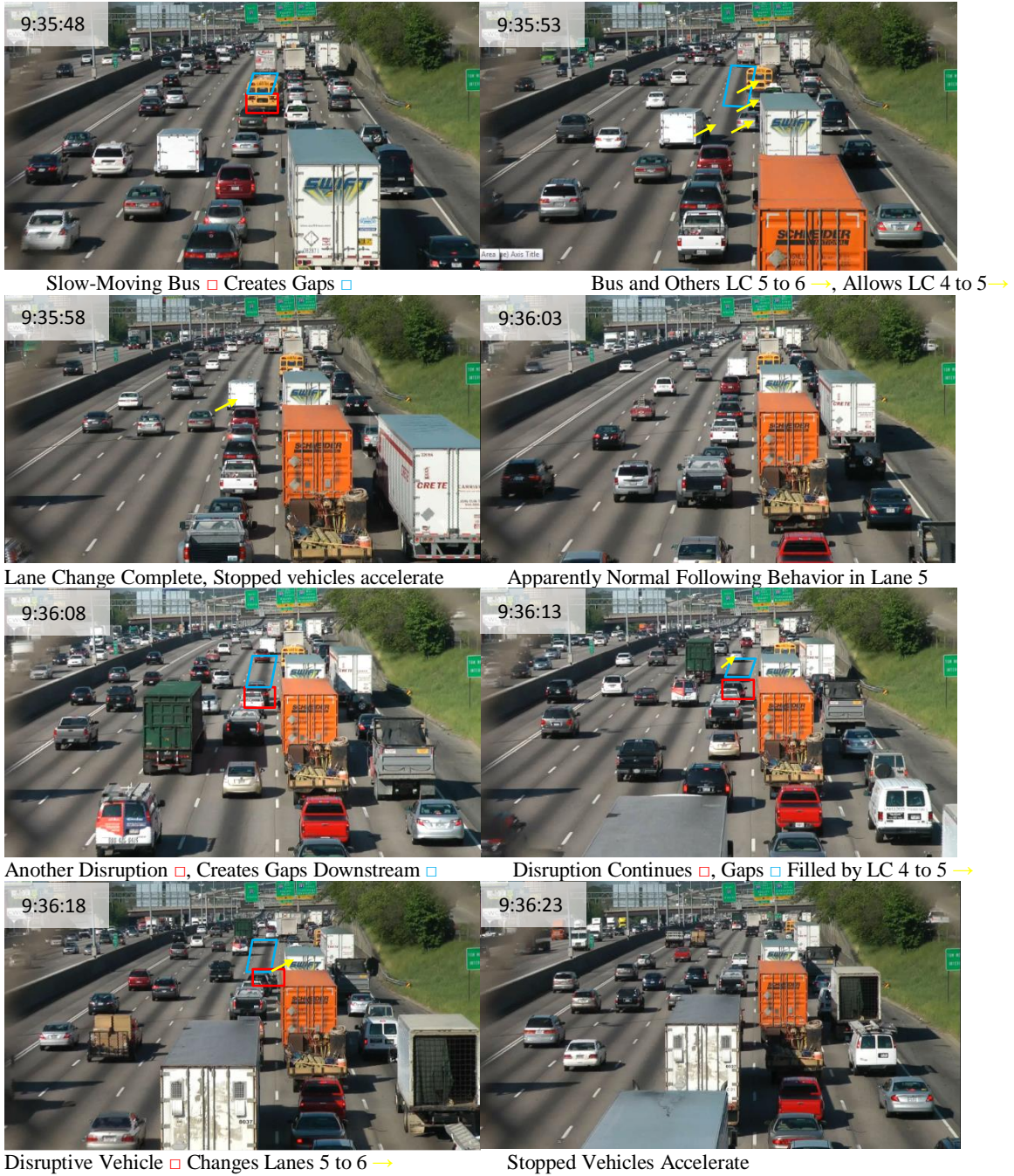


Figure 48: Disruptive Lane Change Progression Example (May 8, 2013)

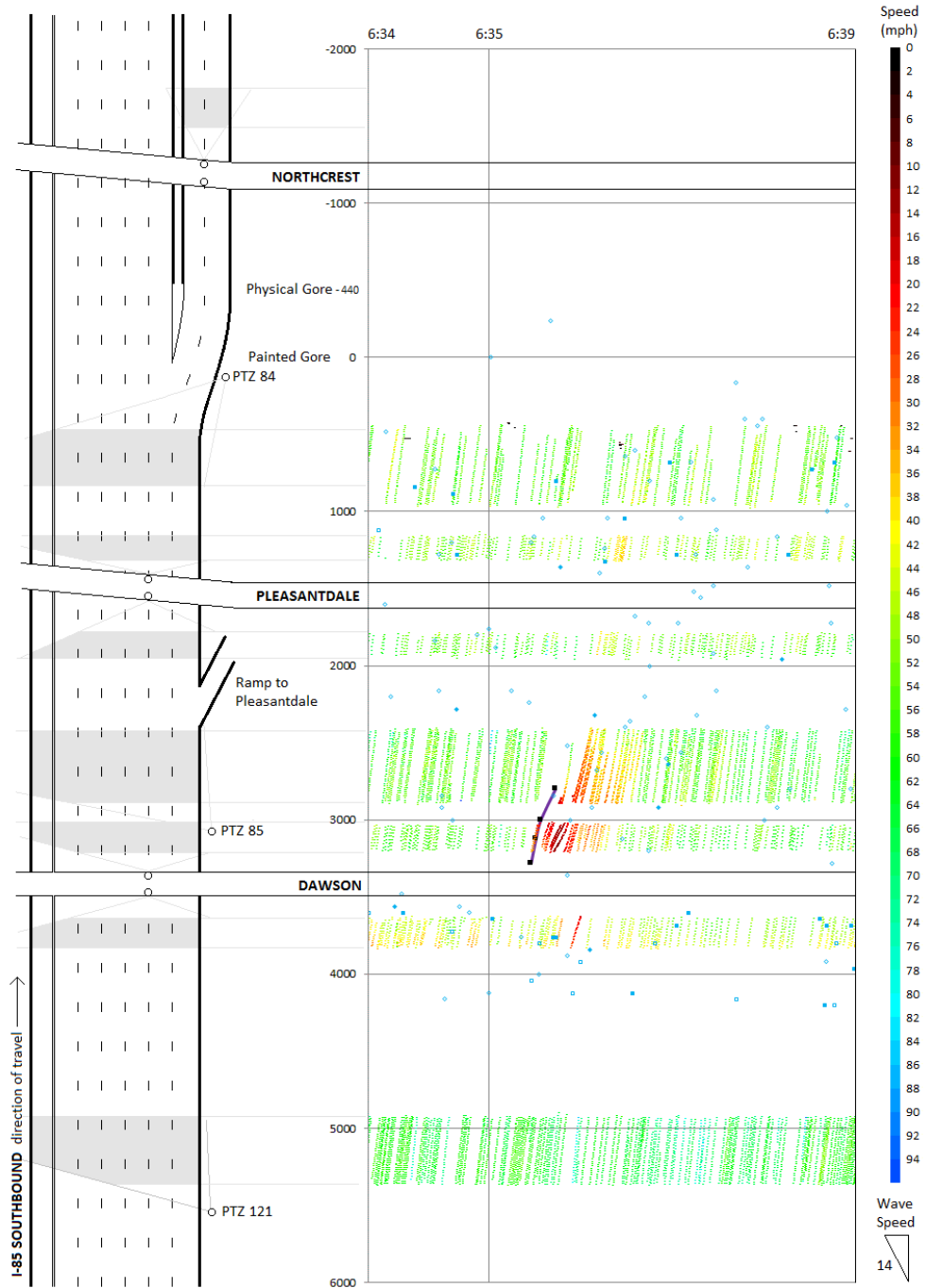
Case Studies

As an introduction to the effect of lane-changing disruptions, a case study of several identified disruptive lane changes are presented in this section. The images show the time-space trajectories of the automatically identified vehicles, which are colored by speed (black-red-yellow-green), and the trajectories of vehicles causing a disruption in the traffic stream of the initial lane (purple). Lane changes locations are displayed as blue dots. Solid dots represent lane changes into the lane, while hollow dots represent lane changes out of the lane. All time-space trajectories shown are of Lane 5, the lane from which vehicles move from to get into the exit lane.

The displayed time-space trajectories are for a subset of the vehicles, which the tracking software was able to automatically identify. Footage is from the PTZ and overpass cameras on the I-85 site (Chapter 3, Figure 7). The vertical axes in the following images represent space, in units of feet, and represent the distance to the beginning of the painted gore. The upstream side of the corridor is at the bottom of the graph, and the downstream side of the corridor is at the top of the graph. The horizontal axis represents time, and progresses from left to right. Hence, are moving from the bottom of the graph to the top of the graph in distance and from left to right in time. The slope of the line indicates velocity, where a stopped vehicle is represented by a horizontal line section. All disruption trajectories are vehicles attempting to change lanes. This is typically evidenced by the utilization of the vehicle's turning signal, and confirmed on the video when the vehicle eventually moves into the ramp lane.

Case Study 1 in Figure 49 takes place before the onset of congestion on May 9, 2013. A driver in Lane 5 (third lane from the right) slows down to move over to the

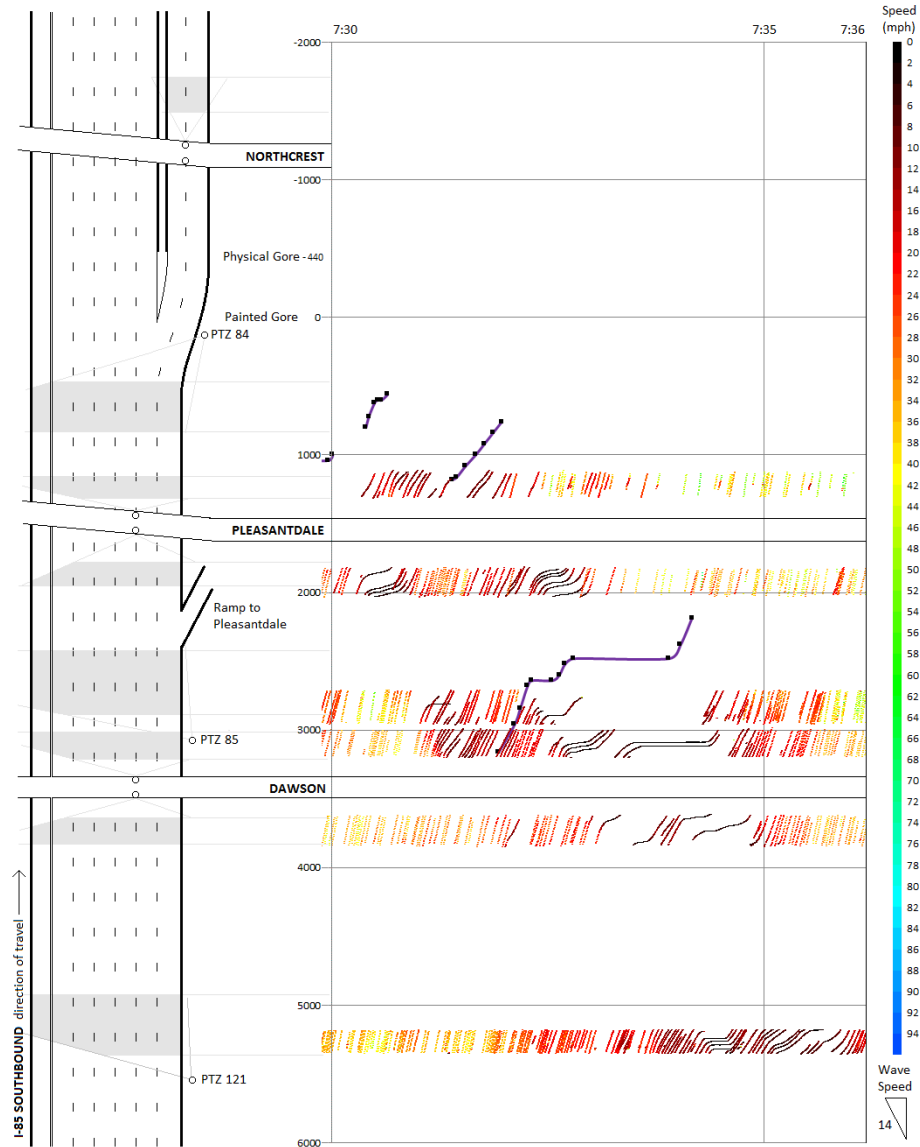
Pleasantdale Road ramp, less than 500' from the painted gore of the ramp. Drivers behind this vehicle are not able to change lanes to avoid the disruption, resulting in the formation of a wave behind the disturbance-causing driver. The upstream traffic state in the lane does not allow the wave to propagate very far upstream. This driver's behavior also has an impact on adjacent lanes. Traffic in the right two lanes slow down to accommodate this driver's move into the ramp lane. Also, although no vehicles are observed moving to the left to bypass the short wave, speeds in Lane 4 decrease, presumably as a result of a friction effect. The disruption in Figure 49 does not impact the system on a large scale (low upstream demand), but provides an excellent example of how the unusual behavior of an individual driver can result in a wave forming in the initial lane, and showcases how disruptive weave behavior works in combination with the friction effect to advance the lateral propagation of congestion.



May 9, 2013 6:34-6:39am, Lane 5

Figure 49: Disruption Case Study 1

In Case Study 2 (Figure 50), a vehicle stops for a longer period of time, resulting in a greater impact on the initial lane. As the downstream traffic begins to dissipate, this driver stays at a stopped state. At this point, traffic remains in a queued state behind the driver, while pockets of free flow appear in front. This is evidenced by vehicles changing lanes in front of the disturbance-causing driver at high rates of speed.

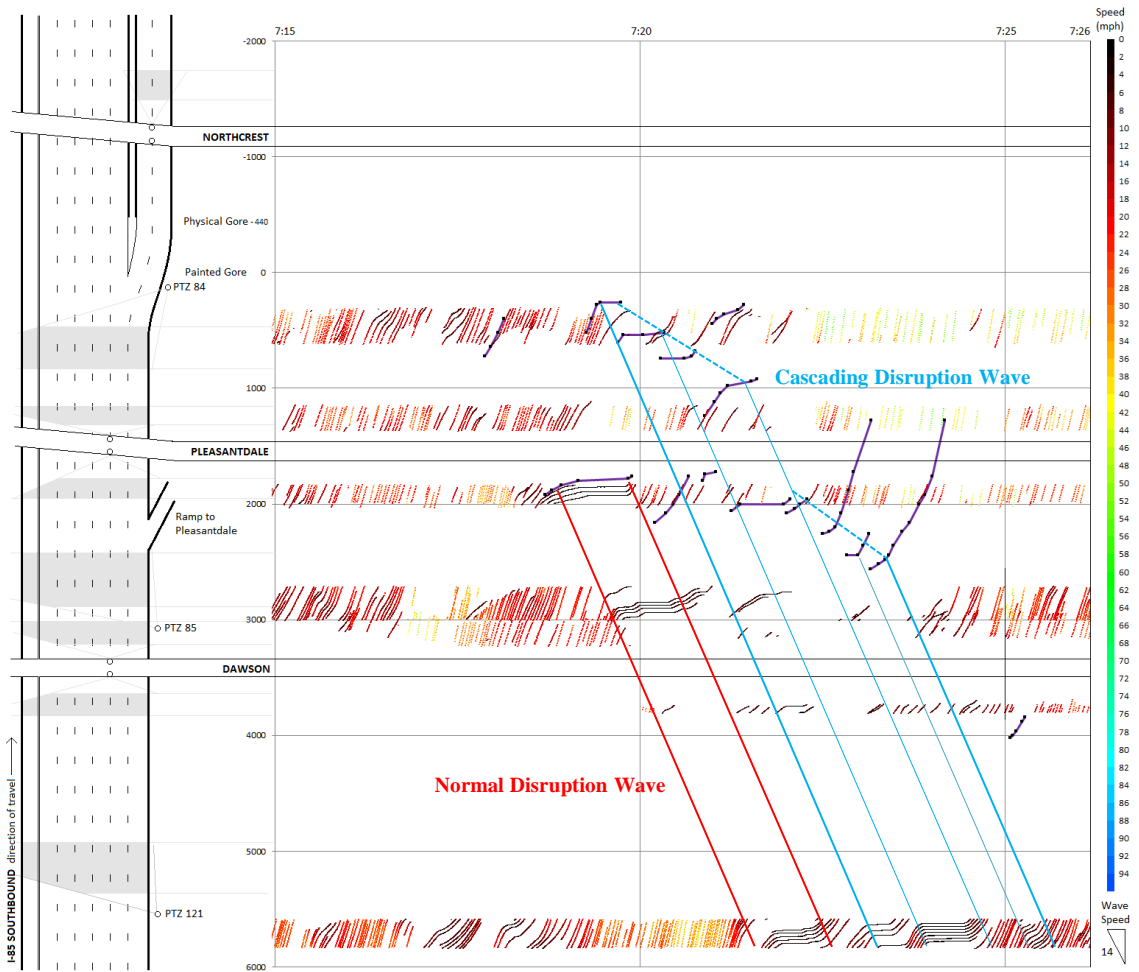


May 8, 2013 7:30-7:36am, Lane 5

Figure 50: Disruption Case Study 2

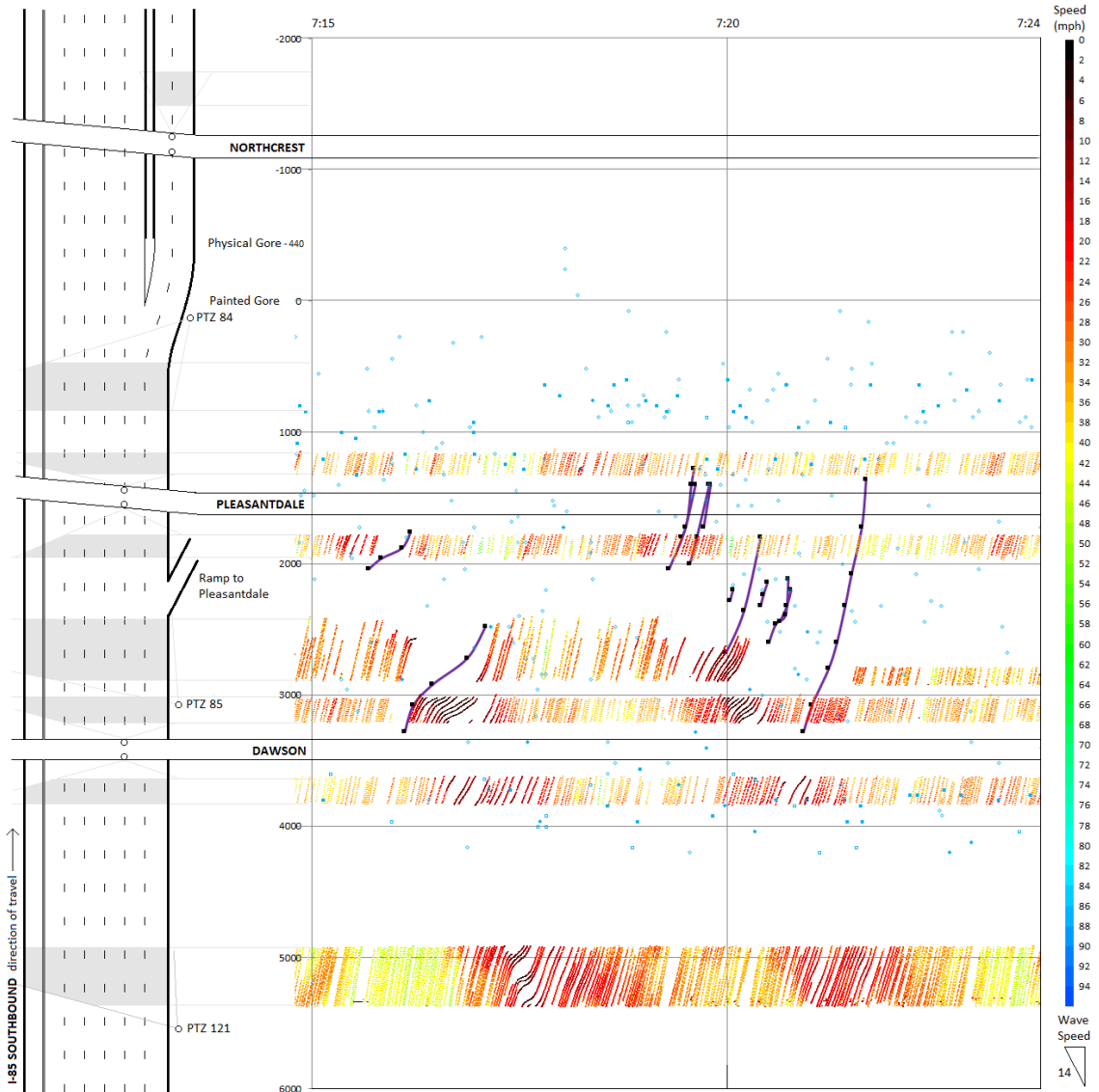
Case Study 3 is presented in Figure 51, using data collected on February 28, 2013, and shows how disruptions affect traffic in the initial lane. However, the upstream traffic condition represents the combined effect of several disturbances. While a majority of the disturbance can be attributed to two drivers, there are several other drivers that play a role in the extension of the original disturbance. Normal car-following models would predict these drivers would accelerate faster and sooner than their behavior indicates. These drivers are attempting to change lanes, but maintain lower speeds as they wait for an opportunity to move into the ramp lane.

The complexity and interdependency of lane changes are evident in this figure. Disruptions build upon each other in a cascading fashion, as demand to enter the exit lane builds because vehicles are not able to enter the congested exit lane. Other opportunity to enter the exit lane is available downstream as the queue in the ramp lane clears, and variance in queued vehicle acceleration provides gaps into which vehicles can move. A second example of this cascading effect is presented in Figure 52. In this figure, downstream conditions are clearly in free-flow, and several disruptive lane changes result in the propagation of a slower traffic state back to the upstream side of the study site.



February 28, 2013 7:18-7:26am, Lane 5

Figure 51: Disruption Case Study 3



May 9, 2013, 7:15-7:24am, Lane 5

Figure 52: Disruption Case Study 4

From the images presented above, drivers causing disturbances do not always change lanes while they are moving at the slowest speed. Often, after decreasing speed, they will speed up before changing lanes, and maneuver into an approaching gap. The increase in speed plays a crucial role in the cooperative lane change process. If a driver

following the lane-changing vehicle accelerates slowly, a large gap forms and another vehicle has an opportunity change into the space that was vacated by the driver making the original weave. Similarly, when a driver moves into the target lane, the response of the vehicle immediately behind the vehicle can result in the creation of another gap that allows for further weaving into the target lane. The acceleration rates and gap creation process of participating vehicles is not well-defined, and is likely to be dependent of the cooperative behavior of drivers in the departure and target lanes.

Regression Analysis

Disruptions are often observed on the I-85 corridor upstream of the ramp to I-285 westbound. Disruption data between the times of 7:05am and 9:20am on May 8, 2013 between the Pleasantdale Road and Dawson Road overpasses are used in this statistical analysis. May 8 was chosen because of the slightly higher likelihood of slower ramp speeds compared to May 7 and 9, which are expected to result in more frequent and more easily observed disruptive lane changing. This site was chosen because the proximity of cameras (2 overpass cameras and PTZ 85) makes it easier to identify and track disruptions. However, the data collected were not expected to represent all disruptions present on this segment of freeway. Disruptive drivers are more easily spotted when traveling at low speeds for a long duration. Because the distance between cameras can be somewhat large, it not always possible to capture the smaller disruptions, which may in turn affect upstream speeds. Overpass-mounted cameras are focused down the boundary between the mainline and exit lanes, and although the lane change itself can be observed, the time-space trajectory of the lane-changing vehicle prior to the lane change cannot be

observed due to larger (occluding) vehicles between the lane changing driver and the overpass camera. Thus, disruptions that occur under these conditions will not be observed.

To affirm that the speeds of vehicles that cause disruptions play a role in the lateral propagation of congestion, a stepwise regression analysis was performed to estimate speeds upstream (dependent variable) of the location of disruptions in the initial lane. Because it has been conceded that not all disruptions can be observed, separate regressions will be performed on periods of time that do and do not contain disruptions. Only 30-second periods that have disruptions longer than 10 seconds are included with the disruption data set. All other data are part of the non-disruption data set. It is assumed that disruptions that last less than 10 seconds may not have a great enough impact to significantly affect the upstream speed. Periods of time when the upstream speed in the initial lane was not available were excluded from the analysis. Periods of free-flow and the congested transition to free-flow conditions were also excluded from this analysis.

Average speed was assessed for a 30-second period at the downstream site. This average speed was paired with the average speed at the upstream site, within the same wave. Traffic states are expected to remain relatively constant within the same wave when traffic is at capacity or in congestion, so speeds at the upstream and downstream sites within the same wave are expected to be correlated. Varying wave speeds were assessed to assess the correlation between speeds at the downstream and upstream sites. A wave speed of 14 miles per hour provides the highest correlation between upstream and downstream speed measurement sites. This value is relatively consistent, provided that traffic upstream is either at capacity or congested. If a disruption occurs during a

period of non-congestion, its effects will be noticed at a later-than-expected time because the traffic state propagation will occur at a lower speed. Alternatively, a disruption may not be noticed at the upstream location if there are too few vehicles succeeding the disruption, as evidenced by the second case study presented above (Figure 50). Thus, only periods when traffic is in a congested state are considered - 7:05am to 9:20am, May 8, 2013.

Several independent variables are considered in the formulation of each regression.

| | |
|--------------|--|
| v_{5D} | Initial lane downstream speed |
| v_{6D} | Target lane downstream speed |
| v_{6U} | Target lane upstream speed |
| v_{dis} | Speed of disruptive vehicles |
| t_{dis} | Duration of disruption |
| v_{hybrid} | Hybrid Speed: f (disruption speed & initial lane downstream speed) |
| LC_{56} | Number of lane change Lane 5 to Lane 6 (full segment) |
| LC_{54} | Number of lane change Lane 5 to Lane 4 (full segment) |
| LC_{65} | Number of lane change Lane 6 to Lane 5 (full segment) |
| LC_{45} | Number of lane change Lane 4 to Lane 5 (full segment) |
| LC_{56up} | Number of lane change Lane 5 to Lane 6 (upstream of disturbance) |
| LC_{54up} | Number of lane change Lane 5 to Lane 4 (upstream of disturbance) |
| LC_{65up} | Number of lane change Lane 6 to Lane 5 (upstream of disturbance) |
| LC_{45up} | Number of lane change Lane 4 to Lane 5 (upstream of disturbance) |

Within each 30-second wave, each disruption can last between 10 and 30 seconds.

That being said, the speed condition upstream is not necessarily a function of the disruption speed only. When disruptions are not present throughout the entire duration of the wave, the upstream speed may also be a function of downstream speed. Thus, the hybrid speed variable was developed, equal to the time-weighted average of the speed of the disruption and downstream speed.

$$v_{hybrid} = \frac{t_{dis} * v_{dis} + (30 - t_{dis}) * v_{5D}}{30} \quad \text{Equation 11: Hybrid Speed}$$

Where v_{hybrid} is the hybrid speed,

v_{dis} is the space mean speed of the disruption(s),

t_{dis} is the length of time over which the disruption(s) occurs, and

v_{5D} is the space mean speed of the initial lane at the downstream overpass.

Figure 53 illustrates the hybrid speed calculation. Between the upstream and downstream speed measurement locations, a vehicle exhibiting disruptive behavior attempts to change lanes (shown in purple). The downstream and disruption speed are displayed, and the time-average of the two (hybrid) is calculated as follows:

- In the first 30-second wave, normal following behavior occurs for the first 10 seconds. This is followed by 20 seconds during which the disruptive vehicle slows to a complete stop (average speed 10 mph). The hybrid speed calculation is 26 mph.
- The disruption lasts completely throughout the second 30-second wave, so the hybrid speed estimation is based completely on the speed of the disrupting vehicle (0 mph)
- In the final 30-second wave, the disruption continues for 10 seconds, after which the disrupting vehicle departs the lane. The remaining vehicles accelerate back to 60 mph and follow normal behavior for 20 seconds. The time-average of the two (hybrid) is calculated as 43 mph.
- The fourth 30-second wave is represented by normal cruise at 60 mph.

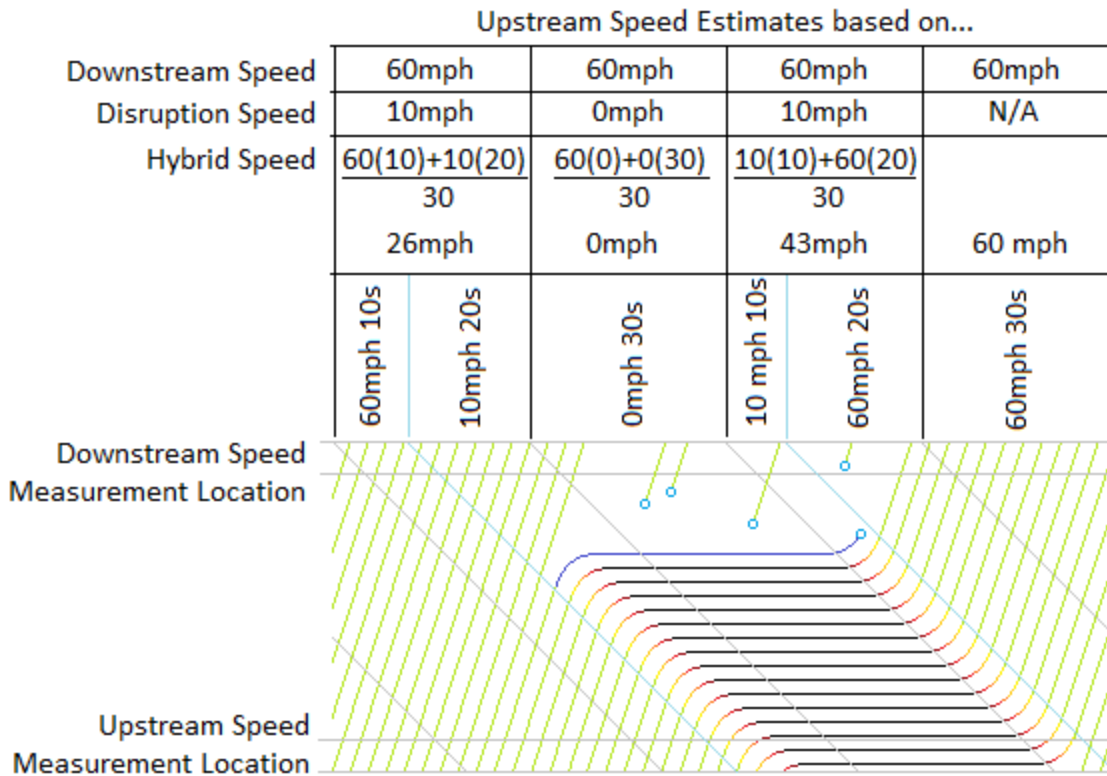


Figure 53: Hybrid Speed Visualization

A site diagram is shown in Figure 54, and the variables used in the regression are labeled. Cameras on the Pleasantdale and Dawson overpasses and a PTZ camera are used for estimating the upstream and downstream speeds in the initial and target lanes. Lane changes into and out of the initial lane are represented by diagonal arrows into and out of Lane 5. The disruption speed is represented by the purple vehicle and the purple time-space trajectory in Figure 54.

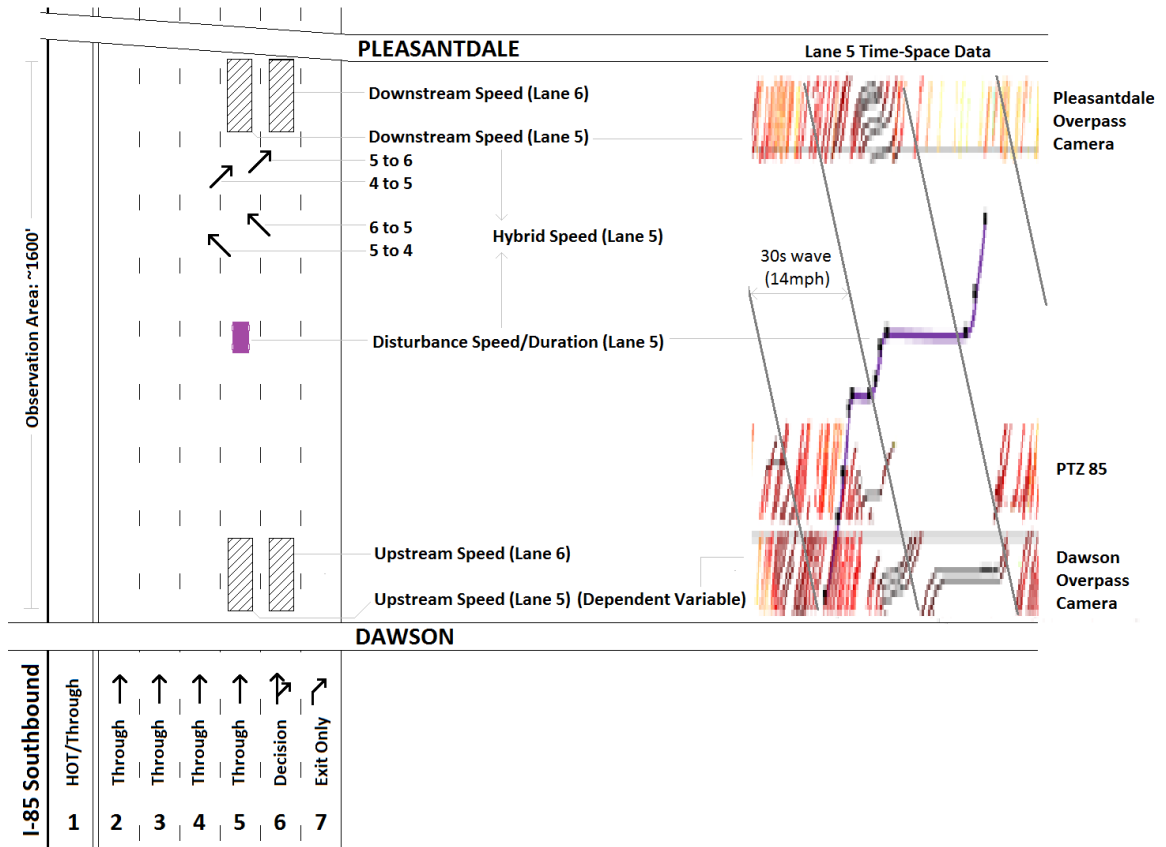


Figure 54: Regression Data Visualization

Disruption Regression

A simple regression of disruption data indicates that the hybrid speed is most significantly correlated with the upstream speed in the initial lanes. All other available regression variables, when paired with the hybrid speed as regressing variables, are insignificant predictors of the upstream speed. When the hybrid speed is zero, the regression-predicted upstream speed is approximately 4 mph. The upstream speed increases at a rate slightly less than the hybrid speed, and the regression predicts the upstream speed is equal to the hybrid speed when the hybrid speed is approximately 40 mph. Ideally, there should be a one-to-one relationship between the hybrid and upstream

speed (slope equal to 1, intercept equal to 0), as the congestion caused by a disruption typically propagates upstream at approximately 14 mph. This difference could be driven by several different factors. Following drivers may brake more slowly in the presence of a disruption, which could account for part of the difference between the hybrid speed and the upstream speed. Another factor influencing the upstream speed may be the number of lane changes out of Lane 5, upstream of the disruption. Lane changes out of Lane 5 open up gaps in the lane and these gaps are closed by following drivers as they approach the vehicle causing the disruption. Because it takes additional time for these gaps to be closed, the rate at which congestion propagates upstream would in theory be slightly reduced, resulting in the upstream estimated speed being greater than the speed of the disruption. Regression statistics, best-fit line, and residuals (relatively homoscedastic) are displayed on the following page.

$$v_{5U} = 0.898 v_{hybrid} + 4.06$$

$$R_{adj}^2 = 0.823$$

$$N = 47$$

Table 17: Disruption Regression Results

| | Estimate | Standard Error | t-Statistic | P-Value |
|--------------|----------|----------------|-------------|----------|
| Intercept | 4.06 | 1.195 | 3.395 | 0.00144 |
| v_{hybrid} | 0.898 | 0.0613 | 14.642 | 9.90E-19 |

N=47

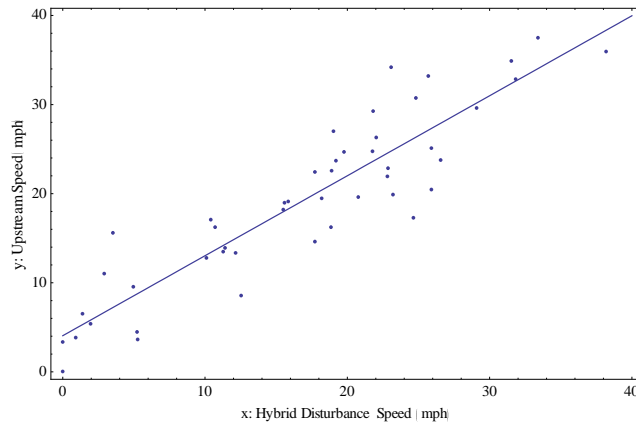


Figure 55: Disruption Regression Fit

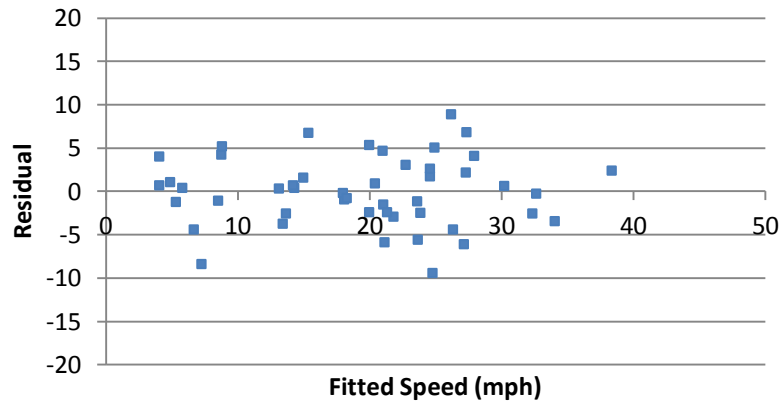


Figure 56: Disruption Regression Residuals

The least insignificant variable, when paired with hybrid speed, was the number of lane changes from Lane 4 to Lane 5. Because drivers that cause disturbances do not display normal following behavior, large gaps are often left in front of drivers causing a disruption. Drivers in Lane 4 change lanes directly in front of these disturbances, resulting in a correlation between the lane changing activity and the occurrence of a disruption. Given a constant likelihood of drivers in Lane 4 moving to Lane 5, more impactful disruptions, are more likely to result in more lane changes from Lane 4 to Lane 5. Also, in the presence of a disruption, higher speed differentials are expected between downstream and upstream locations, and are less likely to be correlated. Thus, the negative correlation between the number of lane changes (from Lane 4 to Lane 5) is plausible.

Non-Disruption Regression

The upstream speed for the remainder of the observations is much less predictable than the upstream speed for data with known disturbances. The same variables are considered as in the previous regression. The downstream speed in the initial lane, the upstream speed in the target lane, and the number of lane changes from Lane 4 to Lane 5 play a significant role in estimating the upstream speed in Lane 5. Regression results are shown in Table 19.

When the hybrid speed and Lane 6 upstream speed are set to 0, approximately 13 lane changes from Lane 4 to Lane 5 are required for the model to estimate the upstream Lane 5 speed as zero, which is unrealistic. Ideally, when the hybrid speed and Lane 6 upstream speed are both equal to zero, the Lane 5 upstream speed should be very close to

zero. Correlation between the hybrid speed and Lane 6 upstream speed ($p = 0.68$) may be responsible for an unrealistic regression fit when the value for both speed variables is low. Furthermore, low hybrid and low Lane 6 upstream speeds were not observed at the same time, indicating such conditions are less likely to be present in the absence of disruptive drivers, and the non-disruption regression should not be used when both speed variables are low. More data may be needed to improve the regression fit in this area. Residuals in Figure 57 indicate the model tends to overestimate the speed at lower predicted speeds, providing further evidence that the model is not doing a very good job at explaining why very low speeds are observed at the Lane 5 upstream location.

Significance of the hybrid speed may be an indicator that normal car-following behavior may be playing a role in the estimation of Lane 5 upstream speed. Significance of the Lane 6 upstream speed may be an indicator that the friction factor or disruptive lane changes may be playing a role in the estimation of Lane 5 upstream speed. Due to the correlation between speed of the target lane and disturbance speed ($p = 0.68$), it is possible that the effects of wave propagation and the friction factor are captured in both of these variables. Both the hybrid speed and Lane 6 upstream speed exhibit positive coefficients, which are expected. As the correlated speeds increase, the estimated Lane 5 upstream speed increases at a slower rate.

Interestingly, the number of lane changes from Lane 4 to Lane 5 is a negatively-correlated significant variable. Two separate effects may be captured in this variable. First, drivers forcing their way from Lane 4 to Lane 5 may be causing following drivers to slow down to maintain a safe following distance. Second, gaps created by unobserved disturbances are more likely to have lane changes occur from Lane 4 to Lane 5

downstream of the disturbance location. The unobserved disturbance in Lane 5 results in a speed decrease upstream in Lane 5, and could be captured by the lane changing regression variable.

The model fit is not as good for the non-disruption dataset, and this is reflected in the wider scatter of the residuals. Additionally, the distribution of the residuals appear slightly heteroscedastic as more error in the Lane 5 upstream speed prediction is likely when fitted speeds are lower.

$$v_{5U} = 0.3345 v_{hybrid} + 0.4764 v_{6U} - 0.8953 LC_{45} + 12.02$$

$$R^2_{adj} = 0.499 \quad N = 214$$

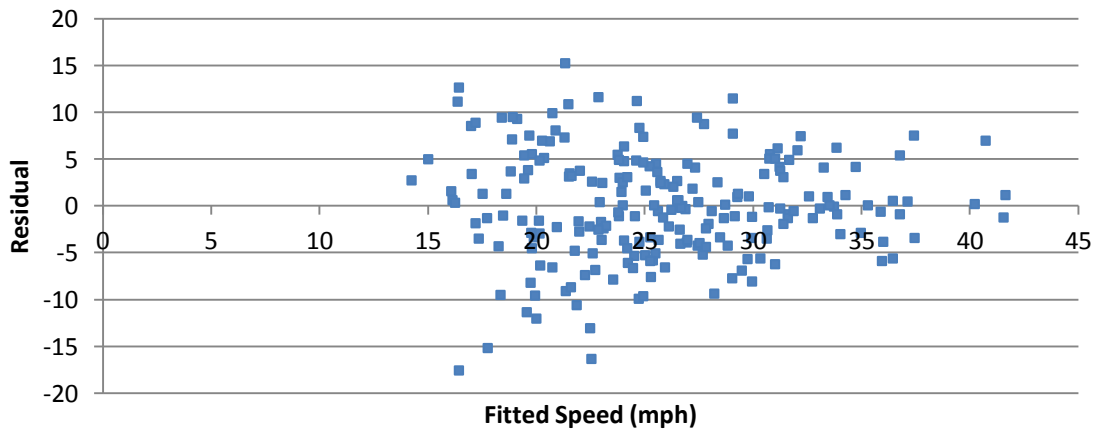


Figure 57: Non-Disruption Regression Residuals

Table 18: Non-Disruption Regression Results

| | Estimate | Standard Error | t-Statistic | p-Value |
|--------------|----------|----------------|-------------|-----------|
| Intercept | 12.02 | 1.476 | 8.14 | 3.366E-14 |
| v_{hybrid} | 0.3345 | 0.0725 | 4.61 | 6.952E-6 |
| v_{6U} | 0.4764 | 0.0655 | 7.16 | 1.349E-11 |
| LC_{45} | -0.8953 | 0.2634 | -3.40 | 8.104E-4 |

Disruptions caused by lane-changing vehicles have been observed and documented in this section. A model using observed disruption data and a model using unobserved disruption data was developed. The model that uses disruption data is able to account for more than 80 percent of the variance in the upstream speed in which the lane disruption occurs. The previous model, in which disturbances could not be observed, indicates that the remaining regression variables do not predict Lane 5 upstream speed as well as a model that includes disruptions. While other variables do appear to help capture the impacts of disruptions, a model can significantly benefit from direct use of observed disruption data. This is likely because the variable helps to differentiate between the effects of wave propagation, friction factors, and disruptions when low upstream Lane 5 speed conditions are observed.

With respect to individual driver disruptive lane changing behavior, the underlying mechanisms responsible for the behavior are mostly unknown. It is important to point out that a change in driver behavior will likely impact the likelihood that disruptions will occur, the duration/severity of individual disruptions, and the affect that the disruptions have on the traffic stream. Given regional differences in driver behavior, extensibility of model is uncertain. Furthermore, the likelihood of disruptive behavior and the impacts of disruptive behavior are expected to change as advances in automated vehicle technology are made.

A regression analysis indicates the speed of disruptive vehicles is better for predicting upstream speed than either the speed of the adjacent lane and the downstream speed. This probably not too surprising given the direct impact that the slow moving vehicle has on the vehicles immediately following. Because of limited camera

coverage, observed disruptions within the study corridor are documented manually. Disruptions are more easily observable when the vehicle causing the disruption is moving at a very slow speed for a prolonged period of time. Not all disruptions can be observed, especially disruptions that occur at greater speeds and shorter durations. Impacts of not-observed disruptions are likely captured in the variable that describes the number of lane changes into the initial lane. While higher speed and shorter duration disruptions may not individually cause a large impact on the lane it is moving out of, the frequency with which they occur is expected to be far greater. As evidenced in the final case study, the impacts of several cascading small disturbances can compound to significantly impact the traffic stream. Aside from target lane speeds that are slower than initial lane speeds, mechanisms that cause lane changing disruptions are unknown. More comprehensive data is needed to generate a model that employs factors which motivate drivers exhibiting disruptive behavior. As ITS and vehicle monitoring technologies continue to advance, it is likely that vehicle monitoring systems can be programmed to identify disruptions (and speed of disrupting vehicles) and use these data for response purposes (such as adjusting variable speed limits to reduce the risk of a crash upstream of the disruption). Enforcement strategies could also be considered to help minimize disruptive lane change behavior.

CHAPTER 8: LANE DISTRIBUTION OF EXITING VEHICLES

Similar to the distribution of lane changes upstream of a ramp, knowledge of how vehicles are distributed across the freeway upstream of a ramp may yield further insight into developing a macroscopic lane change model. The lane-changing model developed in Chapter 6 considers lane changing behavior between the through and exit lanes. While data are available for lane changing between other lanes, there is currently no system in place to efficiently associate lane changes made by the same vehicle within the study area. The ability to make these associations would lead much greater insight into lane changing behavior of drivers that have different destinations (i.e., to I-285 westbound exit, I-285 eastbound exit, or I-85 southbound through).

However, RFID tag-reading gantries placed periodically throughout the corridor allow the lane choice of the subset of vehicles containing RFID tags (Peach Pass) to be studied. Each tag has a unique identifier, so individual vehicle activity can be assessed. Though there are limitations when only a subset of vehicles can be detected, the advantage of the system is that vehicles can be tracked from gantry to gantry, allowing the lane choice of drivers exiting at different off-ramps to be studied. This study and accompanying discussion are presented in this chapter.

The distribution of vehicle lane choices (at a given location) is directly related to a flow boundary condition, and the (inflow-outflow) lane changing distribution between the boundary location and the given location. That is, final lane positions are a function of initial lane positions and weaving activity within the section. Thus, the results of this

analysis and the macroscopic lane changing model are relatable, though at different scales, due to the spacing of RFID gantries along the corridor.

There are limitations to using the Peach Pass data. It is important to note before any data are analyzed that there are many other factors other than distance upstream of a ramp that influence lane choice, such as the presence on-ramps and off-ramps. Within this study several on-ramps will increase traffic density in the rightmost lanes, which may cause through drivers to move to the left. There may be correlations between time-of-day, trip purpose and driver behavior that influence lane choice, and these factors cannot be captured by analyzing Peach Pass data alone. Additionally, driver behavior may be linked to demographic characteristics, which can influence lane choice, especially when an HOT lane is present. Despite limitations, the analyses will at the very least open up the discussion as to how vehicles with different origins and destinations are distributed across the freeway at locations where Peach Pass data are available, and will provide insight on general lane choice, in advance of differentiating across time-of-day, trip type, demographic, or other potentially significant characteristics.

SRTA Peach Pass Data can be used to estimate fractions of vehicles in each lane travelling to different destinations (off-ramps). The primary purpose of these RFID tags is for tolling on the I-85 HOT lane, and enforcing weaving behavior. RFID tag-reading gantries are placed every one-half to one-third of a mile in the HOT lane. Unique to I-85, is that gantries are also placed across each of the general purpose lanes every two to four miles. Each time a vehicle passes under a gantry, its tag identification number, timestamp, and a gantry identifier are recorded. The recorded information can be used to monitor lane choice of drivers that have a Peach Pass in their vehicle.

These data also provide a basis for discussing the potential impacts that operating speeds have on the lane change distribution of exiting vehicles upstream of the exit point. Because more exiting vehicles choose the left lanes when travel speed is lower, more lane changes must be made by these vehicles to exit the freeway, on average. Thus, a correlation between speed and the number of lane changes is expected. The analyses proceed under the assumption that nearly all of the vehicles in the HOT lane have a Peach Pass. Drivers in the HOT lane without Peach Passes may, or may not, behave differently than drivers with a Peach Pass, but the number is so small it is not expected to significantly impact results.

Relationship Between Lane Choice and Freeway Speed

The SRTA Peach Pass data stream contains RFID tag reads for drivers using the general purpose lanes for those vehicles equipped with an RFID tag. This allows their cars to be tracked throughout the corridor for analysis of lane choice, and to estimate their destinations based on the last gantry a vehicle is detected at for each trip. A driver's origin and destination is expected to play a role in lane choice throughout the driver's trip along the corridor. The speed of the freeway may also play a role in lane choice, particularly for HOT lane usage when low speeds in the general purpose lane are expected to motivate drivers to use the HOT lane. Assuming freeway access points are on the right side of the roadway, the position of drivers is expected to be closer to the right side of the freeway shortly after entering the freeway, and shortly before exiting the freeway.

Before any discussion of lane choice, it is important to note that the fraction of vehicles in the traffic stream that have a Peach Pass vary throughout the day. To estimate the fraction of drivers with a Peach Pass, GDOT VDS count data can be used to estimate the total number of vehicles on the roadway where VDS count data are available. A VDS station around upstream of the Jimmy Carter interchange, known to provide reliable data (Guensler, et. al, 2013), is in the vicinity of a Peach Pass tag-read gantry. An hour-by-hour comparison of Peach Pass and VDS volumes can be used to estimate the penetration of Peach Pass vehicles in the traffic stream. Table 19 and Figure 58 list the estimated fraction of vehicles with a Peach Pass by time of day, for VDS and Peach Pass data collected on October 1, 2012. The data indicate that a larger fraction of vehicles have a Peach Pass during the morning hours compared to the afternoon and evening hours. The larger fraction likely results because total afternoon traffic volumes include non-commute and non-peak-direction trips, and these vehicles are less likely to be Peach-Pass-equipped. While the data are more representative of the morning period, a Peach Pass penetration rate between 7% and 12% during afternoon hours should still provide reliably representative O/D and lane choice data.

Table 19: Fraction of Drivers with Peach Pass by Time of Day (I-85 Southbound 10/1/12)

| | Time Period | Peach Pass Volume | VDS Volume | Peach Pass Fraction |
|---------|-------------|-------------------|------------|---------------------|
| AM Peak | 6:00-7:00 | 2005 | 9664 | 0.207 |
| | 7:00-8:00 | 2614 | 10284 | 0.254 |
| | 8:00-9:00 | 2241 | 6419 | 0.349 |
| | 9:00-10:00 | 1476 | 4240 | 0.348 |
| PM Peak | 15:00-16:00 | 544 | 6276 | 0.086 |
| | 16:00-17:00 | 491 | 7059 | 0.070 |
| | 17:00-18:00 | 752 | 7744 | 0.097 |
| | 18:00-19:00 | 666 | 5603 | 0.118 |

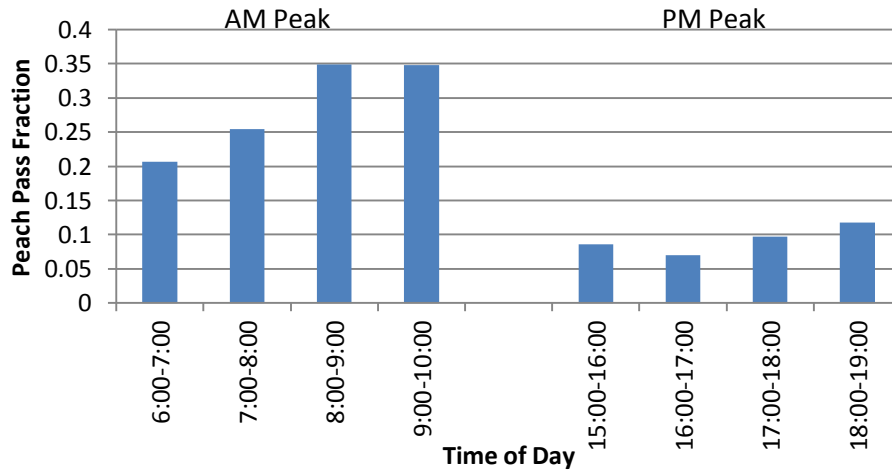


Figure 58: Fraction of Drivers with Peach Pass by Time of Day (I-85 Southbound 10/1/12)

O/D fractions and trip purpose are expected to vary throughout the day, and there is a concern that drivers may exhibit different lane choice behavior depending on origins and destination of other drivers on the freeway and the driver's trip purpose. It is difficult to capture these variables with the given data. Thus, this will limit the conclusions that can be made with available data. If a greater percentage of vehicles are equipped with Peach Pass RFID tags, more conclusive results can be made. Alternative analyses could be performed with automated license plate recognition (ALPR).

Lane Choice Analysis

Peach Pass data will be used to perform a lane choice analysis, and discuss behavior of drivers making these lane changes. Because drivers entering and exiting the freeway at different locations are expected to utilize the freeway differently, any lane choice analysis should only be performed using data from vehicles with similar entry and exit points. The three highest-demand origin/destination pairs being assessed are presented and discussed below.

- I-85 (beginning of HOT corridor) to I-85 (end of HOT corridor)
- I-85 (beginning of HOT corridor) to I-285 Eastbound
- I-85 (beginning of HOT corridor) to I-285 Westbound

Vehicles starting at the beginning of the corridor and ending at the end of the corridor may be in any lane at the beginning/end of the trip. However, traffic exiting to either of the I-285 exits must exit on the right side of the freeway.

Drivers are assumed to choose a lane based on experienced freeway conditions. To best estimate conditions that a driver has experienced, the average freeway speed (space-mean) between two gantries over a 5-minute period is used. The space-mean speed is calculated by taking the total travel time for all Peach Pass-equipped vehicles that pass the downstream gantry during the 5-minute period, and dividing by the total distance traveled by these vehicles. The calculated speed is assumed to represent the conditions experienced by vehicles passing the downstream gantry during the 5-minute period.

For each O/D pair and each gantry location, the density of vehicles in each lane should provide the most accurate metric for assessing the lane choice distribution. The

density of Peach Pass users in a lane (vehicle/lane-mile) for a given five-minute period is estimated by taking the total travel time for all vehicles with a Peach Pass that pass the downstream gantry during the 5-minute period, and dividing by the area of the time-space region (product of 5-minutes and distance between upstream and downstream gantries). For a given general purpose average speed range, a lane-by-lane density fraction of Peach Pass users can be estimated. The fraction of Peach Pass users in a given lane for a given general purpose lane average speed at a given time is calculated by taking the density of the given lane divided by the sum of all lane densities during the given time period.

Figure 59, Figure 61, and Figure 62 provide the lane distribution of Peach-Pass-equipped vehicles for all weekdays in October 2012 for three different O/D pairs:

1. Beginning of corridor through the end of the corridor, past I-285, Figure 59
2. Beginning of corridor to I-85 eastbound, Figure 61
3. Beginning of corridor to I-85 westbound, Figure 62

Each figure displays two graphs for each gantry. In each figure, The graphs on the left display the fraction of Peach-Pass-equipped vehicles that used the lane for the trip, split into percent observed in the HOT lane at each location vs. the GP lanes at that location, for each 10 mph general purpose speed bin (for that Figure's O/D pair). In each left hand graph, the sum of the fractions for every 10mph bin equals one (percent of vehicles observed in the HOT lane vs. GP lanes at each location for that speed condition). The average speed of general purpose lanes is expected to impact the fraction of vehicles using the HOT lane, because users are paying to obtain higher and more reliable speeds. As expected, across all locations and O/D pairs, the probability that Peach-Pass-equipped vehicles will be using the HOT lanes is higher when general purpose lane speeds are

lower (until the point where the vehicles have departed the corridor and HOT lane use is zero).

The impact of average general purpose lane speeds on the lane distribution of vehicles not using the HOT lane can also be ascertained by studying the lane choice distribution conditioned for vehicles not using the HOT lane. In Figure 59, Figure 61, and Figure 62, the graphs on the right reflect the lane choice distribution of Peach-Pass-equipped vehicles electing not to use the HOT lane for their trip. In each right hand graph, the sum of the fractions for every 10mph bin equals one (percent of vehicles observed in each GP lane at each location for that speed condition).

The subsections that follow will separately analyze the lane choices for each of the previously listed O/D pairs. For each O/D pair, the fraction of Peach Pass-equipped vehicles using the HOT lane is first discussed starting from the upstream gantry (Gantry 1), and moving toward the destination. The lane choice of Peach-Pass-equipped vehicles not using the HOT lane is then discussed.

I-85 (beginning of HOT corridor) to I-85 past I-285 (end of HOT corridor)

Peach Pass-equipped vehicles moving from the beginning of the corridor to the end of the corridor (Figure 59) tend to use the HOT lane more as the average general purpose speed decreases at the upstream gantry (Gantry 1). Moving downstream to Gantry 2, the fraction of vehicles using the HOT lane increases for all general purpose speed ranges (as additional vehicles join the HOT lane). The increased fraction is most notable at lower general purpose speeds. The fraction of Peach Pass-equipped vehicles

using the HOT lane remains relatively constant between Gantry 2 and Gantry 3 for all general purpose speeds. Between gantries 3 and 4, however, the fraction of Peach-Pass-equipped drivers using the HOT lane decreases. The decreasing fraction persists between gantries 4 and 5, especially when general purpose speeds are lower. This is interesting considering weaving into and out of the HOT lane is not permitted between the downstream-most gantry and the previous gantry. At this point, the vehicles have nearly reached the end of the HOT corridor. Some HOT drivers may need to exit to Chamblee-Tucker Road, which may be partially responsible for a smaller fraction of drivers using the HOT lane at Gantry 5.

Peach-Pass-equipped drivers using the general purpose lanes at Gantry 1 are most likely to be driving in Lane 2 or Lane 3. General purpose lane choice appears to be consistent at different average general purpose speeds. The same trend is noticed at the next gantry downstream. At the next-downstream gantry (Gantry 2), the largest fraction of Peach Pass drivers in the general purpose lanes are observed in Lane 2, while a lower fraction of vehicles are present in other lanes, despite an additional lane on the right. General purpose lane choice at Gantry 3 is much like the first gantry. A lower fraction of vehicles are observed in Lane 2, and more vehicles are observed in other freeway lanes (particularly in Lane 3 and Lane 4). Moving to Gantry 4, more Peach-Pass-equipped vehicles are in the right lanes, although a majority of vehicles are still in Lane 2. Interestingly, this gantry is less than half a mile downstream of the I-285 westbound off-ramp, which is typically congested, with congested conditions propagating upstream and laterally to other lanes on I-85. Perhaps some drivers are taking advantage of lower density traffic states on the right side of the freeway as traffic exits to I-285 westbound.

At the final gantry, a lower fraction of Peach-Pass-equipped vehicles are in Lane 2, and more are spread throughout the other general purpose lanes. The likelihood of finding traffic on the right lanes may be increasing partially due to the exit to Chamblee-Tucker road downstream of Gantry 5. Also at Gantry 5, general purpose lane choice appears to change with the average general purpose speed. At higher speeds, a higher fraction of vehicles are more likely to be found in Lane 2, and at lower speeds, vehicles are less likely to be found in Lane 2 and spread across other lanes. However, it is important to note that the number of observations in lower speed ranges is very small, and may not be representative of lane choice at low general purpose speeds.

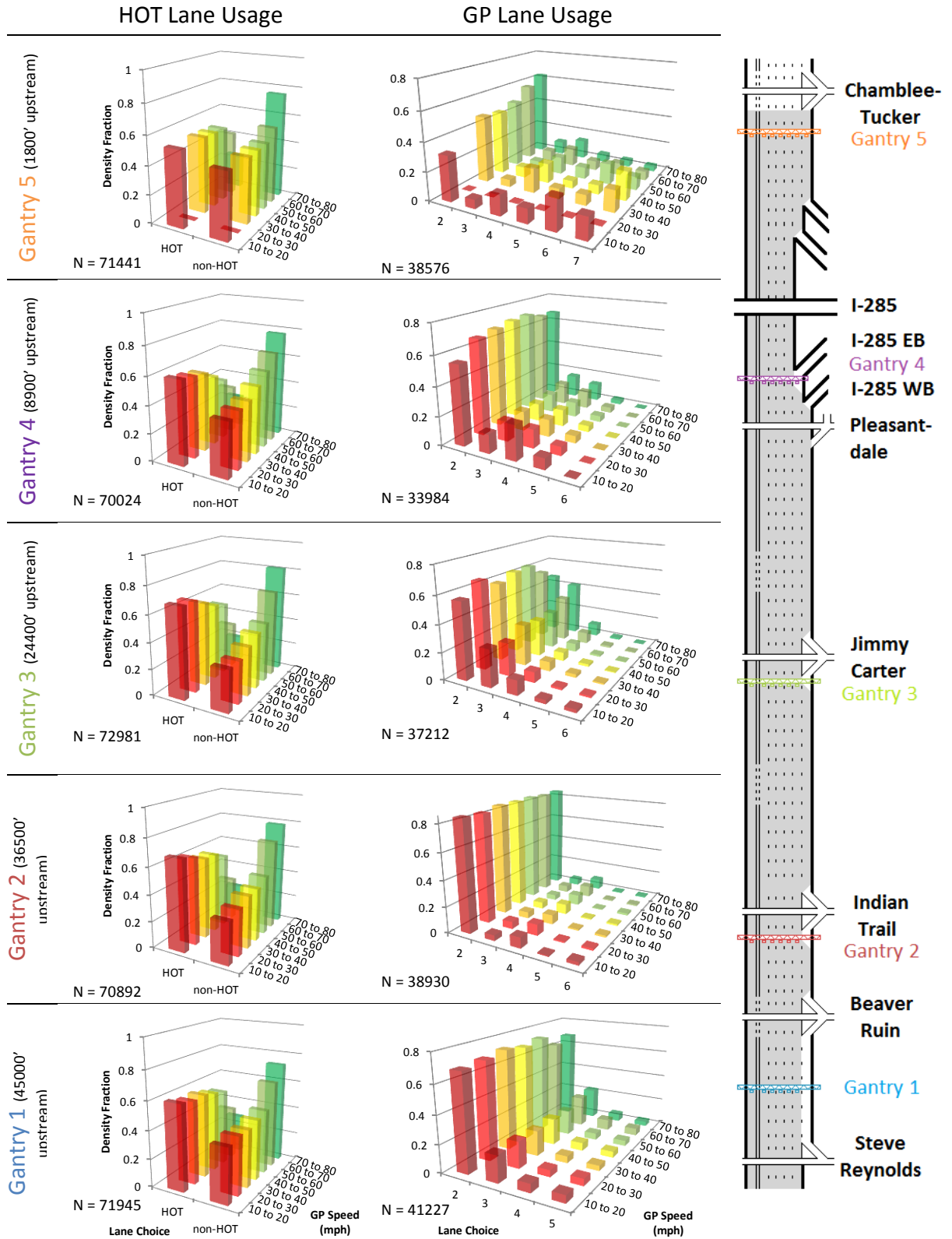


Figure 59: Lane Distribution - Beginning of Corridor to End of Corridor (weekdays, October, 2012)

I-85 (beginning of HOT corridor) to I-285 Eastbound

Drivers travelling from the beginning of the corridor to the I-285 eastbound ramp (Figure 61) near the end of the corridor exhibit similar behavior to the I-85 beginning-to-end drivers when they are far upstream of the ramp. At Gantry 1, a large fraction of vehicles use the HOT lane at lower speeds, and this fraction decreases as speeds increase. At Gantry 2, a larger fraction of drivers are observed in the HOT lane for all general purpose speeds, compared to Gantry 1; similar to drivers going to the end of the corridor. At Gantry 3, the likelihood of a driver using the HOT lane remains roughly the same as Gantry 2. The final gantry (Gantry 4) is only 1100' upstream of the ramp to I-285 eastbound. Very few drivers exiting to I-285 eastbound are using the HOT lane at this location, as expected. Four lane changes are required to exit from the HOT lane, which is very difficult to accomplish over the course of 1100 feet. However, two percent of drivers are observed to be moving from the HOT lane to the ramp when the average general purpose speeds are between 10 and 20 mph. These vehicles are essentially diving from the HOT lane to the exit lane over a very short distance. During the one-hour peak of the peak period, this constitutes about 40 to 50 vehicles per hour undertaking this potentially destructive weaving activity from the HOT lane to the I-285 eastbound ramp.

Peach-Pass-equipped vehicles traveling in the general purpose lanes to I-285 eastbound are predominately found in Lane 2 at the upstream gantry location. A larger portion of the Peach-Pass-equipped general purpose traffic is found in Lane 2 at Gantry 2, compared to Gantry 1. However, at Gantry 3, general purpose lane usage begins to distribute across the lanes. Slightly less than 50% of drivers are observed using Lane 2, around 25% use Lane 3, and 20% use Lane 4, when general purpose average speeds are

lower. There appears to be a tradeoff between Lane 2 (decrease) and Lane 3 (increase) usage as average general purpose lane speeds increase at Gantry 3. This may be a sign that general purpose drivers are moving over toward the exit lanes earlier when general purpose lanes are operating at faster speeds. That is, there may be less advantage to staying in the leftmost lanes when traffic is flowing well in all lanes. At Gantry 4, 1100' upstream of the exit, Peach-Pass-equipped general purpose drivers are predominately found in lanes 5 and 6, which are the two exit lanes for the ramp to I-285 eastbound. At any given average general purpose speed, about 8% of exiting drivers are also found in Lane 4 at this location, and are making their lane change into the exit lane over the last 1100' upstream of the ramp. Again, the influence of last-minute lane changes may have some effect on the performance of the lanes upstream of the exits and should be investigated in more detail.

It is interesting to note that as general purpose speeds increase, an increasing fraction of drivers estimated to be exiting to I-285 eastbound were noted in Lane 2 and Lane 3. It is not known why this occurs. In fact, this observation may be due to suspected errors in the data stream associated with gantry tag reader alignment at this location. If a vehicle is not detected at a gantry downstream of this location, it is assumed the vehicle exited to I-285 eastbound. If the vehicle passes under a downstream gantry, but the gantry equipment does not detect the vehicle, the assumption stated above will lead researchers to believe the vehicle had exited even though it did not. Shown in Figure 60, a suspected misaligned RFID tag reader in Lane 2 on the next-downstream gantry may be responsible for missing vehicles that stay in/move to Lane 2 between the gantry just upstream of the ramp to I-285 eastbound and the downstream gantry.



Figure 60: Misaligned General Purpose Detector

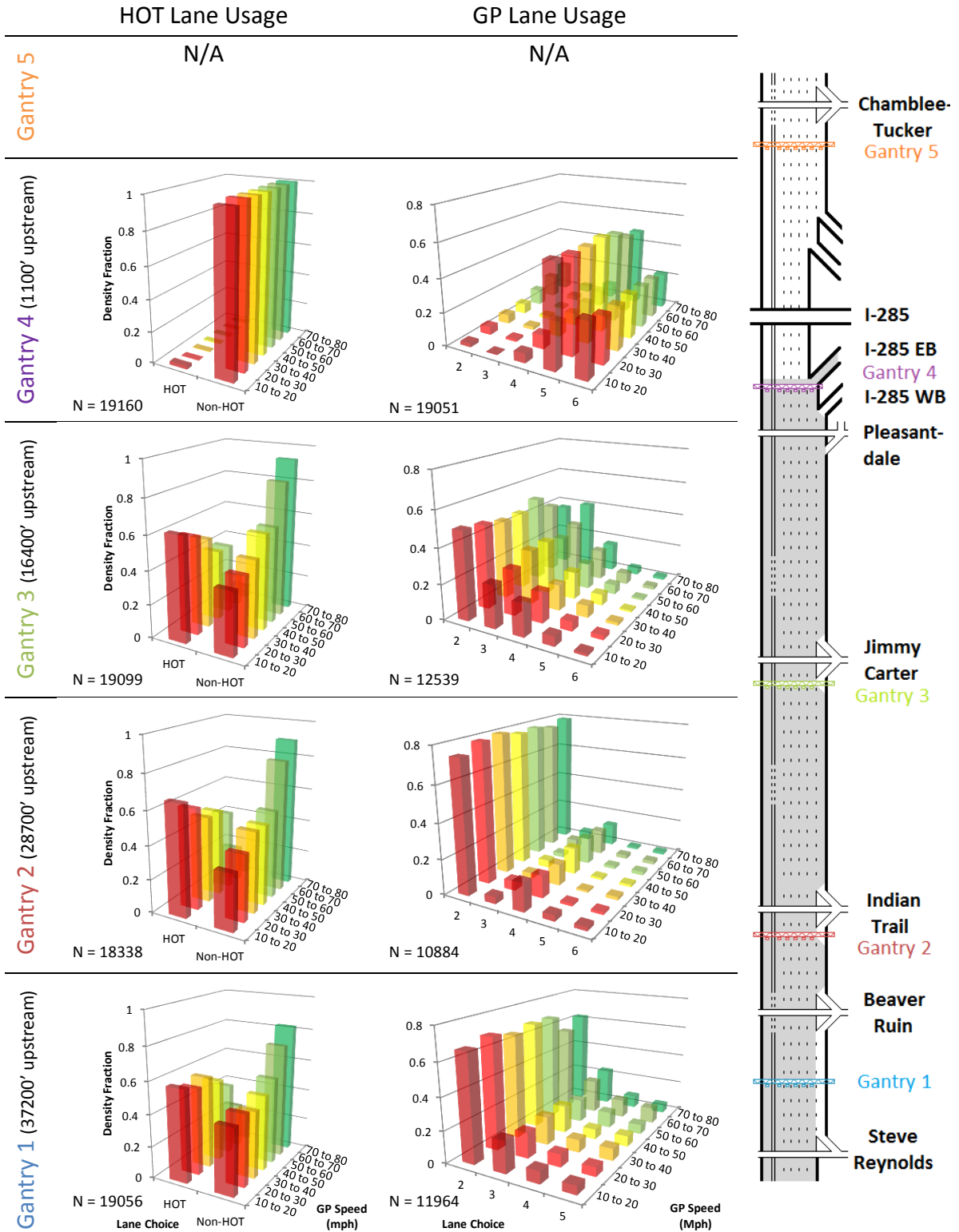


Figure 61: Lane Distribution - Beginning of Corridor to I-285 Eastbound (weekdays, October, 2012)

I-85 (beginning of HOT corridor) to I-285 Westbound

For traffic traveling from the beginning of the corridor to the I-285 westbound ramp (Figure 62), the proportion of traffic using the HOT lane follows the same trend as for traffic traveling to other destinations. As expected, Peach-Pass-equipped vehicles tend to use the HOT lane at lower general purpose speeds. Moving to Gantry 2, the fraction of drivers traveling in the HOT lane remains roughly the same for all general purpose speeds. HOT lane utilization decreases between gantries 2 and 3. Given that Gantry 3 is approximately 2.75 miles upstream of the ramp, a portion of HOT traffic may be starting to leave the HOT lane to exit.

At the upstream-most gantry (Gantry 1), roughly half of Peach-Pass-equipped general purpose drivers are in Lane 2, and the other half are relatively evenly distributed across other general purpose lanes. At Gantry 2, a higher percentage of Peach-Pass-equipped general purpose drivers use Lane 2, compared to the observation at Gantry 1. At Gantry 2, general purpose lane choice indicates a larger fraction of drivers in Lane 2, Lane 4, and Lane 6 compared to Lane 3 and Lane 5. This lane distribution is highly unusual, and may be a result of over-sensitive or misaligned RFID detectors in these lanes. The next gantry (Gantry 3) is the final gantry before traffic exits to I-285 westbound, and is located approximately 2.75 miles upstream of the ramp. Interestingly, Peach-Pass-equipped vehicles in the general purpose lanes are evenly distributed across the general purpose lanes for any given average general purpose speed. Compared to Gantry 2, Peach-Pass-equipped vehicles at Gantry 3 exiting to I-285 westbound are more likely to have moved to the right, most likely to prepare to exit.

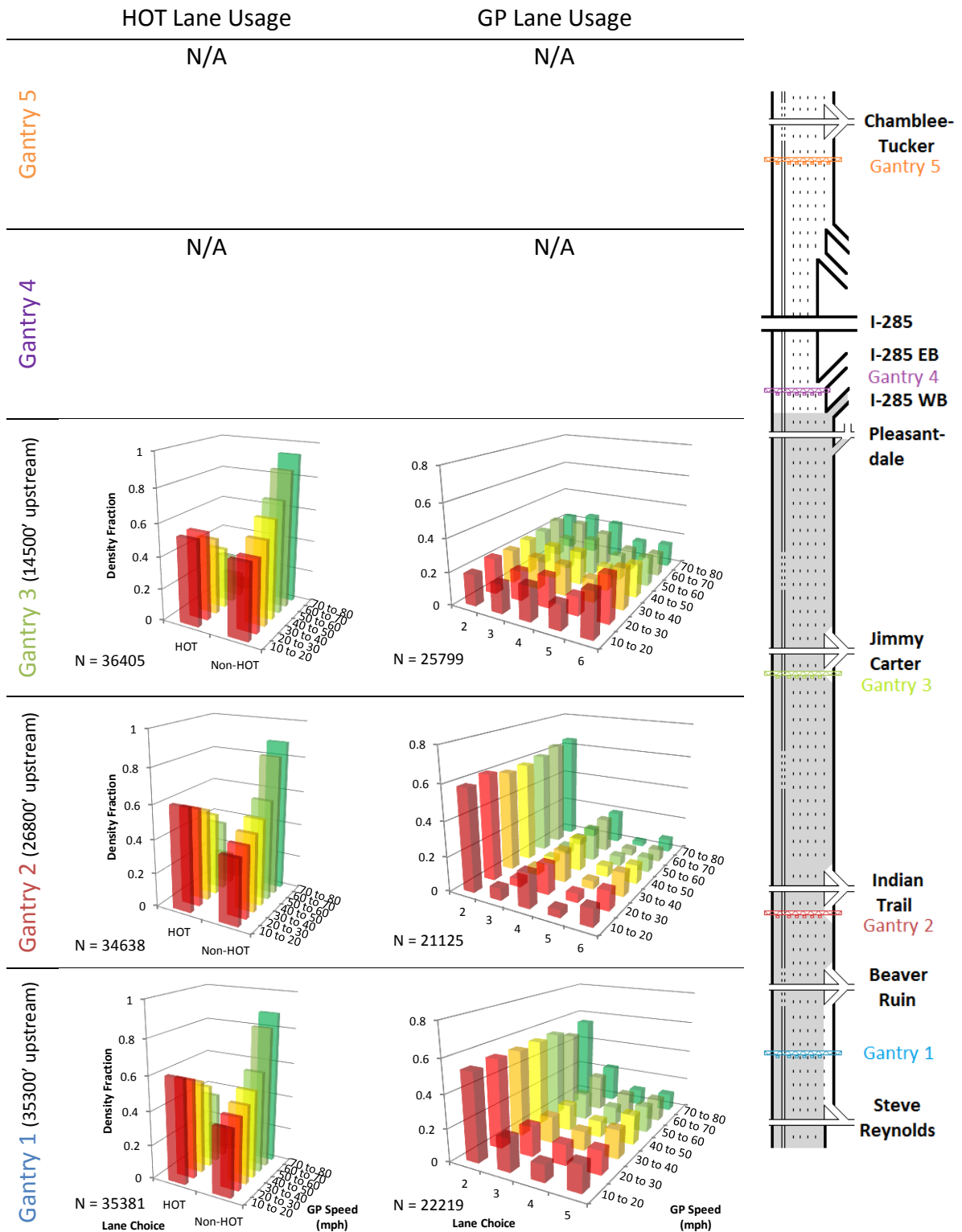


Figure 62: Lane Distribution - Beginning of Corridor to I-285 Westbound (weekdays, October, 2012)

The general purpose lane distribution of Peach-Pass-equipped vehicles shows a stark contrast between drivers exiting to I-285 westbound (Figure 62, Gantry 3) and traffic exiting to I-285 eastbound (Figure 61, Gantry 3). Despite exiting 1100' further downstream, general purpose traffic exiting to I-285 eastbound is much more likely to be found in Lane 2 or Lane 3 than in other general purpose lanes (compared to drivers exiting to I-285 westbound). Thus, it is not only the location of the destination, but the presence of other ramps (queues) upstream of the destination that may be influencing driver decision. This assumes drivers traveling along the corridor are familiar with traffic conditions and ramp locations.

Similar to traffic exiting to I-285 eastbound, the opportunity exists for HOT drivers to exit the HOT lane at the last minute, and make 5 lane changes over a short distance in order to exit to I-285 westbound. In the segment of freeway after the weaving section before the ramp, 40 to 50 vehicles per hour illegally weave from the HOT lane to the I-285 westbound ramp during the peak hour for illegal weaves.

Comparison of HOT Usage for Different O/D Pairs

As expected, the fraction of drivers using the HOT lane increases as average general purpose speed decreases for each studied O/D pair. The percentage of drivers using the HOT lane is largely influenced by general purpose speeds. At locations far upstream of the destination (i.e., Gantry 1 and 2), the fraction of drivers in the HOT lane is relatively uniform between the three studied O/D pairs. At free-flow speeds, the drivers traveling from the beginning to the end of the corridor are more likely to be in the HOT lane, compared to the fraction of vehicles traveling to either I-285 eastbound or

westbound. Despite being very far upstream from the I-285 ramps, drivers may be less likely to use the HOT lane if they have to exit and general purpose speeds are moderate to high. Demographic differences between drivers with different O/D pairs may also be playing a role here, as drivers with a certain O/D may be more likely to pay to use the HOT lane even when general purpose lanes are in free-flow.

As the drivers exiting to I-285 eastbound or to I-285 westbound approach their respective exits, they are less likely to be observed in the HOT lane. This is illustrated by the data from Gantries 3 and 4 presented in Figure 63. This figure presents the fraction of drivers using the HOT lane for each of the origin/destination pairs for different general purpose speeds. Fewer vehicles are observed in the HOT lane at locations closer to the ramp because drivers have left the HOT lane in order to make the required lane changes to reach the exit ramps.

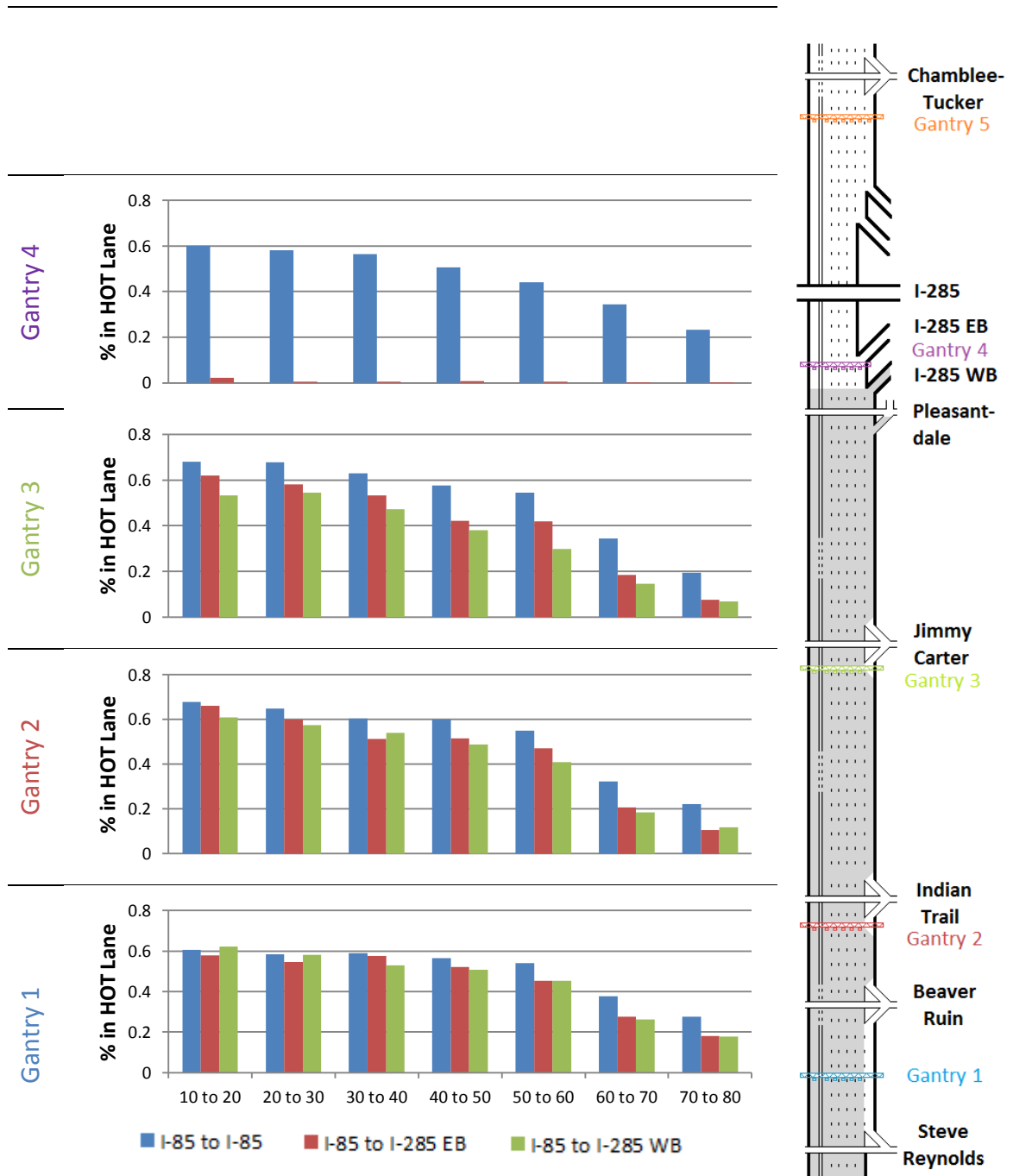


Figure 63: HOT Usage Comparison

One of the more interesting findings is that when a Peach-Pass-equipped vehicle is using a general purpose lane, the lane distribution of vehicles does not drastically change with respect to average freeway speed. However, for vehicles using the HOT lane, drivers exiting the corridor (on the right-hand side of the freeway) appear to prefer to stay in the HOT lane for a longer period of time compared to drivers in the leftmost general purpose lane, which tend to select move toward the right earlier (further upstream).

Several factors may result in exhibited behavioral differences between exiting drivers using the HOT lane and drivers exiting from the general purpose lanes. Drivers in general purpose lane can begin migrating to the right hand lanes at any point along the segment. However, the I-85 HOT lane only permits ingress and egress at certain locations. As evidence in Figure 64, approximately 80 percent of lane changes out of the HOT lane occur in the legal weaving area. The remaining 20 percent make illegal egress maneuvers between the legal weaving sections.

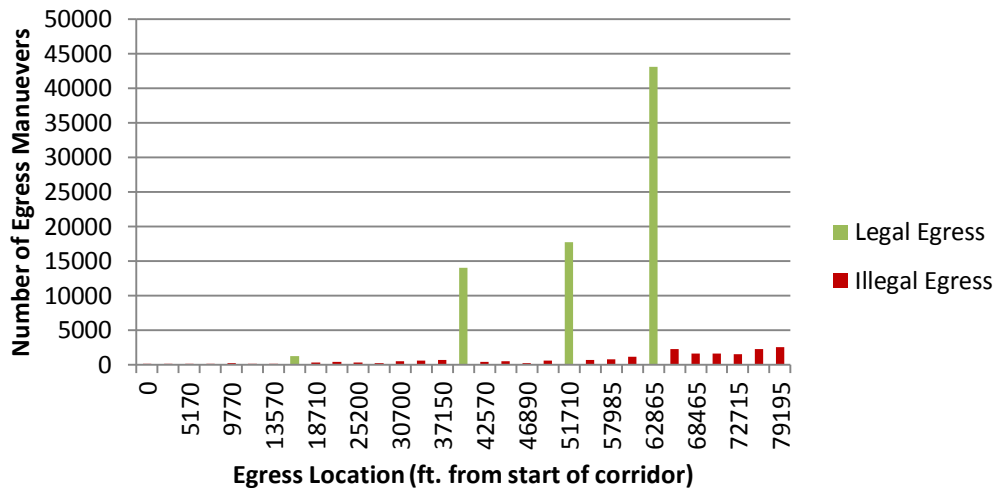


Figure 64: HOT Egress Counts by Location (weekdays, October 2012)

The weaving section prior to the I-285 ramps also contains signage indicating drivers should leave the HOT lane at this location if they wish to exit. Hence, the location of weaving sections and placement of signage likely plays a large role in the lane-changing behavior of HOT drivers. Also, because HOT drivers are paying a toll to use the HOT lane, they may desire to stay in the HOT lane to bypass as much congestion as possible before making the required exit maneuver. The decision to use the HOT lane is generally predicated on time savings compared to the general purpose lanes. Presumably, the magnitude of the toll to use the lane also plays a role in the likelihood that a driver will use the HOT lane. Thus, HOT drivers may wait longer to exit if travel time is reduced. It is currently not known whether drivers are exhibiting this behavior because they are in the HOT lane, or if HOT lane is more likely to be used by drivers exhibiting late lane-changing behavior. While the significance of each factor cannot be determined with the data at hand, more closely-spaced gantries in the HOT lane allow the egress behavior of HOT drivers to be studied.

HOT Egress Behavior of Exiting Drivers

An estimate of lane choice preference has been established based on a driver's origin and destination, as well as the speed of the general purpose lane. As the speed of the general purpose lanes decrease, the likelihood of a vehicle with a given O/D to be in the HOT lane increases. Vehicles moving from the HOT lane to the exit lane can affect freeway operations. Each lane change has the potential to reduce effective lane capacity and decrease throughput. As the proportion of vehicles making lane changes increases, so does the potential for throughput reduction. Not only is the proportion of vehicles

making the HOT-to-ramp maneuver expected to play a role in throughput reduction, but the egress location (in relation to the position of the ramp) of HOT-to-ramp traffic is also important. Vehicles that leave the HOT lane later (closer to the exit) increase the lane changing density in the area immediately upstream of the off-ramp. Egress behavior of the vehicles observed leaving the HOT lane to exit is studied in this section. Separate O/D analyses are performed for traffic originating at the beginning of the corridor and travelling to I-285 eastbound, and traffic originating at the beginning of the corridor and travelling to I-285 westbound. Egress behavior for vehicles traveling from the beginning of the corridor to the end of the corridor (not required to exit) is also analyzed to compare the egress behavior of traffic that must leave the HOT lane to exit against behavior of vehicles that are not exiting.

Figure 65 shows HOT egress data for vehicles exiting to the I-285 ramps, the rolling average of egress location (solid line for those vehicles exiting to I-285 westbound and a dashed line for those vehicles exiting to I-285 eastbound) and is color coded to reflect general purpose lane speed readings. What is most evident in this figure is the shift in the average egress position toward the exit ramp as general purpose lane speeds decrease (the solid and dashed lines representing the average egress location move up in the figure toward the exit ramp location). On the day these data were collected (10/23/2012), the average egress position for vehicles leaving the HOT lane within 35,000 feet of the ramp shifts from an average location of about 16,000 feet upstream of the ramp to an average location of about 10,000 feet upstream of the ramp as congestion builds.

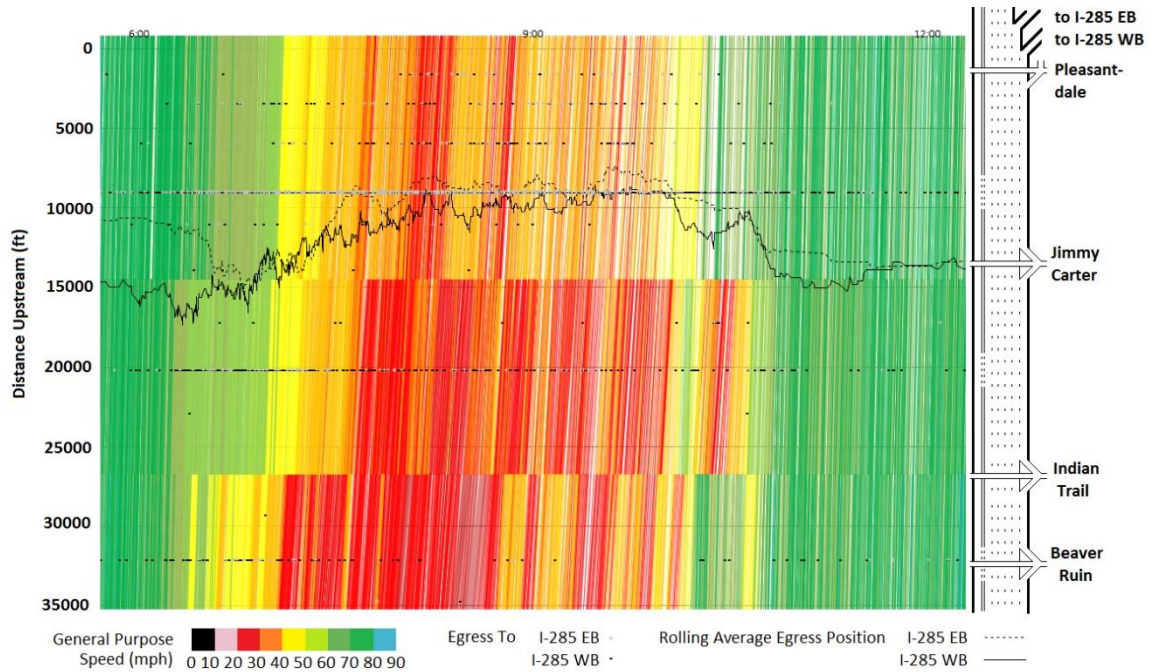


Figure 65: HOT Egress Behavior (10/23/12)

From Figure 65, it appears that average general purpose lane speed is likely to be a primary factor related to average HOT egress location. It will be of interest to ascertain the correlation between general purpose lane speeds as HOT drivers pass an upstream gantry, and the average egress location. The general purpose lane speed can be estimated using the space-mean speed of Peach-Pass-equipped drivers in the general purpose lanes for all drivers that pass the upstream gantry over a 5-minute period. The 5-minute period is determined according to the time the driver in the HOT lane passes the upstream gantry. Downstream general purpose speeds are then aggregated into 10 mph bins. These speed bins can be used to assess the role that general purpose speeds may play in average egress position. The average HOT egress position will be estimated for all vehicles that pass under each gantry:

- Gantry 1, ~35,300'/37,200' upstream of ramp to I-285 WB/EB
- Gantry 2, ~26,800'/28,700' upstream of ramp to I-285 WB/EB
- Gantry 3, ~14,500'/16,400' upstream of ramp to I-285 WB/EB

Gantry 1 is the furthest away from the ramp, and the average lane change position for HOT drivers passing under Gantry 1 is expected to be further away from the ramp. Gantry 3 is closer to the ramp, and the average HOT egress position is expected to be closer to the ramp. The average HOT egress position and confidence intervals are displayed in Figure 66.

In Figure 66, there seems to be a trend that reinforces the discussion of the case study from Figure 65. For all drivers in the HOT lane at the upstream gantry (GP Gantry 1, in blue, Figure 66), relatively stable average egress positions are noted for general purpose speeds greater than 50 mph. As the general purpose lane speeds decrease below 50 mph, the location from which exiting traffic leaves the HOT lane tend to move closer to the ramp. An exception arises for general purpose speeds between 0 and 10 mph. However, there are very few observations in this 0 to 10 mph regime and other factors may be at play here. Because the general purpose speed is based on the travel time to the next gantry, it is possible the traffic further downstream has cleared, and traffic moves outside of the HOT lane earlier than expected. This effect is discussed after the presentation of Figure 66. Early egress from the HOT lane when GP speeds are in the 0 to 10mph are also potentially the result of toll caps in place on the HOT lane that are not able to effectively manage demand for use of the lane (resulting in failure of HOT lane operations). When toll prices fail to ensure that demand remains below HOT lane

capacity, HOT lane speeds decrease, and drivers may start leaving the lane because they are receiving no value from paying the toll.

Given that an HOT driver passes Gantry 2 (in red, Figure 66), it is not surprising that the likely location of HOT egress is closer to the ramp. However, the general purpose speed appears to play a less significant role in the average location of the HOT egress. Although, the trend seems to indicate that as speeds increase, so does the average egress position upstream of the ramp.

Once HOT drivers pass Gantry 3 (in green, Figure 66), lane changes occur even closer to the ramp, and general purpose lane speeds appear to have very little influence on the average egress position. Difference in the average HOT egress location is meaningfully insignificant (~50') between the low and high general purpose speeds.

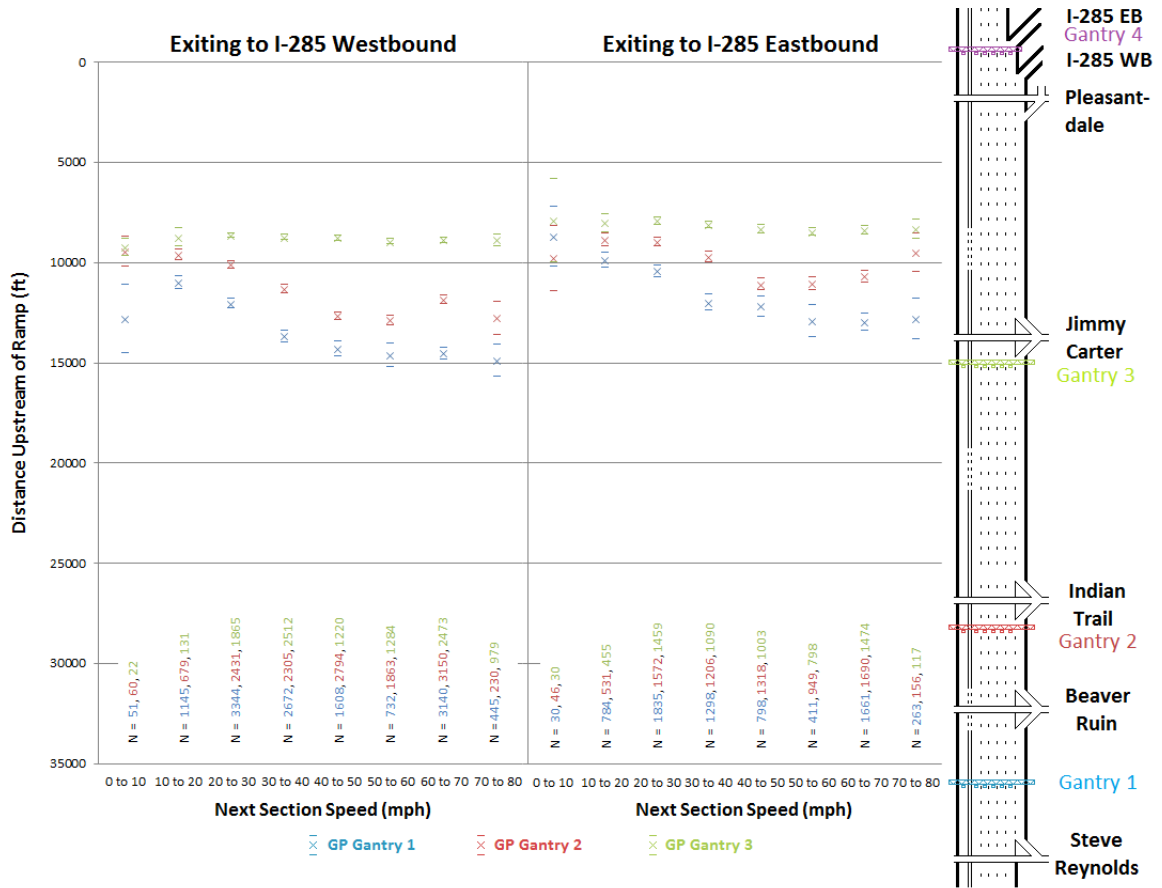


Figure 66: Average HOT Egress Location (exiting to I-285 WB/EB)

For any given gantry and general purpose speed, the average HOT egress location is closer to the ramp for drivers exiting to I-285 eastbound than it is for drivers exiting to I-285 westbound. On one hand, this is not surprising given that the I-285 eastbound ramp is 2,000' downstream of the I-285 westbound ramp. However, egress behavior differences for the two exiting groups is quite interesting, given that drivers exiting to either of these ramps from the HOT lane have the same opportunity to move from the HOT lane into the general purpose lanes via the designed access locations.

Figure 67 illustrates the average egress location for vehicles passing the upstream gantry, given the speed of vehicles in the general purpose lanes in the previous segment and in the upcoming segment. As already discussed in this chapter, the general purpose speed of the segment an HOT driver has already passed appears to play a role in the average egress position. However, the speed of general purpose traffic in the upcoming segment also appears to play a role in the estimation of the average egress position. For a given upcoming-segment general purpose speed, the average HOT egress location moves further away from the ramp as the previous segment general purpose speed decreases. In Figure 67, the impact of next-segment general purpose speeds is particularly noticeable when general purpose speeds of the previous segment are very low (10-20mph). When subsequent segment speeds are low, drivers appear to wait longer to leave the HOT lane (closer to ramp), but leave earlier (further upstream of the ramp) when next-segment general purpose speeds increase.

HOT drivers observing general purpose traffic conditions may notice that general purpose speeds are increasing. The greater the speed improvement, the more likely drivers may be to leave the HOT lane at the next available chance. As more drivers desire to leave the HOT lane sooner, the average egress position moves further and further upstream of the ramp.

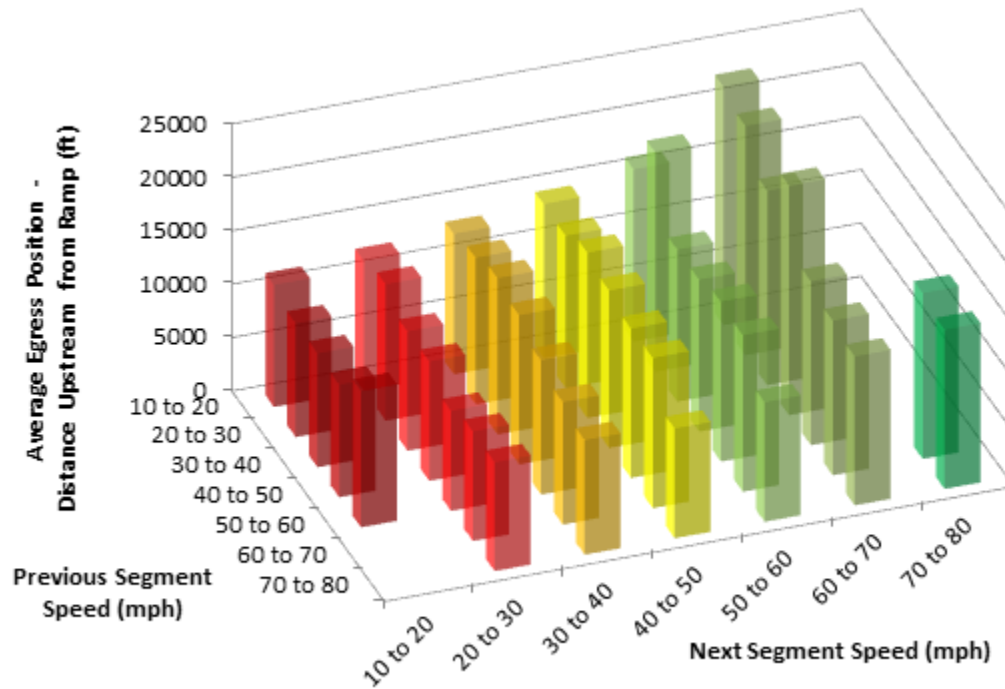


Figure 67: Average HOT Egress Location Vs. Previous and Next Segment GP Speed

Speed in the general purpose lanes is probably not the only factor that drivers consider when deciding when to leave the HOT lane. Some drivers may habitually use the lane, and have behavioral preferences regarding egress location independent of conditions in the general purpose speed.

The general purpose speed is correlated with the propensity for a driver with a given O/D to use the HOT lane. This was evidenced in the data presented in Figure 59, Figure 61, and Figure 62, which assess the likelihood of HOT usage, given a driver's O/D and speed in the general purpose lanes. The data also indicate that O/D and general purpose speed may play a role in general purpose lane choice, particularly when drivers

get closer to an off-ramp. Additionally, data presented in Figure 66 and Figure 67 appears to show correlation between general purpose speeds and the location from where vehicles leave the HOT lane to exit. Drivers tend to wait longer before leaving the HOT lane when general purpose lane speeds are moving slower.

As general purpose speeds decrease, there is an increased likelihood that drivers will use the HOT lane, coupled with an increased likelihood that these drivers will wait longer and leave the HOT lane closer to their destination. The end result is increased lane changing density in the vicinity of off-ramps, which have the potential to further negatively impact already-congested freeway operations. Given that HOT lanes are typically built along congested corridors and attempt to relieve congestion, consideration should be given to HOT-driver lane-changing behavior to minimize the potential negative impacts on general purpose lanes, especially in the vicinity high-demand off-ramps.

Given the complexity of the findings presented in Chapters 6, 7, and 8, there is clearly a need for a further assessment of lane choice and lane changing behavior. With the data at hand, there are limits to the conclusions that can be made. However, the framework for future model development has been established. Chapter 9 provides an overview of future model development needs within the context of the findings presented in this dissertation.

CHAPTER 9 FUTURE MODEL DEVELOPMENT

Research presented in this dissertation indicates that there is a relationship between speed and the position of lane changes between the ramp lane and mainline lanes, on a macroscopic scale. Findings warrant further investigation into lane changing behavior for use in the development of a more generalized macroscopic lane changing model that can be applied to more complex systems. Future research needs can be broken into two areas:

1. Research that can be completed using current data collection capabilities and processing techniques
2. Research that can be completed with more extensive data collection capabilities and with improvements on current data processing techniques

Research Utilizing Current Capabilities and Techniques

Given the infrastructure of the sites used in this study, if more detailed data were available, further conclusions regarding the shapes of the lane changing distributions could likely be made for given different infrastructure characteristics. At the moment, video acquisition technology is available to efficiently collect data at a reasonable cost. Unfortunately, a sufficient number of cameras are not in place to collect the data needed. More cameras are needed to obtain broader and continuous coverage of vehicle activity, and the number of cameras needed depends upon whether high-resolution or low-resolution (current standard) cameras are installed. For this study, a congested, high-demand off-ramp was chosen for analysis. When appropriate camera equipment becomes

available, current processing capabilities will allow further studies to be conducted designed assess the impacts of physical infrastructure design on the lane change distributions. Other infrastructure characteristics that are likely to affect weaving distributions may include:

- Lane drops
- Lane adds
- On-ramps
- Weaving sections (i.e., cloverleaf or diamond ramps)
- Auxiliary lanes (weaving section between on-ramp and off-ramp)
- Controlled or uncontrolled access points
- Barrier or buffer separated HOV, HOT, express, and collector-distributor lanes.
- Temporary work zone lane closures
- Etc.

Each type of infrastructure is expected to impact the lane changing distribution differently. First, lane changing resulting from each type of infrastructure should be assessed in isolation, absent the influence of other infrastructure elements that may cause additional lane changing to occur. This will provide a baseline for how each type of infrastructure affects lane changing. Based on the research presented in this paper, the inter-related locations of physical infrastructure elements and the speed of traffic are expected to play the largest role in the estimation of the lane changing distribution. Given knowledge about how each piece of infrastructure affects lane changing, the overall lane changing distribution resulting from clusters of infrastructure can be disaggregated to trace the shape of the lane changing distribution back to each individual infrastructure element. Studies can then proceed to assess the interaction of closely spaced infrastructure, where more continuous data (described in the next section) will be required to evaluate lane changing interactions between infrastructure too far apart to be evaluated given current data collection capabilities.

Also, with current capabilities, relationships between primary (first-order effect) lane changes and other induced (higher-order effect) lane changes, can begin to be established for different types of sites. For instance, in the case of a lane drop, the primary lane change movement is between the dropped lane and the lane adjacent to the dropped lane, e.g. the infrastructure (dropped lane) forces these lane changes to occur. Secondary lane changes are made from the adjacent lane to the next lane over, to avoid the merging maneuver or the slowdown resulting from merging vehicles. Similar lane changing habits are expected in the vicinity of high-volume on-ramps. On the other hand, in a lane add, more gaps are created in the traffic stream when vehicles move into the added lane. Vehicles in other higher-density lanes may fill in gaps created by the primary lane changes. Secondary, and other higher-order lane changes, are not required for a driver continue on the roadway, but are made by changes in lane preference due to the effects of first-order lane changes on the traffic stream. In the case when primary lane changes result in a higher-density traffic stream (i.e., lane drop, on-ramp merge), it is hypothesized that higher-order lane changes will occur upstream of lower-order lane changes. When primary lane changes result in a lower-density traffic stream (i.e., lane add, off-ramp), it is hypothesized that higher-order lane changes will occur downstream of lower-order lane changes. Assessing lane change behavior in response to created gaps will be critical to this research element and will require detailed vehicle position data that can only be afforded with improved video deployment.

Equally important to the locations of physical infrastructure, varying demands from different O/D (on-ramp/off-ramp) pairs promises to further complicate the analysis. The general flow of vehicles from origins to destinations may affect the intensity of

weaving depending upon the location of origin or destination ramps and prevailing traffic conditions faced by the drivers. Additional SRTA data can be used to assess the impacts of varying volumes and fractions of O/D pairs, general purpose lane speed, and time-of-day differences in driver behavior for given O/D pairs. For freeways that do not have RFID capabilities (similar to I-85), properly placed ALPR equipment could potentially provide similar data to study the impacts of origin and destination on lane choice. Additional RFID tag reader installations at specific locations of interested would help support these research efforts.

Research Utilizing Improved Capabilities and Techniques

In developing improved lane changing models, addressing the need for adequate data collection infrastructure and equipment is paramount. Comprehensive video coverage is needed to allow more complex macroscopic lane changing models to be developed. One way this can be accomplished is by positioning PTZ camera locations close enough together so that vehicles can be tracked from camera to camera. To be tracked through the field of view, vehicle images need to remain a minimum of approximately 100 pixels in size during tracking. With current standards of high-definition (1920x1080), PTZ-mounting poles need to be placed approximately every one third of a mile, assuming two cameras are mounted on each pole, pointing in opposite directions (a third camera is generally needed to monitor the occluded area near the mounting equipment) to ensure the minimum 10x10 pixel tracking size requirement is met for each vehicle. As the resolution of video able to be collected by cameras increases, the distance required between the mounting equipment will increase, presumably

decreasing the cost to monitor a given length of corridor. Additional opportunities will likely be available to cost-efficiently collect complete corridor data with the advent and evolution of drone technology and ever-increasing video resolution.

Being able to monitor vehicles from camera to camera as they traverse the corridor will allow a vehicle to be tracked back from its destination to estimate the fraction of drivers in a given lane attempting to reach a certain destination. However, funding has to be allocated to camera infrastructure installation to support required data acquisition (which is the primary limiting factor for continuing research). With additional camera infrastructure, especially with the availability of high-definition camera views, time-space trajectories for larger portions of the freeway can be collected, and microscopic behavior analyzed to further test the hypotheses proposed in this research. With the ability to accurately track all vehicles, microscopic gap acceptance choice models can be developed (as opposed to models based on speed or density averages) to estimate the likelihood of a driver to change lanes, given O/D, current lane choice, and distance to the destination. Microscopic choice-based models can be compared against macroscopic findings to verify they are working properly.

Aside from tracking vehicles between camera views, it is also important to emphasize the importance of monitoring to provide a continuous data stream. The ability to track vehicles over long distances opens up many possibilities for future research, including analysis of corridor level behavior as a function of traffic conditions and origin/destination supply/demand throughout the day. Whereas RFID gantry data can only be used to estimate O/D and lane choice for a subset of vehicles where RFID-

detection equipment is installed, continuous camera coverage potentially allows the lane choice for all vehicles to be monitored at all locations throughout the corridor.

Vehicles moving between the mainline and exit lanes are generally making a mandatory lane-changing decision. However, between other lane boundaries, it is currently not known whether a vehicle is making a mandatory or discretionary lane change, as the lane change cannot be linked to a particular destination or freeway egress point. The macroscopic lane changing characteristics exhibited by drivers with a certain destination can be compared against drivers with other destinations. Given a known destination, the predictability of the population can be estimated for a given lane given the distance upstream from a ramp. This is important because it will allow us to understand how lanes are being utilized by drivers with different origins and destinations.

With corridor-level data in hand, interactions of lane changing effects caused by different physical infrastructure and demand can be assessed. While it is useful to understand how individual pieces of infrastructure affect the lane changing distribution, knowledge of how they interact with each other to create more complex lane changing distributions will be useful in modeling realistic corridor-level lane changing behavior.

Changing the location of infrastructure and varying O/D demand will affect lane changing activity along a corridor. A fully-developed lane-change model is expected to accurately predict lane-changing activity for a specified set of infrastructure elements and O/D demand. Knowledge of how infrastructure will affect lane changing is crucial in highway engineering. Infrastructure (multiple elements) can be designed to minimize the adverse impacts of lane changing on the traffic stream, and minimize the creation of freeway zones in which lane changing may pose a safety concern. Additionally,

knowledge of how demand is expected to change over time (travel demand modeling) can be used to assess the impacts changing O/D demand will have on lane changing activity, and ultimately, traffic flow.

CHAPTER 10 CONCLUSIONS AND FUTURE RESEARCH

Speed and lane change data collected from video cameras in the field indicates that there is a relationship between the number of lane changes, speed of the target lane, and the distance upstream of the congested off-ramp. The data exhibited a parabolic relationship between the average number of lane changes in a wave and target lane speed, and a gamma-distributed relationship between the number of lane changes and position. Parameters of the distribution can be derived as a linear function of the downstream speed of the target lane. The combined shape of the macroscopic lane changing distributions indicates that for a given target lane speed, lane changing is least likely at locations nearest the physical gore, and increases until a limiting distance is reached upstream of the ramp, before decreasing and then tailing off. The location at which the maximum expected number of lane changes occurs increases as target lane speed increases, and overall lane changing intensity increases in parabolic form with respect to speed, peaking around 30 to 40 mph.

The decreasing intensity of lane changing at lower speeds likely results from fewer available gaps in the target lane. The decreasing intensity of lane changing at higher speeds is likely a result of fewer vehicles available or desiring to fill gaps in the target lane (assuming relatively homogeneous conditions when ramp lane is in free flow). The shape displaying the relationship between speed, location and number of locations for the I-85 study site is shown in Figure 68.

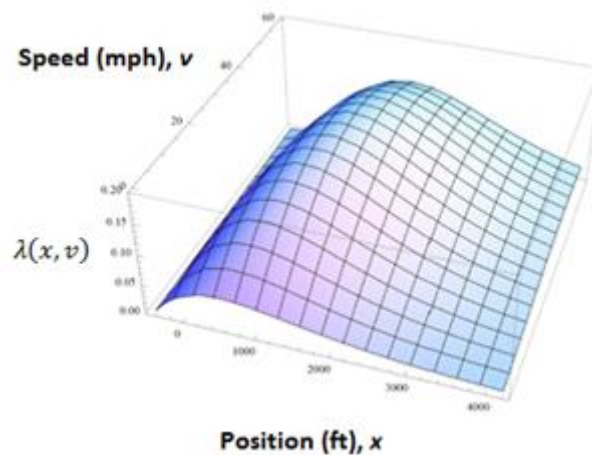


Figure 68: Best-Fit Model

Video data suggests that along with the friction factor between exiting vehicles and through vehicles, queue jumpers may be slowing down in the rightmost through lane as they try to enter the slower-moving exit lane. More often than not, these queue jumpers hold up traffic in the rightmost through lane, likely reducing the discharge capacity of the mainline through lanes. Stopped vehicles, attempting to move from the rightmost through lane to the exit lane, cause a congestion wave to form in the rightmost through lane, which also likely increases the friction factor on upstream left-hand lanes, and may cause additional disruptive lane changes from drivers exiting from the second and then later from the third through lane (etc.). The propagation of the higher density traffic state to other lanes of the freeway may result from these disruptive lane changes.

Implications for Design

Analysis of Peach Pass data suggests exiting drivers are more likely to choose the HOT lane on the left side of the freeway at a given location upstream of the off-ramp, as freeway speeds decrease. Because HOT drivers are waiting longer to get over, more lane

changes are being made over a shorter distance at a location closer to the ramp. Advance knowledge of HOT-to-ramp maneuvers and freeway speeds can be used by HOT system designers for the placement of weaving sections, or can be used as justification for direct-access ramps for certain high-demand maneuvers.

Implications for Safety

Lane changes that cause disruptions in the initial lane are partially responsible for the lateral propagation of congestion. Some disruptions cause more congestion than others. Given a prolonged queue in the ramp lane, large disruptions are somewhat unavoidable. However, there is an opportunity to educate drivers on how to change lanes in a safe and legal manner that minimizes their impact on the system. A few of the major takeaways of such a campaign would be to only change lanes before traffic comes to a stop, otherwise, keep moving forward at a reasonable pace, until gaps become available in the exit lane. Typically, gaps appear in the traffic stream as drivers accelerate, which presents an opportunity for changing lanes (Laval, Toth, Zhou, 2013). In conjunction with a driver education program, an automated enforcement strategy can be put into place to minimize the likelihood of a driver exhibiting disruptive behavior.

Limitations

Currently, one of the major limitations to constructing more in-depth data-driven lane changing models is the lack of infrastructure from which data can be collected. Vehicle-tracking tools necessary for processing the data are available (Park, 2012). However, video data for use in these analyses are generally not available.

Another limitation of this research is the difficulty of locating the most ideal sites for data collection. In the best circumstance, data could be collected from a site with no off-ramps upstream of the ramp of interest. Although the Pleasantdale Road off-ramp did not significantly impact the results of this study, the off-ramp presence is likely to have played a role in the lane changing distribution in its vicinity. Additionally, with regard to site selection, it would be ideal for there to be no on-ramps upstream of the site. Without ramps, the fraction of vehicles exiting and staying on the mainline may be homogeneous (approximately) across all lanes at some point upstream of the congested off-ramp. Unfortunately, sites with such a description are not easy to come by, especially considering areas that experience freeway congestion are typically in urban areas, which are more likely to have more closely spaced ramps.

Future Research

With respect to the spatial distribution of lane changes outside of the study area, it is important to recognize that transferability of the current shape functions remains uncertain. The cause-effect relationships that drive the shape of the distribution are still undefined and will require additional research efforts with higher-resolution data. Given that infrastructure plays a role in the location where lane changes are made, there is likely an on-ramp or off-ramp upstream of the study site that will result in an increase/decrease of lane changing in certain areas. However, under the most ideal infrastructure, a freeway with no high-demand ramps or major bottlenecks immediately upstream of a high-demand ramp, the gamma distribution may accurately represent the macroscopic spatial lane changing distribution for making the mandatory lane change into a ramp lane.

However, for data collection and analysis purposes, it becomes increasingly difficult to differentiate between mandatory and discretionary lane changes further and further upstream from the ramp. The fraction of discretionary lane changes (compared to mandatory lane changes) may increase, and occur at random or as a function of driver demographics, but such hypotheses cannot be tested without additional detailed data. Driver observation data generated by the naturalistic driving studies conducted under the SHRP2 program may help in this regard (Hedlund, 2013).

Although the site selection for this research attempted to minimize the number of confounding variables, future research (given current data collection and processing capabilities) should first focus at sites where off-ramps and on-ramps do not play a role in affecting the spatial distribution of mandatory lane changes. Unfortunately, there are not many ideally-designed freeways from which empirical studies can be performed (i.e., no on-ramps or off-ramps). It is simply the nature in which how infrastructure is designed to get drivers where they need to go. Once the impacts of individual pieces of infrastructure are assessed, interactive effects of multiple pieces of infrastructure can be studied.

At the microscopic level, it will be important to assess whether drivers making mandatory lane changes (from the through lane into the exit lane) are forcing their way in, or whether they are simply waiting for gaps. Findings in this research reveals that the speed of a congested exit lane decreases further upstream of a ramp. A decrease in speed is not a surprise, given the fact that vehicles are entering the exit lane via a lane change. However from the data in hand, a quantitative assessment cannot be made as to whether lane changes are a result of gap creation from slowly accelerating vehicles, or if drivers are forcing their way into small gaps causing drivers behind to decrease speed as they

relax their following distance (Laval and Leclercq, 2008). Obviously, both hypotheses are likely to play a role, but the relative extent is currently unknown. A microscopic assessment of the interaction between lane changing vehicles and vehicles in the exit lane may provide insight into why the speed of the ramp lane tends to decrease upstream of the ramp.

Lane changing appears to affect congestion propagating wave speed. As the number of lane changes increases, the speed at which a wave appears to propagate backwards appears to decrease. This is especially evident when traffic in the ramp lanes has been at a standstill for a prolonged period of time (greater than 30 seconds), and the number of vehicles needing to make the maneuver from the mainline into the ramp lane begins to accumulate, because there are rarely gaps for vehicles to enter the traffic stream when the target lane is operating at jam density. As traffic in the ramp lanes begins to move again, gaps are quickly filled by drivers moving from the mainline to the ramp lanes. Regardless of whether the driver already in the ramp lane is aiding the lane-changing driver, or the lane-changing driver is forcing his way in front of the driver currently occupying the target lane, it is hypothesized that the driver currently in the target lane is staying stopped longer than they would be in the absence of the lane-changing driver, resulting in the wave propagating back more slowly. Further research is needed in this area to better understand how lane changing plays a role in the propagation of traffic states.

Contributions

Data and processing techniques introduced in this study have never been used before. The data collected in this study (video and processed) can be used in future studies of driver behavior and freeway operations. Given the video processing tools, other researchers can collect data at other sites, and perform similar or alternative studies. The analysis is completed in a straightforward manner, and does not rely on complicated theories, arguments, or assumptions to make conclusions about lane changing at the macroscopic level.

The most significant contribution of this study is introduction of a statistical basis for macroscopic lane changing relationships that can be integrated into simulation models and expanded and tested in other locations. The research effectively analyzes the data in hand to establish a preliminary model for changing lanes into an off-ramp. The preliminary model advances the state of the practice, and provides a starting point from which extensions can be made.

Other contributions include the identification of disruptive weaving behavior exhibited by a small fraction of drivers that results in the lateral propagation of congestion, and that a driver's origin and destination and the speed of general purpose lanes affects lane choice. Transportation engineering design and operational policies can be informed by these findings in an effort to reduce destructive weaving, improve operations, implement variable speed limits as a function of O/D patterns and operating conditions, and better design the placement and design of weaving sections as a function of local demand patterns.

Steps for future research have been identified to work toward a corridor level macroscopic lane changing model that captures the complexities of driver behavior as it pertains to the location of infrastructure, speed of the roadway, and O/D pairs. When higher-resolution, comprehensive data becomes available, more sophisticated models can be developed that control for such complexities.

**APPENDIX A: PROCEDURES FOR CHANGING TMC PTZ
CAMERA VIEWS DURING I-85 VIDEO DATA COLLECTION
EFFORTS**

December 14, 2010

Randall Guensler, Professor

Jorge Laval, Professor

Michael Hunter, Professor

Angshuman Guin, Research Engineer

Vetri Elango, Research Engineer

Christopher Toth, Graduate Research Assistant

Felipe Castrillon, Graduate Research Assistant

School of Civil and Environmental Engineering

790 Atlantic Drive, Atlanta, GA 30332-0355

Georgia Institute of Technology

Atlanta, GA 30332-0355

Procedures for Changing I-85 TMC PTZ Camera Views

The GDOT Traffic Management Center uses pan-tilt-zoom (PTZ) cameras to monitor incidents and adverse traffic conditions. Using the cameras for any other purpose is of secondary priority to this incident monitoring function. Beginning in January 2011, Georgia Tech Faculty and Staff Assistants will be collecting video data from the PTZ cameras along the I-85 corridor for weaving and effective capacity analysis. Georgia Tech staff plan to move the cameras for the purposes of video data collection only when TMC staff members are not actively using the camera views. This report describes the proposed protocols that Georgia Tech staff will follow in changing PTZ camera views along the I-85 corridor for data collection purposes.

Background

Beginning in January 2011, the Georgia Tech team will begin collecting video data from the I-85 HOV-to-HOT corridor for the purposes of assessing effective capacity of the managed lanes before and after HOT conversion.

Processing of video data for weaving analysis involves assessment of the gap separation between vehicles when a weave occurs. Baseline camera views for each camera are pre-assigned and distance calibration is performed for each baseline view. With proper calibration, video post-processing provides reasonable estimates of gap separation based upon the pixel separation of vehicles on the video image. To be useful, weaving analysis video must be collected from each camera's baseline camera position. The primary use of the cameras is for the TMC operators to monitor incidents and adverse traffic conditions. The Georgia Tech data collection effort is secondary to TMC

use of the cameras. The team will be collecting a very large amount of video data to ensure that data loss associated with the relocation of camera views by TMC operators to monitor incidents should not cause any major problems in analytical efforts. However, the Georgia Tech team will need to return each camera to its baseline position before the video will provide useful data for weaving analyses.

TMC Notification

Maintaining continuous baseline camera positions significantly helps in the data collection efforts. Hence, it will help if TMC operators can avoid moving camera views on the corridor for non-incident-related purposes during video data collection periods. The Georgia Tech team will provide a schedule to the TMC indicating when the I-85 cameras will be used for data collection. The Georgia Tech team will also call 511 each morning and afternoon that data are being collected to remind the operators about the data collection effort.

Procedures for Moving Camera Views

Georgia Tech staff will periodically monitor the camera views to determine when a camera has been moved from its baseline data collection position. If a camera has been moved by a TMC employee during the recording period, the camera view will not be automatically or immediately repositioned by Georgia Tech staff.

GT staff will first look for any obvious cause of the camera movement by studying the field of view and looking for an incident or an adverse traffic condition. Under no circumstances will cameras be moved if adverse traffic conditions are being monitored or an incident is active. Once an incident ends, GT staff members will wait at

least 10 minutes prior to repositioning the camera back to its baseline view. Even if no incident or adverse traffic conditions are present in the camera view, the research group will wait 10 minutes before moving the camera back to its original baseline position in case the TMC operator was looking at some other condition. If after GT staff reposition the camera, the camera is again repositioned by TMC staff with no obvious incident in the field of view, GT staff will leave the camera in its current position and will call 511 to ask whether the TMC staff still need that camera view or whether the view can be returned to the baseline position for data collection.

In summary, GT staff will not move camera views when:

- The camera is monitoring an incident or adverse traffic condition
- Ten minutes after an incident or adverse traffic conditions has ended
- Ten minutes after a camera has been moved by a TMC operator

APPENDIX B: SCREENSHOTS OF CAMERA VIEWS USED DURING RECORDING



1. PTZ camera 84



2. PTZ camera 85



2. PTZ camera 121



4. PTZ camera 86

APPENDIX C: OTHER MODEL CONSIDERATIONS

Last-Second Lane Changing

Very few lane changes are observed within 120 feet of the physical gore and these lane changes did not fit the model well, due to the fact that the number of lane changes predicted by the model in this zone is extremely small. Given the lack of data near the physical gore, it is very difficult to estimate the fitting shape with any accuracy. Hence, there is no discernible relationship between general purpose lane speed and number of lane changes expected within each of the final three 40-foot increments approaching the gore. Figure 69 shows the number of lane changes into the exit lane for each of the final three lane changing locations upstream of the physical gore.

Given the lack of data, aggregating across all locations may be helpful for estimating the relationship between the number of lane changes and ramp speed. The number of lane changes observed in each 10 mph speed bin is displayed in the graph in Figure 70, and reveals that the relationship between speed and the fraction of lane changes that occur during the final 120 feet may decrease in a linear fashion.

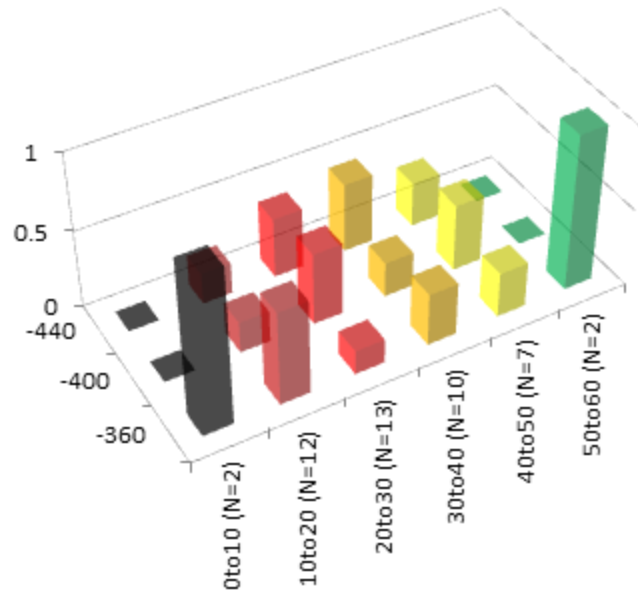


Figure 69: Spatial Distribution of Last-Minute Lane Changes by Speed

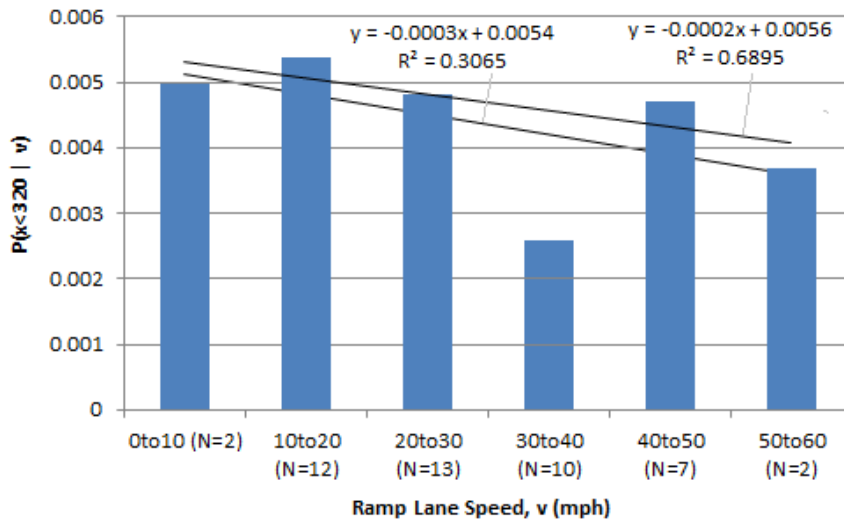


Figure 70: Relationship between Ramp Lane Speed and Last-Minute Lane Changing

Earlier in this chapter, the total number of expected lane changes was estimated as a parabolic function of speed. However, this does not seem to be the case for lane

changing in the last 120 feet. The trend indicates that lane changing in the last 120 feet may decrease with respect to ramp speed. Excluding the potentially outlying data in the 30 to 40 mph range, the linear fit greatly improves. Surprisingly, the lane changing rate does not dramatically decrease, especially at higher speeds when more gaps are expected to be available in the exit lane traffic stream. This may be partially explained by assessing conditions that drivers experienced immediately before reaching the gore area. If the ramp lane moves at slow speeds for a prolonged period of time, a driver trying to enter the ramp lanes may have to wait until the very last minute to enter the ramp lane. Alternatively, last-second lane changing may be an inherent part of some drivers' behavior. The goal of drivers with this type of behavior may be to travel as quickly as possible by waiting until the last second to move into the ramp lane. Less than one half of one percent of observed lane change data occurs in the final 120 feet. More data are needed to make accurate assessments regarding driver behavior in this area. However, given the congestion implications of these late lane changes, supplemental research is warranted.

Secondary Lane-Changing Effects

Physical infrastructure is expected to play an important role in the location of lane-changing maneuvers. Around 2000' upstream of the off-ramp is the Pleasantdale Road overpass and the off-ramp to Pleasantdale Road. Both of these features have the potential to impact lane changing. Drivers may be more hesitant to change lanes under an overpass, or perhaps more likely, driver may be more likely to change lanes into the ramp

lanes just downstream of the Pleasantdale off-ramp as exiting drivers create additional gaps thereby facilitating the lane changing.

A proper analysis of this phenomenon would require microscopic data between the Pleasantdale off-ramp and the Pleasantdale overpass. Because these data do not exist, the hypotheses above are still speculative. The model is not intended to estimate the effects associated with upstream ramps. This opens up the discussion for why the inflection in the spatial distribution exists at this location. Perhaps the effect can be attributed to the presence of the overpass or the off-ramp, but this cannot be assessed at this time with the current data.

Analysis of observed and model-estimated numbers of lane changing (see Figure 36 through 38) on the I-85 site indicate a short period of underestimation, followed by a period of overestimation in the area between the Pleasantdale overpass and the off-ramp to Pleasantdale. Not surprisingly, the trend in the residuals is particularly noticeable in the middle speed regimes when the most lane-changing is occurring.

To model the inflection in the vicinity of the off-ramp, an additional shape derived from the normal distribution, and represented by the equation below, is added to the fitting equation. The shape contains three parameters which control for the location, period (variance), and amplitude of the inflection.

$$\lambda(x, v) = (a_1 + a_2v + a_3v^2) \frac{\exp\left(-\frac{440+x}{a_6+a_7v}\right) (440+x)^{-1+a_4v+a_5} (a_6v+a_7)^{-a_4v+a_5}}{\Gamma|a_4v+a_5|} + \exp\left(\frac{(x-a_8)^2}{a_9^2}\right) \left(\frac{x-a_8}{a_9a_{10}}\right) \quad x > -320$$

Equation 12: Model Fit with Inflection

The model results are shown in Table 20 on the following page. The shape of the final fitting curve is shown in Figure 71. All three additional parameters are significant, especially the inflection location estimator. All other coefficients remain significant.

Table 20: Parameter Estimates for Best-Fit Curve (Inflection)

| Coefficient | Estimate | Standard Error | t-Statistic | P-Value |
|-------------|-----------|----------------|-------------|---------------------------|
| a_1 | -0.258076 | 0.0202023 | -12.7746 | 2.40488×10^{-37} |
| a_2 | 19.7462 | 1.19553 | 16.5167 | 3.25163×10^{-61} |
| a_3 | 118.85 | 16.5493 | 7.18156 | 6.93168×10^{-13} |
| a_4 | 0.0317279 | 0.004739 | 6.69455 | 2.17282×10^{-11} |
| a_5 | 2.18155 | 0.145238 | 15.0206 | 5.99231×10^{-51} |
| a_6 | -3.11021 | 1.34313 | -2.31564 | 0.0205798 |
| a_7 | 820.49 | 48.7313 | 16.837 | 1.54581×10^{-63} |
| a_8 | 1737.1 | 28.8741 | 60.1614 | 6.7064×10^{-777} |
| a_9 | 404.83 | 44.0183 | 9.19678 | 3.74515×10^{-20} |
| a_{10} | 10272 | 1405.6 | 7.30846 | 2.71901×10^{-13} |

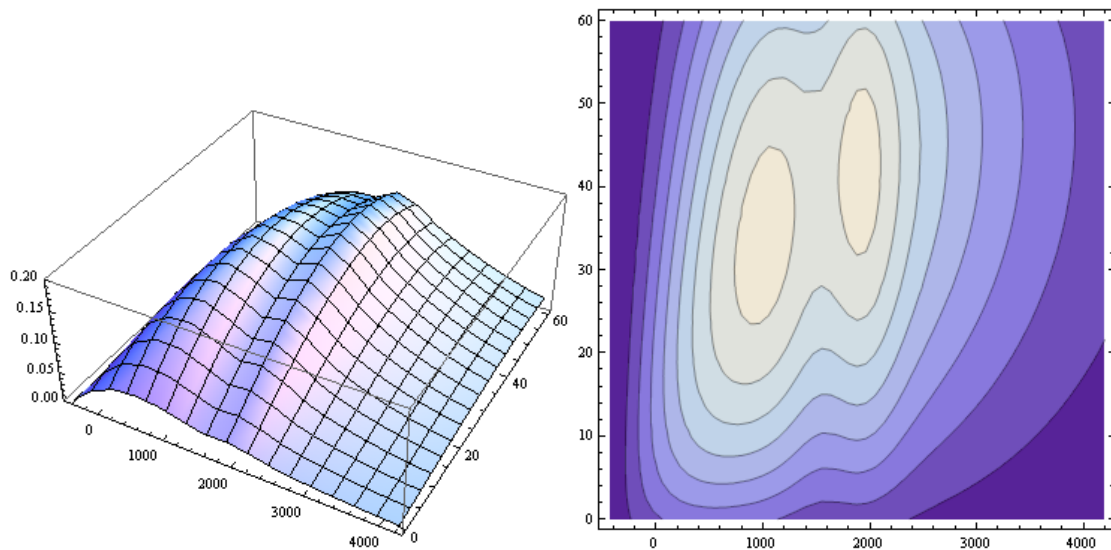


Figure 71: Three-Dimensional and Contour Plots for Best Fit Model With Inflection

Table 21: Chi-Squared Test Results for Best-Fit Curve (Inflection)

| Speed (mph) | 0-5 | 5-10 | 10-15 | 15-20 | 20-25 | 25-30 | 30-35 | 35-40 | 40-45 | 45-50 | 50-55 |
|---------------|-------|-------|-------|-------|-------|-------|-------|-------|-------|-------|-------|
| N 30s periods | 28 | 143 | 121 | 76 | 41 | 32 | 21 | 24 | 10 | 19 | 6 |
| Chi-sq | 86.1 | 118.9 | 94.5 | 117.0 | 101.0 | 130.6 | 124.0 | 125.4 | 119.1 | 97.0 | 100.6 |
| p-value | 0.949 | 0.244 | 0.838 | 0.283 | 0.694 | 0.078 | 0.154 | 0.135 | 0.239 | 0.789 | 0.704 |

Chi-square critical value at 5% significance(109 d.o.f.): 134.37

The chi-square test in Table 17 indicates an improved fit at higher speeds (greater than 20mph), but a worse fit in lower speed bin (less than 20mph) compared to the fit curve without an inflection. This may be due to the location, amplitude, or period of the inflection changing with respect to speed. However, with the given data, the improvement in model fit is offset by the additional fitting parameters. That is, the addition of variables to the model introduces additional degrees of freedom to the analysis and essentially results in over-specification.

Despite improvements in the model fit, there is not enough evidence with the given dataset to make any conclusive remarks regarding the impacts of an uncongested off-ramp on freeway lane changing. The number of parameters may also be overfitting the data, as the relationship between speed, lane change location, and infrastructure location cannot be further refined without studying additional sites. However, this opens up the discussion as to how an off-ramp may play a role in macroscopic lane changing, and that adding an inflection into the model may be necessary when modeling macroscopic lane changes in the vicinity of a low-demand off-ramp. Presence of infrastructure elements such as ramps or construction zones may result in more complex shapes, as indicated above. With enough continuous weaving activity data, it seems likely that if these more complex shape functions are consistent they will be predictable as a function of infrastructure design and traffic demand.

APPENDIX D: VIDEO PROCESSING SOFTWARE

The tracking of the vehicles through the camera view was performed using the Gygax software developed at the Georgia Institute of Technology. Red tracking boxes are drawn around each vehicle. This is the image the program attempts to follow frame-to-frame. Tracking parameters are specified to help the program determine the rate at which vehicles position and size will shift from frame to frame. The pixel coordinates of the corners of each red tracking box are used to determine each box's centroid. However, the scale of the image changes from the foreground to the background of the image. To correct for this, a coordinate transformation is specified to convert pixel coordinates to real-world coordinates. The time at each frame, the real-world (horizontal and longitudinal) coordinates of the centroid of each box, and the lane number (based on the horizontal coordinate) is written to a text document. To ensure for quality and correctness of the data, each processed frame is recorded in the event the output data becomes questionable (e.g. in the case of partially-occluded vehicles, or in the case where a track is dropped and the box skips around the screen). In these cases, the recorded frames can be referenced to determine if any parts of any trajectories should be excluded from the data.

Trucks traveling in the right lanes result in occlusion of vehicles, usually a single lane to the left of the truck. When occlusion occurs, the centroids of some red boxes may be shifted in a way that does not accurately represent the occluded vehicle's trajectory. In these instances, the boxes are deleted and re-drawn if/when the vehicle comes back in view. This process is done for all vehicles in all lanes.

Tracking

The tracking algorithm of the proposed methodology is based on Ross et al. []. Within the methodology, inference on affine parameters is made through particle filtering. The parameters include x , y , scale, aspect ratio, rotation, and skew of a parallelogram that encloses a vehicle. The appearance of the vehicle is modeled with principal components of eigen-images. Unlike the original method, the one in the proposed system considers x and y coordinates converted to road coordinates instead of using image pixel coordinates in particle filtering. The use of road coordinates facilitates imposing a priori knowledge of vehicle behaviors on the tracking process, which allows improved performance and automated termination of failed tracking. A set of affine parameters is estimated by modeling each parameter with an independent Gaussian distribution. In the proposed method, standard deviations (STD's) of the distributions for x and y are determined by the previous information. For example, STD_x and STD_y at time t are updated as $x_t - x_{t-1}$ and $y_t - y_{t-1}$, respectively. In this way, the current state of a vehicle is well reflected in the Gaussian distribution. Also, a priori knowledge that vehicles do not move backward on roads, especially on highways, is infused into the particle filtering by enforcing y_t to be larger than y_{t-1} for each particle. For the first inference when x_{t-1} and y_{t-1} do not exist, STD_x and STD_y are determined based on the average speed of a certain number of previous vehicles per lane.

Tracking results are integrated with detection results to determine whether each detected region indicates a new vehicle or one that has already detected and tracked. Detection and tracking are processed simultaneously for every frame. If a detection result matches a corresponding tracking result in terms of both their road coordinates and pixel

coordinates, they are regarded as the same vehicle. The criteria that describe this determination are presented below.

$\text{INFLATE}(R_d, 0.1)$ contains more than two points out of R_t 's centroid point and four corner points, vice versa.

Here, r_D and r_T refer road coordinates of the detected and tracked region. $v_{\text{smooth},y}$, R_D , and R_T indicates the y-direction smoothed velocity of a tracked vehicle in road coordinates, the detected and the tracked image region, respectively.

$\text{INFLATE}(\text{region}, \text{factor})$ is a function that inflates the given region by the factor of its original size. R_D is represented by a rectangle while R_T is represented by a parallelogram. The y-axis of the road coordinate system is set as the road's longitudinal direction. The criterion (a) is established on the basis of the average vehicle length, the safe distance between vehicles, and the average road width. When either of the two criteria is satisfied, the two results are determined to be the same vehicle. In this case, the tracking result is adjusted by substituting the corresponding detection result. If a detection result has no tracking match, it initiates a new tracking.

Calibration

A fixed camera view is calibrated to establish the transformation between the pixel coordinate and the real-world road coordinate. VWL (one vertical vanishing point, one known width, and one known length) method [] is selected for this purpose since the vanishing point can be located on the basis of parallel lane lines and the road width (12ft) and the dimension of the lane line pattern (40ft for each) are known. A manual interaction

is required to specify the known dimensions. It requires to locate six points and to input the appropriate width and length (Figure 8). Once the user input is set up, a transformation matrix and its inverse matrix are calculated for each specified height (rz). The transformation of rz converts pixel coordinates to the plane that is parallel to the road plane and in a distance of rz . The proposed system uses the centroid of the detected and tracked region as a representative location of a vehicle. The height (rz) of the representative location varies depending on the vehicle's size. Therefore, transformation matrices are generated for several heights so that an appropriate one is chosen for each detected vehicle according to its height.

REFERENCES

- Ahmed, K., M. Ben-Akiva, H. Koutsopoulos, and R. Mishalan (1996). Models of Freeway Lane Changing and Gap Acceptance Behavior. In: Proceedings of the 13th International Symposium on the Theory of Traffic Flow and Transportation.
- Ahmed, Kazi (1999). Modeling Drivers Acceleration and Lane Changing Behavior. Massachusetts Institute of Technology, Dept. of Civil and Environmental Engineering.
- Akaike, Hirotugu (1974). A New Look at the Statistical Model Identification. IEEE Transactions on Automatic Control, Vol AC-19, No. 6.
- Ben-Akiva, M., C. Choudhury, and T. Toledo (2006). Lane Changing Models. In: Proceedings of the International Symposium of Transport Simulation.
- Cassidy, M. J., S.B. Anani, & J.M. Haigwood (2002). Study of freeway traffic near an off-ramp, Transportation Research – Part A, Vol. 36, No. 6, pp. 563-572.
- Cassidy, Michael J, Kitae Jang, and Carlos F. Daganzo (2008). The Smoothing Effect of Carpool Lanes of Freeway Bottlenecks. Transportation Research – Part A. Vol. 44, No. 2, pp. 65-75.
- Chang, Gang-Len, and Yang-Ming Kao (1991). An Empirical Investigation of Macroscopic Lane Changing Characteristics of Uncongested Multilane Freeways. Transportation Research – Part A. Vol. 25A, No. 6, pp. 375-389.
- Choudhury, Charisma (2005). Modeling Lane-Changing Behavior in Presence of Exclusive Lanes. Massachusetts Institute of Technology, Dept. of Civil and Environmental Engineering.
- Coifman, B., R. Mishalani, & C. Wang (2006). Impact of Lane-Change Maneuvers on Pilot Study, 152–159, Transportation Research Record Volume 1965, pp. 152-159.
- Daganzo, Carlos F. and Michael J. Cassidy (2008). Effects of High Occupancy Vehicle Lanes of Freeway Congestion. Transportation Research – Part B. Vol. 42, No. 10, pp. 861-872.
- Efron, B., and R. Tibshirani (2003). An Introduction to the Bootstrap – Monographs on Statistics and Applied Probability, Volume 57, Chapman & Hall.

- Grant, Christopher (1998). Representative vehicle operating mode frequencies : measurement and prediction of vehicle specific freeway modal activity. Dissertation. Georgia Institute of Technology. Dept. of Civil and Environmental Engineering.
- Guensler, R., S. Araque, C. Toth, A. Guin, V. Elango, M. Hunter (2013). "Atlanta I-85 HOV-to-HOT Conversion: Analysis of Changes in Weaving Activity." Final Draft for Review and Comment. Prepared for the Georgia Department of Transportation, Atlanta, GA. Georgia Institute of Technology. Atlanta, GA.
- Guin, A., M. Hunter, and R. Guensler (2008). Analysis of Reduction in Effective Capacities of High-Occupancy Vehicle Lanes Related to Traffic Behavior. *Transportation Research Record*, Volume 2065, pp. 47-53.
- Gurupackiam, Saravanan, Steven Lee Jones Jr. (2012). Empirical Study of Accepted Gap and Lane Change Duration within Arterial Traffic under Recurrent and Non-Recurrent Congestion. *International Journal for Traffic and Transport Engineering*, Volume 2, No. 4, pp. 306-322.
- Hedlund, J. (2013) SHRP 2 Naturalistic Driving Study Overview, Retrieved from : <http://www.ghsa.org/html/meetings/pdf/2013am/pres/wed.hedlund.pdf>. Accessed: August 2014.
- Hidas, P. (2005). Modelling vehicle interactions in microscopic simulation of merging and weaving. *Transportation Research – Part C*. Vol. 13, No. 1, pp. 37-62.
- Highway Capacity Manual (2000) - Chapter 13
- J. A. Laval and L Leclercq (2010). Continuum Approximation for Congestion Dynamics Along Freeway Corridors. *Transportation Science* 44: 87 – 97.
- Jian Zheng, Koji Suzuki, Motohiro Fujita (2014). Predicting driver's lane-changing decisions using a neural network model, *Simulation Modelling Practice and Theory*, Volume 42, March 2014, Pages 73-83.
- Laval Jorge A. & Carlos F. Daganzo (2005). Lane Changing in Traffic Streams. *Transportation Research – Part B*. Vol. 40, No. 3, pp. 251-264.
- Laval, J. A., & Leclercq, L. (2009). Continuum Approximation for Congestion Dynamics Along Freeway Corridors. *Transportation Science* 44(1):87-97
- Laval, J., and L. Leclercq (2008). Microscopic Modeling of the Relaxation Phenomenon Using a Macroscopic Lane-Changing Model. *Transportation Research Part B*, Vol. 42, No. 6, pp. 511-522.

- Laval, Jorge A. and Carlos F. Daganzo (2004). Multi-Lane Hybrid Traffic Flow Model: Quantifying the Impacts of Lane-Changing Maneuvers on Traffic Flow. Institute of Transportation Studies, Research Reports, Working Papers, Proceedings, Institute of Transportation Studies, UC Berkeley,
- Laval, Jorge A., C. Toth, Y. Zhou (2014). A Parsimonious Model for the Formation of Oscillations in Car-Following Models. *Transportation Research Part B*, Vol. 70, pp. 228-238.
- Laval, Jorge A., Michael Cassidy, Carlos Daganzo (2007). Impacts of Lane Changes at Merge Bottlenecks: A Theory and Strategies to Maximize Capacity. Springer Berlin Heidelberg, *Traffic and Granular Flow*, pp 577-586.
- Leclercq, L., Laval, J. A., & Chiabaut, N. (2011). Capacity Drops at Merges : an endogenous model, *Procedia*, Vol. 17, pp. 12–26.
- Leclercq, N Chiabaut, J Laval, and C Buisson (2007). Relaxation phenomenon after changing lanes: Experimental validation with NGSIM data set. *Transportation Research Record*, Volume 1999: 79-85.
- Lee, Joon Ho (2008). Observations on Traffic Behavior in Freeway Weaving Bottlenecks: Empirical Study and Theoretical Modeling. University of California Berkeley.
- Lehman, E.L. (1986), *Testing Statistical Hypotheses* (second ed.). New York: Springer Verlag.
- Ma, T., & Ahn, S. (2008). Comparisons of Speed-Spacing Relations Under General Car Following Versus Lane Changing. *Transportation Research Record: Journal of the Transportation Research Board*, 2088(-1), 138–147. doi:10.3141/2088-15
- Massey, Frank T (1951). The Kolmogorov-Smirnov Test for Goodness of Fit. *Journal of the American Statistical Association*, Vol. 46, No. 253 (Mar., 1951), pp. 68-78
- Massey, William A., Geraldine A. Parker, and Ward Whitt (1995). Estimating the Parameters of a Nonhomogeneous Poisson Process with Linear Rate. *Telecommunication Systems* 5, pp.361-388 AT&T Bell Laboratories.
- Menendez, Monica and Carlos F. Daganzo (2006). Effects of HOV Lanes on Freeway Bottlenecks. *Transportation Research Part B*, Vol. 41, No. 8, pp. 809-822.
- Muñoz, J. C., & Daganzo, C. F. (2000). Experimental Characterization of Multi-Lane Freeway Traffic Upstream of an Off-Ramp Bottleneck, California Partners for Advanced Transit and Highways.

- P.G. Gipps (1986). A model for the structure of lane-changing decisions, *Transportation Research Part B: Methodological*, Volume 20, Issue 5, October 1986, Pages 403-414
- Park, Man-Woo (2012), *Automated 3D Vision-Based Tracking of Construction Entities*. Dissertation. Georgia Institute of Technology, Department of Civil and Environmental Engineering.
- Sarvi, M., O. Ejtemai, and A. Zavabeti (2011). *Modeling Freeway Weaving Maneuver*. Australasian Transport Research Forum 2011 Proceedings.
- Smirnov N (1948). "Table for estimating the goodness of fit of empirical distributions". *Annals of Mathematical Statistics* 19, pp. 279–281.
- Smith, S. A., (1985). *Freeway data collection for studying vehicle interaction*. Tech. Rep. FHWA/RD-85/108, FHWA, U.S., Department of Transportation
- Tomer Toledo, Charisma Choudhury, Moshe Ben-Akiva (2005). *Modeling Lane-Changing Behavior in Presence of Exclusive Lanes*. *Transportation Research Record*, Vol. 1934, pp. 157-165.
- Wei, H., Eric Meyer, Joe Lee, Chuen Feng (2000). *Characterizing and Modeling Observed Lane-Changing Behavior Simulation on Urban Street Network*. *Transportation Research Record*, Vol. 1710, pp. 104-113.

VITA

CHRISTOPHER STEPHEN TOTH

TOTH was born in Columbus, Ohio. He attended public schools in Pickerington, Ohio, received a B.S. in Civil Engineering from Case Western Reserve University, Cleveland, Ohio in 2009 and a M.S. in Civil Engineering from Georgia Institute of Technology, Atlanta, Georgia in 2011 before pursuing a doctorate.